

Finite volume form factors and correlation functions at finite temperature

Ph.D. thesis

Balázs Pozsgay

Supervisor: Gábor Takács, D.Sc.

Eötvös University, Budapest

Physics Doctoral School

Particle Physics and Astronomy Program

Doctoral School leader: Zalán Horváth

Program leader: Ferenc Csikor

Theoretical Physics Group of the
Hungarian Academy of Sciences,
Theoretical Physics Department
Eötvös University, Budapest

Contents

| | |
|--|-----------|
| Introduction | 1 |
| Acknowledgements | 6 |
| 1 Integrable Models and Conformal Field Theories | 7 |
| 1.1 Exact S-matrix theories | 7 |
| 1.1.1 Conserved charges and factorization | 7 |
| 1.1.2 Bound states – The bootstrap principle | 9 |
| 1.2 Integrable theories in finite volume | 10 |
| 1.2.1 One-particle states | 10 |
| 1.2.2 Many-particle states | 11 |
| 1.3 Scattering theories as perturbed CFT's | 13 |
| 1.3.1 CFT in a cylindrical geometry | 13 |
| 1.3.2 Perturbing CFT's | 14 |
| 1.3.3 The Lee-Yang model | 15 |
| 1.3.4 The Ising-model in a magnetic field | 16 |
| 1.3.5 Finite size spectrum from Conformal Field Theory – the Truncated Conformal Space approach | 17 |
| 2 Finite Volume Form Factors – Analytic results | 19 |
| 2.1 The form factor bootstrap program | 19 |
| 2.2 Finite volume form factors without disconnected pieces | 20 |
| 2.2.1 Elementary form factors | 20 |
| 2.2.2 Generic form factors without disconnected pieces | 24 |
| 2.2.3 Estimation of the residual finite size corrections | 25 |
| 2.2.4 Comparison with an exact result | 28 |
| 2.3 Diagonal matrix elements | 30 |
| 2.3.1 Form factor perturbation theory and disconnected contributions . . | 30 |
| 2.3.2 Generalization to higher number of particles | 34 |
| 2.3.3 Diagonal matrix elements in terms of connected form factors | 34 |

| | | |
|----------|--|-----------|
| 2.3.4 | Consistency with Saleur's proposal | 39 |
| 2.4 | Zero-momentum particles | 42 |
| 2.4.1 | Theories with one particle species | 42 |
| 2.4.2 | Generalization to more than one particle species | 45 |
| 3 | Finite Volume Form Factors – Numerical analysis | 47 |
| 3.1 | Form factors from truncated conformal space | 47 |
| 3.1.1 | Truncated conformal space approach for scaling Lee-Yang model | 47 |
| 3.1.2 | Exact form factors of the primary field Φ in the Lee-Yang model | 48 |
| 3.1.3 | Truncated fermionic space approach for the Ising model | 49 |
| 3.1.4 | Ising model – Form factors of the energy density operator | 50 |
| 3.1.5 | Evaluating matrix elements of a local operator \mathcal{O} in TCFA | 50 |
| 3.2 | Vacuum expectation values and one-particle form factors | 54 |
| 3.2.1 | Scaling Lee-Yang model | 54 |
| 3.2.2 | Ising model in magnetic field | 57 |
| 3.3 | Two-particle form factors | 61 |
| 3.3.1 | Scaling Lee-Yang model | 61 |
| 3.3.2 | Ising model in magnetic field | 65 |
| 3.4 | Many-particle form factors | 68 |
| 3.4.1 | Scaling Lee-Yang model | 68 |
| 3.4.2 | Ising model in a magnetic field | 70 |
| 3.5 | General form factors without disconnected pieces | 71 |
| 3.5.1 | Scaling Lee-Yang model | 71 |
| 3.5.2 | Ising model in magnetic field | 73 |
| 3.6 | Diagonal matrix elements | 80 |
| 3.6.1 | Diagonal one-particle and two-particle form factors | 80 |
| 3.6.2 | The general result | 80 |
| 3.7 | Zero-momentum particles | 80 |
| 3.7.1 | Lee-Yang model | 80 |
| 3.7.2 | Ising model in magnetic field | 87 |
| 4 | Residual finite size effects | 89 |
| 4.1 | One-particle states | 89 |
| 4.1.1 | Numerical analysis | 92 |
| 4.1.2 | Comparison with the TBA for excited states | 97 |
| 4.2 | Multi-particle states | 98 |
| 4.2.1 | Bethe-Yang quantization in the bound state picture | 98 |
| 4.2.2 | Multi-particle states – Numerical analysis | 100 |
| 4.3 | Finite volume form factors | 101 |

| | | |
|----------|---|------------|
| 4.3.1 | Elementary one-particle form factors | 102 |
| 4.3.2 | One-particle form factors – Numerical analysis | 104 |
| 4.3.3 | Elementary multi-particle form factors | 106 |
| 5 | Correlation functions at finite temperature | 113 |
| 5.1 | The form factor expansion for correlation functions | 113 |
| 5.1.1 | Comparison of the LeClair-Mussardo and the Delfino approaches . . | 115 |
| 5.2 | Low-temperature expansion for the one-point function | 117 |
| 5.2.1 | Corrections of order e^{-mR} | 119 |
| 5.2.2 | Corrections of order e^{-2mR} | 119 |
| 5.2.3 | Corrections of order e^{-3mR} | 120 |
| 5.3 | Low-temperature expansion for the two-point function | 125 |
| 5.3.1 | Comparison with the LeClair-Mussardo proposal | 126 |
| 6 | Conclusions | 129 |
| | Bibliography | 133 |

Introduction

Finite size effects play an important role in modern statistical physics and quantum field theory. From a statistical point of view, it is known, that no phase transitions take place in a finite volume system, and the specific heat $c(T)$ that is divergent at the critical point in infinite volume, becomes finite if the system has a finite size. Moreover, it is only in an interval around the critical temperature T_c that finite size effects are relevant. Away from this interval, they are negligible because it is only near T_c that the correlation length is comparable with the size of the system. An important fact is that the specific heat and other critical quantities have a scaling behaviour as a response to varying the size L , which is fixed by the critical exponents of the infinite volume system [1, 2].

Interesting phenomena occur in quantum field theories as well. The most prominent example is the Casimir force between two neutral macroscopic bodies in vacuum [3]. This force can be determined from the volume dependence of the ground state energy, which is usually obtained by summing vacuum fluctuations. The crucial point is that besides the extensive bulk and boundary contributions (which are proportional to the volume of the domain and the surface of the boundaries, respectively) there are additional terms, which (in massive theories) decay exponentially with the distance of the boundary plates. In analogy with the Casimir energy, masses of stable particles also get exponentially small corrections in a finite volume [4] and the two-body interaction is also modified [5].

The knowledge of the properties of finite volume QFT is of central importance in at least two ways. On one hand, numerical approaches to QFT necessarily presume a finite volume box, and in order to interpret the results correctly a reliable theoretical control of finite size corrections is needed. Consider for example lattice QCD, where in order to approach the continuum limit the lattice spacing has to be adjusted as small as possible. The number of lattice points is limited by the computational resources, therefore it is typically not possible to choose a volume L^3 , which is large enough to neglect finite size effects.

On the other hand, working in finite volume is not necessarily a disadvantage. On the contrary, the volume dependence of the spectrum can be exploited to obtain (infinite volume) physical quantities like the elastic scattering phase shifts [5, 6] or resonance widths [7, 8].

In this work we investigate finite size effects in 1+1 dimensional integrable field theories. The main subjects of interest are finite volume form factors (matrix elements of local operators on eigenstates of the finite volume Hamiltonian) and expectation values and correlation functions at finite temperature.

1+1 dimensional integrable models attracted considerable interest over the past thirty years. This interest is motivated by the fact that low dimensional integrable models represent nontrivial interacting field theories that are exactly solvable: numerous physical quantities can be exactly calculated in these models. Phenomena qualitatively known in higher dimensions, such as universality, duality, etc. can be quantitatively investigated in 1+1 dimensions.

There is also a second motivation which is of a more practical nature. Several systems of condensed matter physics can be described by 1+1 dimensional effective field theories that in many cases lead to integrable models. Some important examples are the Kondo effect [9, 10], and the effect of impurities in transport processes in general [11, 12, 13, 14], behaviour of the edge states in the fractional quantum Hall effect, problems concerning spin chains, polymers, carbon nanotubes, etc.

Besides the applications mentioned above two dimensional field theories also play a central role in string theory: they describe the dynamics of the string on the world sheet.

In statistical physics, two dimensional critical systems can be described by conformal field theories (CFT) which are fixed points of the renormalization group flow. In this sense, off-critical theories correspond to perturbations of CFT's by some of their relevant operators. Off-critical models do not possess the infinite dimensional symmetry algebra of the fixed point CFT, in particular scale invariance is lost. However, it was observed by A. B. Zamolodchikov [15, 16, 17] that in certain situations there remains an infinite number of conserved quantities. In this case the resulting theory is still integrable and can be described by a factorized scattering theory. The integrals of motion restrict the possible bound state structure and mass ratios in the theory. Assuming further the bootstrap principle, ie. that all bound states belong to the same set of asymptotic particles, it is possible to construct the S-matrix with only a finite number of physical poles.

Integrability can be exploited to gain information about the off-shell physics as well. Applying the ideas of analytic S-matrix theory and the bootstrap principle to form factors one obtains a rather restrictive set of equations which they have to obey [18]. These equations can be considered as axioms for the form factor bootstrap, and supplied with the principles of maximum analyticity and the cluster property they contain enough information to determine the form factors completely [18, 19]. Once the form factors are known, it is possible to construct correlation functions through the spectral expansion, although the explicit summation of the series is only possible in some simple cases [20, 21, 22].

Integrability also offers powerful methods to explore the finite size properties of these models. It is possible to obtain the exact Casimir energy by means of the Thermodynamic Bethe Ansatz (TBA), both with periodic boundary conditions [23] or in the presence of non-trivial (integrable) boundary reflection factors [24]. A great deal of information is known about the excited state spectrum as well. Exact methods include the excited state TBA [25, 26] and nonlinear integral equations derived from lattice regularizations [27, 28].

However, less is known about finite size corrections to off-shell quantities. By Euclidean invariance correlation functions in a finite volume invariance correspond to the evaluation of thermal correlations. These objects can be compared directly to experiments, and it is not surprising that they attracted quite a lot of interest over the last decade [29, 30, 31, 32, 33, 34, 35, 36, 37, 38, 39, 40]. One possible way to approach finite temperature correlation functions is by establishing an appropriate spectral representation in finite volume. This constitutes the first motivation for our work, because finite volume form factors play a central role in this approach. Prior to our work only semiclassical results were known [41, 42] and also an exceptional exact result in the case of a free theory [43, 44, 45].

Besides being a promising tool to obtain correlation functions, finite volume form factors provide means to verify the bootstrap approach to form factors. The connection between the scattering theory and the Lagrangian (or perturbed CFT) formulation is rather indirect, however, it is generally believed, that the solutions of the bootstrap axioms correspond to the local operators of the field theory. Evidence includes a direct comparison of the space of the form factor solutions with the space of primary operators of the CFT [46, 47, 48]; the evaluation of correlation functions both through the spectral representation and from perturbation theory around the CFT [19, 49]; the evaluation of sum-rules like Zamolodchikov's c -theorem [50] and the Δ -theorem [51], both of which can be used to express conformal data as spectral sums in terms of form factors. These tests concern quantities which are constructed from various integrals over the form factors, whereas the multi-particle matrix elements themselves have not been accessible. On the other hand, finite volume form factors can be obtained numerically in the perturbed CFT setting by means of the Truncated Conformal Space Approach (TCSA), and establishing the connection to infinite volume form factors provides a way to directly test the solutions of the form factor bootstrap. This constitutes the second motivation for our work.

The first part of this thesis (chapters 3, 4 and 5) is devoted to the study of finite volume form factors in diagonal scattering theories. We show that these objects can be obtained in terms of the infinite volume form factors; in fact they are related by a proportionality factor which can be interpreted as a density of states of the finite volume spectrum.

To our best knowledge, the first result on finite volume form factors in an interacting QFT was derived by Lellouch and Lüscher in [52], where they considered the finite size dependence of kaon decay matrix elements. It was pointed out by Lin et.al. in [53] that

the final result of [52] can be explained simply by a non-trivial normalization of states in finite volume; they also derived a formula for arbitrary two-particle matrix elements. Our arguments are similar to the ones used in [53]. However, in integrable models it is possible to extend the calculations to arbitrary multi-particle states, because the factorized nature of the S-matrix allows of an analytic description of the whole finite size spectrum.

Having established the connection to infinite volume form factors, we can directly access the form factor functions along certain one-dimensional sections of the rapidity-space parameterized by the volume L . The choice of the section corresponds to which multi-particle states we pick from the finite volume spectrum and it is only limited by the increasing numerical inaccuracy for higher lying states. This procedure provides a non-trivial check of our analytical calculations on finite volume form factors, and also a direct test of the bootstrap approach to form factors, as explained above.

In the second part of the work (chapter 6) we develop a method to evaluate correlation functions at finite temperature: we introduce finite volume as a regulator of the otherwise ill-defined Boltzmann sum. We develop a systematic low-temperature expansion using finite volume form factors and show that the individual terms of this series have a well defined $L \rightarrow \infty$ limit. In fact, they can be transformed into integral expressions over the infinite volume form factors.

There have been previous attempts to attack the problem of finite temperature correlations. LeClair and Mussardo proposed an expansion for the one-point and two-point functions in terms of form factors dressed by appropriate occupation number factors containing the pseudo-energy function from the thermodynamical Bethe Ansatz [30]. It was argued by Saleur [31] that their proposal for the two-point function is incorrect; on the other hand, he gave a proof of the LeClair-Mussardo formula for one-point functions provided the operator considered is the density of some local conserved charge. In view of the evidence it is now generally accepted that the conjecture made by LeClair and Mussardo for the one-point functions is correct; in contrast, the case of two-point functions (and also higher ones) is not yet fully understood. We contribute to this issue by comparing the low-temperature expansion obtained using finite volume form factors to the corresponding terms in the LeClair-Mussardo proposal.

The thesis is organized as follows. In the next chapter we give a brief summary of factorized scattering theory and its connection to CFT, with a section devoted to the finite size properties of these models. Chapter 2 includes our analytic calculations concerning finite volume form factors, with two separate sections devoted to form factors including disconnected pieces. In chapter 3 we present our numerical studies: we test the analytic results of the previous chapter using TCSA in the Lee-Yang model and the Ising model in a magnetic field. In chapter 4 we study the leading exponential corrections (the μ -term) to scattering states and form factors. Chapter 5 deals with the evaluation of a

low-temperature expansion for correlation functions and also with the comparison of our results to previous proposals. The last chapter contains our conclusions.

The material presented in this thesis is based on the papers

- Balázs Pozsgay and Gábor Takács: *Form factors in finite volume I: form factor bootstrap and truncated conformal space* Nucl. Phys. **B788** (2007) 167-208, [arxiv:0706.1445\[hep-th\]](#)
- Balázs Pozsgay and Gábor Takács: *Form factors in finite volume II: disconnected terms and finite temperature correlators* Nucl. Phys. **B788** (2007) 209-251, [arxiv:0706.3605\[hep-th\]](#)
- Balázs Pozsgay: *Lüscher's mu-term and finite volume bootstrap principle for scattering states and form factors* Nucl.Phys. **B802** (2008) 435-457, [arxiv:0803.4445\[hep-th\]](#)

Acknowledgements

First of all, I would like to express my gratitude to my supervisor Gábor Takács for his continuous support over the last four years. He introduced me to the field of two dimensional integrable models, and his guidance in the research was of unvaluable help. I am especially indebted to him for his personal encouragement during the early stages of my Ph.D.

I am also grateful to Zoltán Bajnok for illuminating discussions concerning this work and related ongoing projects.

I am indebted to Hubert Saleur, who acted as a supervisor during my visit to the IPhT Saclay, and also to the organizers and lecturers of the 89. Summer School of the École de Physique Les Houches. The four months I spent in France significantly contributed to my enthusiasm for the field of integrable models and theoretical physics in general.

I would like to thank Gábor Zsolt Tóth, Márton Kormos and Constantin Candu for lots of useful advice and encouragement during the writing of this PhD thesis.

Finally, I would like to thank my family and all my friends, who supported me during the research and pushed me to complete the dissertation.

Chapter 1

Integrable Models and Conformal Field Theories

1.1 Exact S-matrix theories

In this section we give a brief summary of the basic properties of factorized scattering theory. For an introduction to this field see the review article of Mussardo [54].

Let us consider a massive scattering theory with n particle types A_a with masses m_a . One-particle states are denoted by $|\theta\rangle_a$, where θ is the rapidity variable. We apply the following Lorentz-invariant normalization:

$${}_a\langle\theta_a|\theta_b\rangle_b = 2\pi\delta_{ab}\delta(\theta_a - \theta_b)$$

Asymptotic states of the theory are defined as tensor products of one-particle states and are denoted by $|\theta_1, \theta_2, \dots, \theta_n\rangle_{a_1 a_2 \dots a_n}$. The ordering of the rapidities is defined as

- $\theta_1 > \dots > \theta_n$ for *in* states
- $\theta_1 < \dots < \theta_n$ for *out* states

1.1.1 Conserved charges and factorization

In integrable models there are an infinite number of conserved quantities, which can be represented on the quantum level as mutually commuting operators Q_s , which act diagonally on the one-particle states:

$$Q_s|\theta\rangle_a = \chi_a^s e^{s\theta}|\theta\rangle_a$$

The quantity χ_a^s is the spin- s conserved charge of particle A_a . The spin represents the behavior under Lorentz-transformations. The charges for $s = 1$ and $s = -1$ correspond to a linear combination of the energy and momentum, therefore $\chi_a^{\pm 1} = m_a$.

The conserved charge operators are local in the sense, that they act additively on multi-particle asymptotic states:

$$Q_s |\theta_1, \theta_2, \dots, \theta_n\rangle_{a_1 a_2 \dots a_n} = \left(\sum_{i=1}^n \chi_{a_i}^s \right) |\theta_1, \theta_2, \dots, \theta_n\rangle_{a_1 a_2 \dots a_n}$$

The conservation of all higher spin charges constrains the S-matrix:

- All scattering processes are elastic: the number of incoming and outgoing particles is the same.
- The set of conserved charges (including the energy and the momentum) is the same for the *in* and *out* states.
- The S-matrix factorizes: the amplitude for an arbitrary scattering process can be obtained by consecutive two-particle scattering processes.

The basic object is therefore the two-particle S-matrix, which is defined for real rapidities by

$$|\theta_1, \theta_2\rangle_{ab} = S_{ab}^{cd}(\theta_1 - \theta_2) |\theta_2, \theta_1\rangle_{cd}$$

The factorization property forces the S-matrix to obey the Yang-Baxter equations [55, 56, 57]

$$S_{a_1 a_2}^{c_1 c_2}(\theta_{12}) S_{c_1 c_3}^{b_1 b_3}(\theta_{13}) S_{c_2 a_3}^{b_2 c_3}(\theta_{23}) = S_{a_1 a_3}^{c_1 c_3}(\theta_{13}) S_{c_1 c_2}^{b_1 b_2}(\theta_{12}) S_{a_3 c_3}^{c_2 b_3}(\theta_{23})$$

where the summation over the repeated indices is understood.

If there are no two particles with the same set of conserved charges, the S-matrix is diagonal:

$$S_{ab}^{cd}(\theta) = S_{ab}(\theta) \delta_{ac} \delta_{bd}$$

In this case the Yang-Baxter equations are automatically satisfied. In this work we only consider diagonal scattering theories.

The S-matrix can be analytically continued to the whole complex plane and it satisfies

$$S_{ab}(\theta) S_{ab}^*(\theta) = 1 \tag{1.1}$$

$$S_{ab}(i\pi - \theta) = S_{\bar{a}\bar{b}}(\theta) \tag{1.2}$$

due to unitarity and crossing symmetry, where $A_{\bar{b}}$ is the charge-conjugate of A_b .

The unitarity condition can be expressed as

$$S_{ab}(\theta) S_{ab}(-\theta) = 1 \tag{1.3}$$

if one assumes real analyticity:

$$S_{ab}(\theta) = S_{ab}(-\theta^*) = S_{ab}^*(-\theta) \tag{1.4}$$

Equations (1.1),(1.3) and (1.4) are rather restrictive and a general solution can be written as

$$S_{ab}(\theta) = \prod_{\gamma \in \mathcal{G}_{ab}} t_{\gamma}(\theta) \quad (1.5)$$

with

$$t_{\gamma}(\theta) = \frac{\tanh \frac{1}{2}(\theta + i\pi\gamma)}{\tanh \frac{1}{2}(\theta - i\pi\gamma)} = \frac{\sinh(\theta) + i \sin(\pi\gamma)}{\sinh(\theta) - i \sin(\pi\gamma)}$$

and $\mathcal{G}_{ab} \subset \mathbb{R}$ is a finite set.

1.1.2 Bound states – The bootstrap principle

The S-matrix (1.5) may contain zeros and simple or multiple poles for purely imaginary rapidities. In a consistent theory, the interpretation for a simple pole is a formation of a bound state.¹ If particle A_c appears to be a bound state of A_a and A_b , then one has

$$\text{Res}_{\theta=i u_{ab}^c} = i(\Gamma_{ab}^c)^2 \quad (1.6)$$

with $\Gamma_{ab}^c \in \mathbb{R}$ and

$$m_c^2 = m_a^2 + m_b^2 + 2m_a m_b \cos(u_{ab}^c)$$

The one-particle state $|\theta\rangle_c$ may be identified with the formal two-particle state

$$|\theta\rangle_c \sim |\theta - i\bar{u}_{ac}^b, \theta + i\bar{u}_{ab}^c\rangle_{ab} \quad (1.7)$$

where the imaginary parts of the rapidities are determined by the conservation of energy and momentum under the fusion process (Fig. 1.1):

$$m_a \sin(\bar{u}_{ac}^b) = m_b \sin(\bar{u}_{ab}^c) \quad m_a \cos(\bar{u}_{ac}^b) + m_b \cos(\bar{u}_{ab}^c) = m_c$$

As a consequence, one also has $u_{ab}^c = \bar{u}_{ac}^b + \bar{u}_{ab}^c$. For the higher spin conserved charges the identification (1.7) requires

$$\chi_c^s = \chi_a^s e^{-is\bar{u}_{ab}^c} + \chi_b^s e^{is\bar{u}_{ab}^c} \quad (1.8)$$

Scattering processes including A_c can be computed due to the factorization property of the S-matrix as

$$S_{dc}(\theta) = S_{da}(\theta - i\bar{u}_{ac}^b) S_{db}(\theta + i\bar{u}_{ab}^c) \quad (1.9)$$

Equations (1.8) and (1.9) represent strong restrictions for the possible set of conserved charges and the sets \mathcal{G}_{ab} describing the scattering processes. The solution of these equations with a finite number of particles is called the *bootstrap procedure*.

¹Higher order poles in the S-matrix are specific to two dimensions and can be explained by the Coleman-Thun mechanism[58, 59, 60].

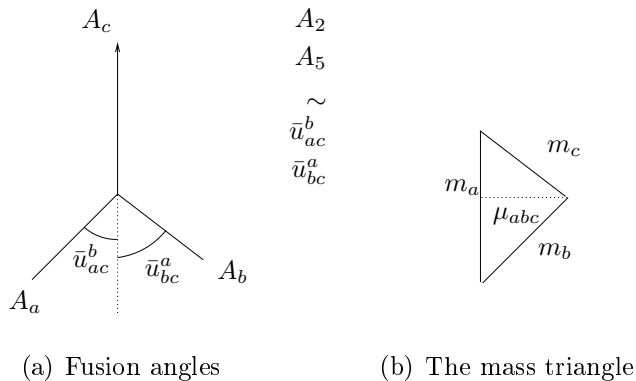


Figure 1.1: Pictorial representation of particle fusions.

1.2 Integrable theories in finite volume

Let us consider the theory defined in a finite box of size L . One of the most characteristic feature of a field theory is the evolution of its discrete energy levels $E_i(L)$, $i = 1 \dots \infty$ as a function of the volume.

In quantum field theories (including realistic 3+1 dimensional models) low-lying one-particle and two-particle states [4, 5, 7] can be described to all orders in $1/L$ in terms of the infinite volume spectrum (particle types and masses) and the elastic scattering amplitudes of the theory. In non-integrable theories higher lying energy levels are far more difficult to access due to the complicated structure of the S-matrix and only partial results are available [61, 62, 63]. On the other hand, the S-matrix of integrable models factorizes and there are no inelastic processes present. These properties enable us to describe the whole finite volume spectrum to all orders in $1/L$.

In this section we briefly describe the main characteristics of the finite volume spectra of diagonal scattering theories. We also introduce some notations which will be used throughout this work. We assume periodic boundary conditions for simplicity.

1.2.1 One-particle states

One-particle states of particle A_a in finite volume can be characterized with the momentum p_a , which (due to the periodicity of the wave function) is constrained to

$$p_a = I \frac{2\pi}{L} \quad I \in \mathbb{N}$$

Therefore, the particle type and the momentum quantum number I (the Lorentz-spin) uniquely determine the one-particle state in question. For convenience we introduce the notation

$$|\{I\}\rangle_{a,L}$$

where the subscript L denotes, that this state is an eigenvector of the finite volume Hamiltonian.

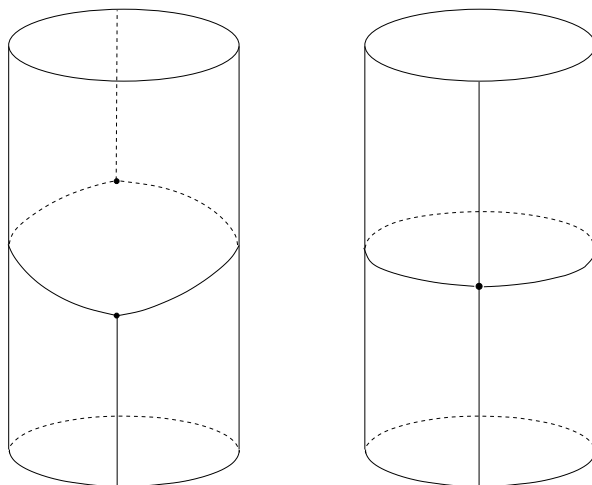


Figure 1.2: The diagram to the left (the μ -term) shows a particle splitting in two virtual, on-shell particles, traveling around the cylinder and recombining. The diagram to the right (the F-term) shows a virtual particle going around the circumference of the cylinder.

The energy is given to all orders in $1/L$ by the relativistic formula

$$E = \sqrt{m_a^2 + p_a^2} \quad (1.10)$$

There are additional correction terms to (1.10), which decay exponentially with the volume. These terms can be attributed to virtual processes which are absent in infinite volume. M. Lüscher calculated the finite size mass corrections of stable particles (energy corrections for $I = 0$); they consist of the so-called μ -term and F-term [4] and are associated to diagrams depicted in figure 1.2. The explicit formulas for one dimensional diagonal scattering theories read [64]

$$\Delta m_a^{(\mu)} = - \sum_{b,c} \theta(m_a^2 - |m_b^2 - m_c^2|) \mathcal{M}_{abc} \mu_{abc} (\Gamma_{ab}^c)^2 e^{-\mu_{abc} L} \quad (1.11)$$

$$\Delta m_a^{(F)} = - \sum_b \int_{-\infty}^{\infty} \frac{d\theta}{2\pi} e^{-m_b L \cosh(\theta)} m_b \cosh(\theta) (S_{ab}(\theta + i\pi/2) - 1) \quad (1.12)$$

where $\mathcal{M}_{abc} = 1$ if A_c is a bound state of A_a and A_b and zero otherwise; μ_{abc} is the altitude of the mass triangle with base m_a (see figure 1.1) and $(\Gamma_{ab}^c)^2$ is the residue of $S_{ab}(\theta)$ corresponding to the formation of the bound state.

1.2.2 Many-particle states

The Bethe-Yang equations [65] serve as quantization conditions for a many-particle state consisting of n particles A_{i_k} with rapidities $\tilde{\theta}_k$:

$$Q_k(\tilde{\theta}_1, \dots, \tilde{\theta}_n)_{i_1 \dots i_n} = m_{i_k} L \sinh \tilde{\theta}_k + \sum_{l \neq k} \delta_{i_k i_l} (\tilde{\theta}_k - \tilde{\theta}_l) = 2\pi I_k \quad , \quad k = 1, \dots, n \quad (1.13)$$

where $\delta_{ij}(\theta) = -i \log S_{ij}(\theta)$.

For each set of particle types and momentum quantum numbers I_k there is a unique solution of the equations above.² The energy of the many-particle state in question is given to all orders in $1/L$ by the additive formula

$$E = \sum_{k=1}^n m_{i_k} \cosh(\tilde{\theta}_k) \quad (1.14)$$

The effect of the interaction between the particles is the shift of the rapidities from the values they would assume in a free theory.

Since many-particle states are completely characterized by the quantum numbers I_k , it is convenient to introduce the following implicit notation for a n -particle state consisting of particles i_1, i_2, \dots, i_n with rapidities $\tilde{\theta}_1, \tilde{\theta}_2, \dots, \tilde{\theta}_n$:

$$|\{I_1, I_2, \dots, I_n\}\rangle_{i_1 i_2, \dots, i_n, L}$$

where it is understood that $\tilde{\theta}_1, \tilde{\theta}_2, \dots, \tilde{\theta}_n$ are solutions of the Bethe-equations with quantum numbers I_1, I_2, \dots, I_n .

To have an unambiguous definition of the quantum numbers I_k , it is convenient to define phase shift functions δ_{ab} which are continuous and odd functions of the rapidity difference θ ; we achieve this using the following convention:

$$S_{ab}(\theta) = S_{ab}(0)e^{i\delta_{ab}(\theta)}$$

where δ_{ab} is uniquely specified by continuity and the branch choice

$$\delta_{ab}(0) = 0$$

and it is an odd function of θ due to the following property of the scattering amplitude:

$$S_{ab}(\theta)S_{ab}(-\theta) = 1$$

(which also implies $S_{ab}(0) = \pm 1$). For a generic complex rapidity one has

$$\delta_{ab}(\theta^*) = \delta_{ab}(\theta)^*$$

Note, that with the convention above the quantum numbers I_k can be both integer and half-integer. Two particle states of the type $A_a A_a$ have generally half-integer quantum numbers, because the particles have fermionic statistics ($S_{aa}(0) = -1$) in all known theories³.

Similar to the one-particle energies, there are exponentially small finite size corrections to (1.14). The μ -term associated to multi-particle energies is investigated in section 4.2.

²The solutions with two or more coinciding momenta for a given particle type do not correspond to eigenstates of the Hamiltonian due to Pauli principle.

³The only exception is the free boson with $S = 1$

1.3 Scattering theories as perturbed CFT's

Conformal Field Theories are two-dimensional Euclidean field theories, which possess invariance under conformal transformations, including scale-invariance. In the space of all possible QFT's they represent fixed points under the renormalization group flow. In statistical physics, they describe fluctuations of critical systems in the continuum limit [66]. Conformal invariance highly constrains the behavior of the correlation functions, and even the operator content of the theory [67]. In this section we quote some basic properties of CFT's and introduce two particular models, which will serve as a testing ground for our results: the scaling Lee-Yang model and the critical Ising model. For a general introduction to conformal field theories see [68, 69].

Scale invariance constrains the energy-momentum tensor $T_{\mu\nu}(x, y)$ to be traceless. Introducing complex coordinates $z = x + iy$ and $\bar{z} = x - iy$ this condition can be expressed as $T_{z\bar{z}} = T_{\bar{z}z} = 0$. Conservation of the energy-momentum tensor on the other hand requires $\partial_{\bar{z}}T_{zz} = \partial_zT_{\bar{z}\bar{z}} = 0$, therefore it is possible to introduce the left- and right-moving (chiral and anti-chiral) components $T(z) \equiv T_{zz}(z)$ and $\bar{T}(\bar{z}) \equiv T_{\bar{z}\bar{z}}(\bar{z})$.

$T(z)$ may be expanded into its Laurent-series around $z = 0$ as

$$T(z) = \sum_{n \in \mathbb{N}} z^{-n-2} L_n$$

The operators L_n satisfy the Virasoro algebra:

$$[L_n, L_m] = (n - m)L_{n+m} + \frac{c}{12}(n^3 - n)\delta_{n+m,0}$$

which is a central extension of the symmetry algebra of the classical conformal group, c being the central charge of the theory.

The value of c includes a great deal of information about the theory. It restricts the possible representations of the Virasoro-algebra, therefore also the operator content and the spectrum of the theory. The simplest theories are the minimal models [70], which contain a finite number of primary fields and possess no additional symmetries. They can be characterized by two coprime integers p and q and the central charge is given by

$$c = 1 - \frac{6(p - q)^2}{pq}$$

These theories are in addition unitary (there are no negative-norm states in the spectrum) if $q = p + 1$.

1.3.1 CFT in a cylindrical geometry

A cylinder with spatial circumference L can be mapped to the complex plane by the conformal transformation

$$z = \exp\left(\frac{2\pi}{L}(\tau - ix)\right) \quad \bar{z} = \exp\left(\frac{2\pi}{L}(\tau + ix)\right) \quad (1.15)$$

where x and τ are the spatial and the imaginary time coordinates, respectively. The transformation properties of the energy-momentum tensor determine the Hamilton-operator (generator of translations in the time-direction):

$$H = \int_0^L dx T_{\tau\tau}(x, \tau = 0) = \frac{2\pi}{L} \left(L_0 + \bar{L}_0 - \frac{c}{12} \right) \quad (1.16)$$

In minimal models the Hilbert-space is given by

$$\mathcal{H} = \bigoplus_h \mathcal{V}_h \otimes \bar{\mathcal{V}}_h \quad (1.17)$$

where \mathcal{V}_h ($\bar{\mathcal{V}}_h$) denotes the irreducible representation of the left (right) Virasoro algebra with highest weight h .

1.3.2 Perturbing CFT's

Conformal field theories represent statistical physical or quantum systems at criticality. However, they can be also used to approach noncritical models.

Let us consider a theory defined by the action

$$A = A_{CFT} + \sum_j g_j \int d^2x \Phi_j(x)$$

where A_{CFT} is the action of some CFT and Φ_j are its relevant operators⁴. This theory is no longer conformal, the coupling constants g_j describe the deviation from criticality. However, if there is only one perturbation present, which only breaks a subset of the conformal symmetries, the theory may still possess an infinite number of conservation laws, and it may remain integrable⁵ [15, 16, 17, 73]. Let us therefore consider that the theory defined by the action

$$A = A_{CFT} + g \int d^2x \Phi(x) \quad (1.18)$$

is integrable. Scale-invariance is broken by the perturbation, the energy scale in the perturbed theory is set by $g^{\frac{1}{2-\Delta_\Phi}}$, where Δ_Φ is the scaling dimension of the field Φ . Depending on the original CFT and the perturbing operator the action (1.18) may define a massive

⁴ In the sense of renormalization group flow, relevant operators describe the departure from the critical system. The perturbation leaves the UV behaviour of the theory unchanged, ie. it is still governed by the CFT. If the scaling dimension of the operator is greater or equal to 1, a renormalization procedure is required to properly define the perturbed theory[71] On the other hand, perturbing with irrelevant operators results in an ill-defined theory in the UV, with an infinite number of counter-terms occurring during renormalization [72].

⁵Perturbations with multiple couplings are not expected to lead to integrable theories. For a short discussion see section 2.3 in [54].

[74] or a massless [75, 76] scattering theory. In this work we only consider the massive case.

The question of which perturbed CFT corresponds to which scattering theory may be answered by different methods. First of all, Zamolodchikov's counting argument [15] provides a sufficient condition for the existence of higher spin conservation laws. A second independent method is the Thermodynamic Bethe Ansatz [23, 77, 78], which provides integral equations to determine the finite size dependence of the vacuum energy in terms of the S-matrix of the theory. It can be used to analytically predict the central charge of the CFT, the non-universal bulk vacuum energy density, and also the scaling dimension of the perturbing field.

A third method is the Truncated Conformal Space Approach (see 1.3.5), which can be used to numerically determine the low-lying energy levels of the finite size spectrum. Matching the numerical data with the predictions of the Bethe-Yang equations (1.13) one can identify multi-particle states and thus directly test the phase shifts $S_{ab}(\theta)$. For the details of this procedure see section 3.1.5.

1.3.3 The Lee-Yang model

The non-unitary minimal model $M_{2,5}$ has central charge $c = -22/5$ and a unique nontrivial primary field Φ with scaling weights $\Delta = \bar{\Delta} = -1/5$. The field Φ is normalized so that it has the following operator product expansion:

$$\Phi(z, \bar{z})\Phi(0, 0) = \mathcal{C}(z\bar{z})^{1/5}\Phi(0, 0) + (z\bar{z})^{2/5}\mathbb{I} + \dots \quad (1.19)$$

where \mathbb{I} is the identity operator and the only nontrivial structure constant is

$$\mathcal{C} = 1.911312699 \dots \times i$$

The Hilbert space of the conformal model is given by

$$\mathcal{H}_{LY} = \bigoplus_{h=0, -1/5} \mathcal{V}_h \otimes \bar{\mathcal{V}}_h$$

where \mathcal{V}_h ($\bar{\mathcal{V}}_h$) denotes the irreducible representation of the left (right) Virasoro algebra with highest weight h .

The off-critical Lee-Yang model is defined by the Hamiltonian

$$H^{SLY} = H_{CFT} + i\lambda \int_0^L dx \Phi(0, x) \quad (1.20)$$

where H_{CFT} is the conformal Hamiltonian. This theory is related to the Lee-Yang edge singularity of the Ising model in an imaginary magnetic field [79, 80, 81]. Despite its lack

of unitarity, it is also relevant in condensed matter physics: it is related to the theory of non-intersecting branched polymers in 4 dimensions [82].

When $\lambda > 0$ the theory above has a single particle in its spectrum with mass m that can be related to the coupling constant as [23]

$$\lambda = 0.09704845636 \dots \times m^{12/5} \quad (1.21)$$

and the bulk energy density is given by

$$\mathcal{B} = -\frac{\sqrt{3}}{12}m^2 \quad (1.22)$$

The S -matrix reads [83]

$$S_{LY}(\theta) = \frac{\sinh \theta + i \sin \frac{2\pi}{3}}{\sinh \theta - i \sin \frac{2\pi}{3}} \quad (1.23)$$

and the particle occurs as a bound state of itself at $\theta = 2\pi i/3$ with the three-particle coupling given by

$$\Gamma^2 = -2\sqrt{3}$$

where the negative sign is due to the non-unitarity of the model. According to the convention introduced in section 1.2 we define the phase-shift via the relation

$$S_{LY}(\theta) = -e^{i\delta(\theta)} \quad (1.24)$$

so that $\delta(0) = 0$.

1.3.4 The Ising-model in a magnetic field

The critical Ising model is described by the unitary conformal field theory $M_{3,4}$ with $c = 1/2$ and has two nontrivial primary fields: the spin operator σ with $\Delta_\sigma = \bar{\Delta}_\sigma = 1/16$ and the energy density ϵ with $\Delta_\epsilon = \bar{\Delta}_\epsilon = 1/2$. The magnetic perturbation

$$H = H_0^I + h \int_0^L dx \sigma(0, x)$$

is massive (and its physics does not depend on the sign of the external magnetic field h). The spectrum and the exact S matrix is described by the famous E_8 factorized scattering

theory [84], which contains eight particles A_i , $i = 1, \dots, 8$ with mass ratios given by

$$\begin{aligned} m_2 &= 2m_1 \cos \frac{\pi}{5} \\ m_3 &= 2m_1 \cos \frac{\pi}{30} \\ m_4 &= 2m_2 \cos \frac{7\pi}{30} \\ m_5 &= 2m_2 \cos \frac{2\pi}{15} \\ m_6 &= 2m_2 \cos \frac{\pi}{30} \\ m_7 &= 2m_4 \cos \frac{\pi}{5} \\ m_8 &= 2m_5 \cos \frac{\pi}{5} \end{aligned}$$

and the mass gap relation is [85]

$$m_1 = (4.40490857 \dots) |h|^{8/15}$$

or

$$h = \kappa_h m_1^{15/8} \quad , \quad \kappa_h = 0.06203236 \dots \quad (1.25)$$

The bulk energy density is given by

$$B = -0.06172858982 \dots \times m_1^2 \quad (1.26)$$

We also quote the scattering phase shift of two A_1 particles:

$$S_{11}(\theta) = \left\{ \frac{1}{15} \right\}_\theta \left\{ \frac{1}{3} \right\}_\theta \left\{ \frac{2}{5} \right\}_\theta \quad , \quad \{x\}_\theta = \frac{\sinh \theta + i \sin \pi x}{\sinh \theta - i \sin \pi x} \quad (1.27)$$

All other amplitudes S_{ab} are determined by the S matrix bootstrap [84]; the only one we need later is that of the $A_1 - A_2$ scattering, which takes the form

$$S_{12}(\theta) = \left\{ \frac{1}{5} \right\}_\theta \left\{ \frac{4}{15} \right\}_\theta \left\{ \frac{2}{5} \right\}_\theta \left\{ \frac{7}{15} \right\}_\theta$$

Our interest in the Ising model is motivated by the fact that this is the simplest model in which form factors of an operator different from the perturbing one are known, and also its spectrum and bootstrap structure is rather complex, both of which stands in contrast with the much simpler case of scaling Lee-Yang model.

1.3.5 Finite size spectrum from Conformal Field Theory – the Truncated Conformal Space approach

Let us assume that the infinite volume scattering theory corresponds to a perturbed conformal theory defined by the action

$$A = A_{CFT} + g \int d^2x \Phi(x) \quad (1.28)$$

If this connection is already established, one can use the conformal data to obtain the finite size spectrum of the theory. The perturbed Hamiltonian is obtained by mapping the cylinder with circumference L to the complex plane. Using the transformation properties of the primary field $\Phi(x)$ one has

$$H = H_{CFT} + 2\pi g \left(\frac{2\pi}{L} \right)^{\Delta_\Phi - 1} \Phi(0, 0) \quad (1.29)$$

where H_{CFT} is the conformal Hamiltonian (1.16). Both the spectrum H_{CFT} and the matrix elements of Φ between its eigenstates can be calculated, therefore the complete and exact finite size spectrum can be obtained in principle by diagonalizing (1.29) in the infinite dimensional Hilbert-space (1.17).

Instead of the impossible task of diagonalizing an infinite matrix Yurov and Zamolodchikov proposed the Truncated Conformal Space Approach (TCSA) [86] as a numerical approximation scheme. The method consists of truncating the Hilbert-space (1.17) to the states which have scaling dimension (eigenvalue under $L_0 + \bar{L}_0$) smaller than some threshold e_{cut} . In this finite Hilbert-space the diagonalization procedure can be performed on a computer, and one obtains eigenvalues $E_i(L, e_{cut})$, which are approximations to the exact energy levels $E_i(L)$, and

$$\lim_{e_{cut} \rightarrow \infty} E_i(L, e_{cut}) = E_i(L)$$

The convergence is faster for the low-lying states.

Besides being an effective tool to obtain finite size quantities, TCSA can also serve as a regulator of the UV divergences of the vacuum energy if $\Delta_\Phi \geq 1$.

In this work (chapter 3) we use TCSA to determine the finite volume form factors of local operators in the scaling Lee-Yang and Ising models. The numerical data is then used to confirm the analytic results of chapter 2. The details of the TCSA methods we used are explained in section 3.1.

Chapter 2

Finite Volume Form Factors – Analytic results

In this chapter we determine the finite volume matrix elements in terms of the infinite volume form factors and the S-matrix of the theory.

In section 2.1 we briefly summarize the ingredients of the so-called form factor bootstrap program, which leads to explicit solutions for the infinite volume form factor functions. In section 2.2 we present our results for finite volume form factors which do not include disconnected pieces.

Disconnected terms occur in the case of diagonal form factors and matrix elements including zero-momentum particles. These two special situations are discussed in sections 2.3 and 2.4, respectively.

2.1 The form factor bootstrap program

The (infinite volume) form factors of a local operator $\mathcal{O}(t, x)$ are defined as

$$F_{mn}^{\mathcal{O}}(\theta'_1, \dots, \theta'_m | \theta_1, \dots, \theta_n)_{j_1 \dots j_m; i_1 \dots i_n} = {}_{j_1 \dots j_m} \langle \theta'_1, \dots, \theta'_m | \mathcal{O}(0, 0) | \theta_1, \dots, \theta_n \rangle_{i_1 \dots i_n} \quad (2.1)$$

In first place they are defined for real rapidities, however they can be analytically continued to the whole complex plane. The properties of the form factor functions are explained in detail in Smirnov's review [18].

With the help of the crossing relations

$$\begin{aligned} F_{mn}^{\mathcal{O}}(\theta'_1, \dots, \theta'_m | \theta_1, \dots, \theta_n)_{j_1 \dots j_m; i_1 \dots i_n} = & \\ & F_{m-1n+1}^{\mathcal{O}}(\theta'_1, \dots, \theta'_{m-1} | \theta'_m + i\pi, \theta_1, \dots, \theta_n)_{j_1 \dots j_{m-1}; j_m i_1 \dots i_n} \\ & + \sum_{k=1}^n \left(2\pi \delta_{j_m i_k} \delta(\theta'_m - \theta_k) \prod_{l=1}^{k-1} S_{i_l i_k}(\theta_l - \theta_k) \times \right. \\ & \left. F_{m-1n-1}^{\mathcal{O}}(\theta'_1, \dots, \theta'_{m-1} | \theta_1, \dots, \theta_{k-1}, \theta_{k+1}, \dots, \theta_n)_{j_1 \dots j_{m-1}; j_m i_1 \dots i_{k-1} i_{k+1} \dots i_n} \right) \quad (2.2) \end{aligned}$$

all form factors can be expressed in terms of the elementary form factors

$$F_n^{\mathcal{O}}(\theta_1, \dots, \theta_n)_{i_1 \dots i_n} = \langle 0 | \mathcal{O}(0, 0) | \theta_1, \dots, \theta_n \rangle_{i_1 \dots i_n}$$

which satisfy the following axioms [87]:

I. Exchange:

$$\begin{aligned} F_n^{\mathcal{O}}(\theta_1, \dots, \theta_k, \theta_{k+1}, \dots, \theta_n)_{i_1 \dots i_k i_{k+1} \dots i_n} = \\ S_{i_k i_{k+1}}(\theta_k - \theta_{k+1}) F_n^{\mathcal{O}}(\theta_1, \dots, \theta_{k+1}, \theta_k, \dots, \theta_n)_{i_1 \dots i_{k+1} i_k \dots i_n} \end{aligned} \quad (2.3)$$

II. Cyclic permutation:

$$F_n^{\mathcal{O}}(\theta_1 + 2i\pi, \theta_2, \dots, \theta_n) = F_n^{\mathcal{O}}(\theta_2, \dots, \theta_n, \theta_1) \quad (2.4)$$

III. Kinematical singularity

$$-i \operatorname{Res}_{\theta=\theta'} F_{n+2}^{\mathcal{O}}(\theta + i\pi, \theta', \theta_1, \dots, \theta_n)_{i_j i_1 \dots i_n} = \left(1 - \delta_{ij} \prod_{k=1}^n S_{i i_k}(\theta - \theta_k) \right) F_n^{\mathcal{O}}(\theta_1, \dots, \theta_n)_{i_1 \dots i_n} \quad (2.5)$$

IV. Dynamical singularity

$$-i \operatorname{Res}_{\theta=\theta'} F_{n+2}^{\mathcal{O}}(\theta + i\bar{u}_{jk}^i/2, \theta' - i\bar{u}_{ik}^j/2, \theta_1, \dots, \theta_n)_{i_j i_1 \dots i_n} = \Gamma_{ij}^k F_{n+1}^{\mathcal{O}}(\theta, \theta_1, \dots, \theta_n)_{k i_1 \dots i_n} \quad (2.6)$$

whenever k occurs as the bound state of the particles i and j .

The essence of the form factor bootstrap program is to obtain explicit analytical solution to the above set of recursive equations [87, 88, 19, 89]. Axioms I-IV are supplemented by the assumption of maximum analyticity (i.e. that the form factors are meromorphic functions which only have the singularities prescribed by the axioms) and possible further conditions expressing properties of the particular operator whose form factors are sought.

2.2 Finite volume form factors without disconnected pieces

2.2.1 Elementary form factors

Here we determine finite volume form factors of the form

$$\langle 0 | \mathcal{O} | \{I_1, I_2, \dots, I_n\} \rangle_{i_1 \dots i_n, L}$$

by comparing the Euclidean two-point functions of arbitrary local operators

$$\langle \mathcal{O}(\bar{x}) \mathcal{O}'(0, 0) \rangle \quad \text{and} \quad \langle \mathcal{O}(\bar{x}) \mathcal{O}'(0, 0) \rangle_L \quad (2.7)$$

defined in the infinite volume theory, and in a finite but large volume L , respectively. Given that one uses the same renormalization prescriptions for the operators, the finite size correction to the correlation function decays exponentially with L :

$$\langle \mathcal{O}(\bar{x})\mathcal{O}'(0) \rangle - \langle \mathcal{O}(\bar{x})\mathcal{O}'(0) \rangle_L \sim O(e^{-\mu L}) \quad (2.8)$$

where μ is some characteristic mass scale. In 2.2.3 we discuss this relation in detail; here we only use the fact, that the finite size correction decays faster than any power of $1/L$.

Choosing $\bar{x} = (\tau, 0)$ and inserting a complete set of states one obtains the spectral representations

$$\begin{aligned} \langle \mathcal{O}(\bar{x})\mathcal{O}'(0, 0) \rangle &= \sum_{n=0}^{\infty} \sum_{i_1 \dots i_n} \left(\prod_{k=1}^n \int_{-\infty}^{\infty} \frac{d\theta_k}{2\pi} \right) F_n^{\mathcal{O}}(\theta_1, \theta_2, \dots, \theta_n)_{i_1 \dots i_n} \times \\ &F_n^{\mathcal{O}'}(\theta_1, \theta_2, \dots, \theta_n)_{i_1 \dots i_n}^+ \exp \left(-\tau \sum_{k=1}^n m_{i_k} \cosh \theta_k \right) \end{aligned} \quad (2.9)$$

and

$$\begin{aligned} \langle \mathcal{O}(\tau, 0)\mathcal{O}'(0, 0) \rangle_L &= \sum_{n=0}^{\infty} \sum_{i_1 \dots i_n} \sum_{I_1 \dots I_n} \langle 0 | \mathcal{O}(0, 0) | \{I_1, I_2, \dots, I_n\} \rangle_{i_1 \dots i_n, L} \times \\ &{}_{i_1 \dots i_n} \langle \{I_1, I_2, \dots, I_n\} | \mathcal{O}'(0, 0) | 0 \rangle_L \exp \left(-\tau \sum_{k=1}^n m_{i_k} \cosh \tilde{\theta}_k \right) \end{aligned} \quad (2.10)$$

where we used multi-particle states and form factors of the infinite volume and finite volume theories, respectively, and in (2.10) it is understood that the rapidities $\tilde{\theta}_k$ are solutions of the Bethe-Yang equations

$$Q_k(\tilde{\theta}_1, \dots, \tilde{\theta}_n)_{i_1 \dots i_n} = m_{i_k} L \sinh \tilde{\theta}_k + \sum_{l \neq k} \delta_{i_k i_l} (\tilde{\theta}_k - \tilde{\theta}_l) = 2\pi I_k \quad , \quad k = 1, \dots, n \quad (2.11)$$

The second form factor in (2.9) is defined as

$$F_n^{\mathcal{O}'}(\theta_1, \theta_2, \dots, \theta_n)_{i_1 \dots i_n}^+ = {}_{i_1 \dots i_n} \langle \theta_1, \dots, \theta_n | \mathcal{O}'(0, 0) | 0 \rangle = F_n^{\mathcal{O}'}(\theta_1 + i\pi, \theta_2 + i\pi, \dots, \theta_n + i\pi)_{i_1 \dots i_n}$$

, which is just the complex conjugate of $F_n^{\mathcal{O}'}$ for unitary theories.

To relate the finite and infinite volume form factors a further step is necessary, because the integrals in the spectral representation (2.9) must also be discretized. Let us consider this problem first for the case of free particles:

$$\left(\prod_{k=1}^n \int_{-\infty}^{\infty} \frac{d\theta_k}{2\pi} \right) f(\theta_1, \dots, \theta_n) = \left(\prod_{k=1}^n \int_{-\infty}^{\infty} \frac{dp_k}{2\pi E_k} \right) f(p_1, \dots, p_n)$$

where

$$p_k = m_{i_k} \sinh \theta_k \quad , \quad E_k = m_{i_k} \cosh \theta_k$$

are the momenta and energies of the particles. In finite volume

$$p_k = \frac{2\pi I_k}{L}$$

and it is well-known (as a consequence of the Poisson summation formula, cf. [5]) that

$$\sum_{I_1, \dots, I_n} g\left(\frac{2\pi I_1}{L}, \dots, \frac{2\pi I_n}{L}\right) = \left(\frac{L}{2\pi}\right)^n \left(\prod_{k=1}^n \int_{-\infty}^{\infty} dp_k\right) g(p_1, \dots, p_n) + O(L^{-N}) \quad (2.12)$$

provided the function g and its first N derivatives are integrable. Recalling that form factors are analytic functions for real momenta, in our case this is true for derivatives of any order, due to the exponential suppression factor in the spectral integrals, provided the form factors grow at most polynomially in the momentum, i.e.

$$|F_n(\theta_1 + \theta, \theta_2 + \theta, \dots, \theta_n + \theta)| \sim e^{x|\theta|} \quad \text{as } |\theta| \rightarrow \infty$$

This is true if we only consider operators which have a power-like short distance singularity in their two-point functions [89]:

$$\langle 0 | \mathcal{O}(\bar{x}) \mathcal{O}(0) | 0 \rangle = \frac{1}{r^{2\Delta}}$$

Therefore the discrete sum differs from the continuum integral only by terms decaying faster than any power in $1/L$, i.e. by terms exponentially suppressed in L . Taking into account that (2.7) is valid for any pair $\mathcal{O}, \mathcal{O}'$ of scaling fields, we obtain

$$\langle 0 | \mathcal{O}(0, 0) | \{I_1, \dots, I_n\}_{i_1 \dots i_n, L} \rangle = \frac{1}{\sqrt{\rho_{i_1 \dots i_n}^{(0)}(\tilde{\theta}_1, \dots, \tilde{\theta}_n)}} F_n^{\mathcal{O}}(\tilde{\theta}_1, \dots, \tilde{\theta}_n)_{i_1 \dots i_n} + O(e^{-\mu' L}) \quad (2.13)$$

where

$$\sinh \tilde{\theta}_k = \frac{2\pi I_k}{m_{i_k} L}$$

and

$$\rho_{i_1 \dots i_n}^{(0)}(\tilde{\theta}_1, \dots, \tilde{\theta}_n) = \prod_{k=1}^n m_{i_k} L \cosh \tilde{\theta}_k \quad (2.14)$$

$\rho_n^{(0)}$ is nothing else than the Jacobi determinant corresponding to changing from the variables $2\pi I_k$ to the rapidities $\tilde{\theta}_k$. The term $O(e^{-\mu' L})$ signifies that our considerations are valid to all orders in $1/L$, although our argument does not tell us the value of μ' : to do that, we would need more information about the correction term in the discretization (2.12).

In the case of interacting particles a more careful analysis is necessary. To generalize (2.13) one has to employ the Jacobian of the mapping $\{I_1, I_2, \dots, I_n\} \rightarrow \{\theta_1, \theta_2, \dots, \theta_n\}$

described by the Bethe-Yang equations. Therefore we define

$$\begin{aligned} \rho_{i_1 \dots i_n}(\theta_1, \dots, \theta_n) &= \det \mathcal{J}^{(n)}(\theta_1, \dots, \theta_n)_{i_1 \dots i_n} \\ \mathcal{J}_{kl}^{(n)}(\theta_1, \dots, \theta_n)_{i_1 \dots i_n} &= \frac{\partial Q_k(\theta_1, \dots, \theta_n)_{i_1 \dots i_n}}{\partial \theta_l}, \quad k, l = 1, \dots, n \end{aligned} \quad (2.15)$$

The finite volume form factors are then given by

$$\langle 0 | \mathcal{O}(0, 0) | \{I_1, \dots, I_n\} \rangle_{i_1 \dots i_n, L} = \frac{1}{\sqrt{\rho_{i_1 \dots i_n}(\tilde{\theta}_1, \dots, \tilde{\theta}_n)}} F_n^{\mathcal{O}}(\tilde{\theta}_1, \dots, \tilde{\theta}_n)_{i_1 \dots i_n} + O(e^{-\mu' L}) \quad (2.16)$$

where $\tilde{\theta}_k$ are the solutions of the Bethe-Yang equations (2.11) corresponding to the state with the specified quantum numbers I_1, \dots, I_n at the given volume L . Note, that the Bethe-Yang equations are correct to all orders in $1/L$, therefore there can be no error terms in (2.16) analytic in $1/L$. In subsection 2.2.3 we consider the error exponent μ' in detail.

The quantity $\rho_{i_1 \dots i_n}(\theta_1, \dots, \theta_n)$ is nothing else than the density of states in rapidity space. It is also worthwhile to mention that relation (2.16) can be interpreted as an expression for the finite volume multi-particle state in terms of the corresponding infinite volume state as follows

$$|\{I_1, \dots, I_n\}\rangle_{i_1 \dots i_n, L} = \frac{1}{\sqrt{\rho_{i_1 \dots i_n}(\tilde{\theta}_1, \dots, \tilde{\theta}_n)}} |\tilde{\theta}_1, \dots, \tilde{\theta}_n\rangle_{i_1 \dots i_n} \quad (2.17)$$

This relation between the density and the normalization of states is a straightforward application of the ideas put forward by Saleur in [31].

To get an idea of the structure of $\rho_{i_1 \dots i_n}(\theta_1, \dots, \theta_n)$ it is instructive to consider the simplest cases. The quantization rule for the one-particle states is identical in the free and interacting cases, therefore

$$\rho_i(\theta) = E_i L \quad \text{with} \quad E_i = m_i \cosh(\theta)$$

In the two-particle case one has

$$\mathcal{J}^{(2)}(\theta_1, \theta_2)_{i_1 i_2} = \begin{pmatrix} E_1 L + \varphi_{i_1 i_2}(\theta_1 - \theta_2) & -\varphi_{i_1 i_2}(\theta_1 - \theta_2) \\ -\varphi_{i_1 i_2}(\theta_1 - \theta_2) & E_2 L + \varphi_{i_1 i_2}(\theta_1 - \theta_2) \end{pmatrix}$$

where we used the symmetric function $\varphi_{i_1 i_2}(\theta) = d/d\theta \delta_{i_1 i_2}(\theta)$ and $E_{1,2} = m_{i_{1,2}} \cosh(\theta_{1,2})$. The two-particle density is therefore given by

$$\rho_{i_1 i_2}(\theta_1, \theta_2) = E_1 E_2 L^2 + (E_1 + E_2) L \varphi_{i_1 i_2}(\theta_1 - \theta_2)$$

The leading term in the expression above is simply the product of two one-particle densities, just like in the free case. This is a general rule: the leading $\mathcal{O}(L^n)$ term in the

n-particle density is given by the product of one-particle densities. The effect of the interaction is the appearance of sub-leading terms proportional to $\varphi_{i_1 i_2}(\theta)$. These terms turn out to be crucial in the calculations of thermal correlations (see section 5.2) and in direct numerical tests of the form factors. The necessity of introducing the full densities (2.15) was first shown in [8] and it is demonstrated in great detail in section 3.

Note, that there is no preferred way to order the rapidities on the circle, since there are no genuine asymptotic *in/out* particle configurations. This means that in relation (2.16) there is no preferred way to order the rapidities inside the infinite volume form factor function $F_n^{\mathcal{O}}$. Different orderings are related by S -matrix factors according to the exchange axiom (2.3), which are indeed phases. Such phases do not contribute to correlation functions (cf. the spectral representation (2.9)), nor to any physically meaningful quantity derived from them. In section 3.2 we show that relations like (2.16) must always be understood to hold only up to physically irrelevant phase factors.

We also remark, that there are no finite volume states for which the quantum numbers of any two of the particles are identical. The reason is that

$$S_{ii}(0) = -1$$

(with the exception of free bosonic theories) and so the wave function corresponding to the appropriate solution of the Bethe-Yang equations (2.11) vanishes. We can express this in terms of form factors as follows:

$$\langle 0 | \mathcal{O}(0, 0) | \{I_1, I_2, \dots, I_n\}_{i_1 \dots i_n, L} \rangle = 0$$

whenever $I_k = I_l$ and $i_k = i_l$ for some k and l . Using this convention we can assume that the summation in (2.10) runs over all possible values of the quantum numbers without exclusions. Note that even in this case the relation (2.16) can be maintained since due to the exchange axiom (2.3)

$$F_n^{\mathcal{O}}(\tilde{\theta}_1, \dots, \tilde{\theta}_n)_{i_1 \dots i_n} = 0$$

whenever $\tilde{\theta}_k = \tilde{\theta}_l$ and $i_k = i_l$ for some k and l .

2.2.2 Generic form factors without disconnected pieces

Using the crossing formula (2.2), eqn. (2.17) allows us to construct the general form factor functions (2.1) in finite volume as follows:

$$\begin{aligned} & {}_{j_1 \dots j_m} \langle \{I'_1, \dots, I'_m\} | \mathcal{O}(0, 0) | \{I_1, \dots, I_n\}_{i_1 \dots i_n, L} \rangle = \\ & \frac{F_{m+n}^{\mathcal{O}}(\tilde{\theta}'_m + i\pi, \dots, \tilde{\theta}'_1 + i\pi, \tilde{\theta}_1, \dots, \tilde{\theta}_n)_{j_m \dots j_1 i_1 \dots i_n}}{\sqrt{\rho_{i_1 \dots i_n}(\tilde{\theta}_1, \dots, \tilde{\theta}_n) \rho_{j_1 \dots j_m}(\tilde{\theta}'_1, \dots, \tilde{\theta}'_m)}} + O(e^{-\mu L}) \end{aligned} \quad (2.18)$$

provided that there are no rapidities that are common between the left and the right states i.e. the sets $\{\tilde{\theta}_1, \dots, \tilde{\theta}_n\}$ and $\{\tilde{\theta}'_1, \dots, \tilde{\theta}'_m\}$ are disjoint. The latter condition is necessary to eliminate disconnected pieces. The rapidities entering (2.18) are determined by the Bethe-Yang equations (1.13); due to the presence of the scattering terms containing the phase shift functions δ , equality of two quantum numbers I_k and I'_l does not mean that the two rapidities themselves are equal in finite volume L . It is easy to see that there are only two cases when exact equality of some rapidities can occur:

1. The two states are identical, i.e. $n = m$ and

$$\begin{aligned} \{j_1 \dots j_m\} &= \{i_1 \dots i_n\} \\ \{I'_1, \dots, I'_m\} &= \{I_1, \dots, I_n\} \end{aligned}$$

in which case all the rapidities are pairwise equal. The discussion of such matrix elements is presented in section 2.3.

2. Both states are parity symmetric states in the spin zero sector, i.e.

$$\begin{aligned} \{I_1, \dots, I_n\} &\equiv \{-I_n, \dots, -I_1\} \\ \{I'_1, \dots, I'_m\} &\equiv \{-I'_m, \dots, -I'_1\} \end{aligned}$$

and the particle species labels are also compatible with the symmetry, i.e. $i_{n+1-k} = i_k$ and $j_{m+1-k} = j_k$. Furthermore, both states must contain one (or possibly more, in a theory with more than one species) particle of quantum number 0, whose rapidity is then exactly 0 for any value of the volume L due to the symmetric assignment of quantum numbers. The discussion of such matrix elements is presented in section 2.4.

We stress that eqns. (2.16, 2.18) are exact to all orders of powers in $1/L$; we refer to the corrections non-analytic in $1/L$ (eventually decaying exponentially as indicated) as *residual finite size effects*, following the terminology introduced in [8].

We would like to remark, that similar arguments that led us to (2.18) were previously used to obtain the finite size dependence of kaon decay matrix elements by Lin et al. [53]. The idea of normalizing finite volume form factors with particle densities also appeared in [90]; however, they used the unsatisfactory free-theory densities.

2.2.3 Estimation of the residual finite size corrections

There are two sources of error terms which may contribute to (2.16):

- Finite size corrections to the correlator $\langle \mathcal{O}(\tau, 0) \mathcal{O}'(0, 0) \rangle_L$.

- Discretization errors introduced in (2.12).

Here we show, that both types of error terms behave as $\mathcal{O}(e^{-\mu L})$ where μ is some characteristic mass scale of the theory.

One can use Lüscher's finite volume expansion introduced in [4] to study finite size effects to the correlator. According to Lüscher's classification of finite volume Feynman graphs, the difference between the finite and infinite volume correlation function is given by contributions from graphs of nontrivial gauge class, i.e. graphs in which some propagator has a nonzero winding number around the cylinder. Such graphs always carry an exponential suppression factor in L , whose exponent can be determined by analyzing the singularities of the propagators and vertex functions entering the expressions. In a massive theory, all such singularities lie away from the real axis of the Mandelstam variables, and the one with the smallest imaginary part determines μ . It turns out that the value of μ is determined by the exact mass spectrum of the particles and also the bound state fusions between them [5, 64]. Therefore it is universal, which means that it is independent of the correlation function considered. In general $\mu \leq m$ where m is the lightest particle mass (the mass gap of the theory), because there are always corrections in which the lightest particle loops around the finite volume L , and so the mass shell pole of the corresponding exact propagator is always present. Contributions from such particle loops to the vacuum expectation value are evaluated in subsection 3.2 (for a graphical representation see figure 3.3), while an example of a finite volume correction corresponding to a bound state fusion (a so-called μ -term) is discussed in subsection 3.2.2 (figure 3.8). The μ -terms associated to scattering states and form factors are analyzed in chapter 4.

The estimation

$$\langle \mathcal{O}(\tau, 0) \mathcal{O}'(0) \rangle - \langle \mathcal{O}(\tau, 0) \mathcal{O}'(0) \rangle_L \sim O(e^{-\mu L}) \quad (2.19)$$

is in fact a pessimistic one. Making use of the Euclidean invariance of the theory and performing the rotation $(\tau, x) \rightarrow (-x, \tau)$, the finite-size effects in the relation above can be obtained by calculating finite temperature corrections to the correlations function with the temperature given by $T = 1/L$. In section 5.3 we consider such contributions; they are of order e^{-mL} , i.e. $\mu = m$ with m being the mass gap of the theory. The absence of correction terms with $\mu < m$ can also be explained by the fact, that it is impossible to draw a relevant finite volume diagram (possibly including a particle fusion) which would carry the suppression factor $e^{-\mu L}$.

Having discussed finite size effects to the the correlator, we now prove that the discretization procedure introduces error terms which behave as $e^{-\mu' L}$, where in fact $\mu' = \mu$.

Recall that the Poisson formula gives the discrete sum in terms of a Fourier transform: the leading term is the Fourier transform of the summand evaluated at wave number 0 (i.e. the integral) and the corrections are determined by the decay of the Fourier transform

at large wave numbers. The function we need to consider is

$$h(p_1, \dots, p_n) = \sum_{i_1 \dots i_n} \rho_{i_1 \dots i_n}(\theta_1, \dots, \theta_n)^{-1} F_n^{\mathcal{O}}(\theta_1, \theta_2, \dots, \theta_n)_{i_1 \dots i_n} F_n^{\mathcal{O}'}(\theta_1, \theta_2, \dots, \theta_n)_{i_1 \dots i_n}^+ \times \exp\left(-r \sum_{k=1}^n m_{i_k} \cosh \theta_k\right) \quad (2.20)$$

where $p_k = m_{i_k} \sinh \theta_k$ are the momentum variables. Due to the analyticity of the form factors for real rapidities, this function is analytic for physical (real) momenta, and together with all of its derivatives decays more rapidly than any power at infinity. Therefore its Fourier transform taken in the momentum variables has the same asymptotic property, i.e. it (and its derivatives) decay more rapidly than any power:

$$\tilde{h}(\kappa_1, \dots, \kappa_n) \sim e^{-\mu'|\kappa|}$$

for large κ . As a result, discretization introduces an error of order $e^{-\mu'L}$. The asymptotic exponent μ' of the Fourier transform can be generally determined by shifting the contour of the integral transform and is given by the position of the singularity closest to the real momentum domain (this is essentially the procedure that Lüscher uses in [4]). Singularities of the form factors are given by the same analytic structure as that of the amplitudes which determine the exponent μ in eqn. (2.8). Thus we find that $\mu' = \mu$.

This argument is just an intuitive reasoning, although it can be made a little more precise. First of all, we must examine whether the determinant $\rho_{i_1 \dots i_n}(\theta_1, \dots, \theta_n)$ can have any zeros. It can always be written in the form

$$\rho_{i_1 \dots i_n}(\theta_1, \dots, \theta_n) = \left(\prod_{k=1}^n m_{i_k} L \cosh \theta_k \right) (1 + O(1/L))$$

The leading factor can only be zero when $\theta_k = \frac{i\pi}{2}$ for some k , which corresponds to $p_k = im_k$, giving $\mu' = m_k$ in case this is the closest singularity. That gives a correction

$$e^{-m_k L}$$

which is the same as the contribution by an on-shell propagator wound around the finite volume, and such corrections are already included in the $e^{-\mu L}$ term of (2.8). Another possibility is that some phase-shift function $\delta(\theta)$ in the $O(1/L)$ terms contributes a large term, which balances the $1/L$ pre-factor. For that its argument must be close to a singularity, and then according to eqn. (1.6) we can write

$$\delta(\theta) \sim \log(\theta - u) \sim O(L)$$

where u is the position of the singularity in the phase-shift. This requires that the singularity is approached exponentially close (as a function of the volume L), but the positions

of all these singularities are again determined by singularities of the vertex functions, so this gives no new possibilities for the exponent μ' .

A further issue that can be easily checked is whether the Fourier integral is convergent for large momenta; the function (2.20) is cut off at the infinities by the factor

$$\prod_{k=1}^n \exp(-m_{i_k} r \cosh \theta_k)$$

which can only go wrong if for some k

$$\Re \cosh \theta_k < 0$$

but that requires

$$\Im \theta_k > \frac{\pi}{2}$$

which is already farther from the real momentum domain than the position of the on-shell propagator singularity.

2.2.4 Comparison with an exact result

As far as we know, the only exact result in the literature was obtained in [45] and independently in [43, 44], where the authors considered the finite volume form factors of the spin-field operator σ in the Ising-model at zero external field. Although the model in question is a free theory (it can be described in terms of free massive Majorana fermions), it is interesting to compare the results with the general rule presented in the previous subsections. On one hand, this confirms our calculations. On the other hand, it might be used in further work as a starting point to study sub-leading exponential corrections (for the leading term, see section 4.3).

The Hilbert space of the theory consists of two sectors: the Neveu-Schwarz (NS) and the Ramond (R) sectors. The fermionic fields are antiperiodic or periodic, respectively, leading to the quantization rule for the particle momenta

$$p = m \sinh(\theta) = \frac{2\pi}{L} k \quad k \in \mathbb{N} + \frac{1}{2} \quad (\text{NS}) \quad (2.21)$$

$$p = m \sinh(\theta) = \frac{2\pi}{L} n \quad n \in \mathbb{N} \quad (\text{R}) \quad (2.22)$$

Multi-particle states are denoted by

$$|k_1, \dots, k_N\rangle_{\text{NS}} \quad \text{and} \quad |n_1, \dots, n_N\rangle_{\text{R}}$$

for states of the NS and R sectors, respectively. For simplicity we only consider the $T > T_c$ phase of the theory, where spin-flip symmetry is unbroken. In this phase the allowed excitations have an even number of particles in both the NS and R sectors.

The spin operator has non-vanishing matrix elements only between states of different sectors. The result for a generic finite volume matrix element reads (eq. 2.12 in [45])

$$\begin{aligned} \text{NS} \langle k_1, k_2, \dots, k_K | \sigma(0, 0) | n_1, n_2, \dots, n_N \rangle_{\text{R}} = \\ S(L) \prod_{j=1}^K \tilde{g}(\theta_{k_j}) \prod_{i=1}^N g(\theta_{n_i}) F_{K,N}(\theta_{k_1}, \dots, \theta_{k_K} | \theta_{n_1}, \dots, \theta_{n_N}), \end{aligned} \quad (2.23)$$

where θ_n (θ_k) stand for the finite-size rapidities related to the integers n (half-integers k) by the equations (2.21)-(2.22). $F_{K,N}$ is the spin-field form factor in infinite-space [88]; the explicit form of this function is not needed for the present purposes. The overall factor $S(L)$ is given by

$$S(L) = \exp \left\{ \frac{(mL)^2}{2} \iint_{-\infty}^{\infty} \frac{d\theta_1 d\theta_2}{(2\pi)^2} \frac{\sinh \theta_1 \sinh \theta_2}{\sinh(mL \cosh \theta_1) \sinh(mL \cosh \theta_2)} \log \left| \coth \frac{\theta_1 - \theta_2}{2} \right| \right\} \quad (2.24)$$

The momentum-dependent leg factors g and \tilde{g} are

$$g(\theta) = e^{\kappa(\theta)} / \sqrt{mL \cosh \theta}, \quad \tilde{g}(\theta) = e^{-\kappa(\theta)} / \sqrt{mL \cosh \theta} \quad (2.25)$$

where

$$\kappa(\theta) = \int_{-\infty}^{\infty} \frac{d\theta'}{2\pi} \frac{1}{\cosh(\theta - \theta')} \log \left(\frac{1 - e^{-mL \cosh \theta'}}{1 + e^{-mL \cosh \theta'}} \right) \quad (2.26)$$

It is straightforward to show, that the exact result (2.23) coincides with our formula (2.18) to all orders in $1/L$; the error terms are of order e^{-mL} . First of all, the normalization factor $S(L)$ does not depend on the form factor in question and for large L its behaviour is given by

$$S(L) \approx 1 + \mathcal{O}(e^{-2mL})$$

The function $\kappa(\theta)$ decays exponentially with L , therefore one has

$$g(\theta) = \frac{1}{\sqrt{\rho_1(\theta)}} + \mathcal{O}(e^{-mL}) \quad \tilde{g}(\theta) = \frac{1}{\sqrt{\rho_1(\theta)}} + \mathcal{O}(e^{-mL})$$

where $\rho_1(\theta) = EL = m \cosh(\theta)L$ is the one-particle density derived from eqs. (2.21)-(2.22). Being a free theory, the products of one-particle densities equals the multi-particle densities entering (2.18) and one has indeed

$$\begin{aligned} \text{NS} \langle k_1, k_2, \dots, k_K | \sigma(0, 0) | n_1, n_2, \dots, n_N \rangle_{\text{R}} \\ = \frac{F_{K,N}(\theta_{k_1}, \dots, \theta_{k_K} | \theta_{n_1}, \dots, \theta_{n_N})}{\sqrt{\rho_K(\theta_{k_1}, \dots, \theta_{k_K}) \rho_N(\theta_{n_1}, \dots, \theta_{n_N})}} + \mathcal{O}(e^{-mL}) \end{aligned}$$

It was shown in 2.2.3 the leading correction term to (2.18) is at most of order $e^{-\mu L}$ where $\mu \leq m$ with m being the mass of the lightest particle. In chapter 4 we show that the leading term (the μ -term) is connected with the inner structure of the particles under

the bootstrap procedure. In fact, in most theories $\mu < m$, whereas in the present case the leading exponential correction is only of order e^{-mL} . The reason for this is simple: the model in question is a free theory, there are no particle fusions. Therefore in this case there is no μ -term present.

2.3 Diagonal matrix elements

In this section we consider diagonal matrix elements of the form

$${}_{i_1 \dots i_n} \langle \{I_1 \dots I_n\} | \Psi | \{I_1 \dots I_n\} \rangle_{i_1 \dots i_n, L}$$

First we derive the first two ($n = 1$ and $n = 2$) cases using form factor perturbation theory [91]. Built on these rigorous results we conjecture the general formula in 2.3.2.

Two additional subsections are devoted to the discussion of our results. In 2.3.3 we examine the connection between two evaluation methods of the infinite volume diagonal form factors. In 2.3.4 we prove that a conjecture made by Saleur in [31] exactly coincides with ours.

2.3.1 Form factor perturbation theory and disconnected contributions

In the framework of conformal perturbation theory, we consider a model with the action

$$\mathcal{A}(\mu, \lambda) = \mathcal{A}_{\text{CFT}} - \mu \int dt dx \Phi(t, x) - \lambda \int dt dx \Psi(t, x) \quad (2.27)$$

such that in the absence of the coupling λ , the model defined by the action $\mathcal{A}(\mu, \lambda = 0)$ is integrable. The two perturbing fields are taken as scaling fields of the ultraviolet limiting conformal field theory, with left/right conformal weights $h_\Phi = \bar{h}_\Phi < 1$ and $h_\Psi = \bar{h}_\Psi < 1$, i.e. they are relevant and have zero conformal spin, resulting in a Lorentz-invariant field theory.

The integrable limit $\mathcal{A}(\mu, \lambda = 0)$ is supposed to define a massive spectrum, with the scale set by the dimensionful coupling μ . The exact spectrum in this case consists of massive particles, forming a factorized scattering theory with known S matrix amplitudes, and characterized by a mass scale M (which we take as the mass of the fundamental particle generating the bootstrap), which is related to the coupling μ via the mass gap relation

$$\mu = \kappa M^{2-2h_\Phi}$$

where κ is a (non-perturbative) dimensionless constant.

Switching on a second independent coupling λ in general spoils integrability, deforms the mass spectrum and the S matrix, and in particular allows decay of the particles which

are stable at the integrable point. One way to approach the dynamics of the model is the form factor perturbation theory proposed in [91]. Let us denote the form factors of the operator Ψ in the $\lambda = 0$ theory by

$$F_n^\Psi(\theta_1, \dots, \theta_n)_{i_1 \dots i_n} = \langle 0 | \Psi(0, 0) | \theta_1 \dots \theta_n \rangle_{i_1 \dots i_n}^{\lambda=0}$$

Using perturbation theory to first order in λ , the following quantities can be calculated [91]:

1. The vacuum energy density is shifted by an amount

$$\delta \mathcal{E}_{vac} = \lambda \langle 0 | \Psi | 0 \rangle_{\lambda=0}. \quad (2.28)$$

2. The mass (squared) matrix M_{ab}^2 gets a correction

$$\delta M_{ab}^2 = 2\lambda F_2^\Psi(i\pi, 0)_{a\bar{b}} \delta_{m_a, m_b} \quad (2.29)$$

(where the bar denotes the antiparticle) supposing that the original mass matrix was diagonal and of the form $M_{ab}^2 = m_a^2 \delta_{ab}$.

3. The scattering amplitude for the four particle process $a + b \rightarrow c + d$ is modified by

$$\delta S_{ab}^{cd}(\theta, \lambda) = -i\lambda \frac{F_4^\Psi(i\pi, \theta + i\pi, 0, \theta)_{\bar{c}\bar{d}ab}}{m_a m_b \sinh \theta}, \quad \theta = \theta_a - \theta_b. \quad (2.30)$$

It is important to stress that the form factor amplitude in the above expression must be defined as the so-called ‘‘symmetric’’ evaluation

$$\lim_{\epsilon \rightarrow 0} F_4^\Psi(i\pi + \epsilon, \theta + i\pi + \epsilon, 0, \theta)_{\bar{c}\bar{d}ab}$$

(see eqn. (2.35) below). It is also necessary to keep in mind that eqn. (2.30) gives the variation of the scattering phase when the center-of-mass energy (or, the Mandelstam variable s) is kept fixed [91]. Therefore, in terms of rapidity variables, this variation corresponds to the following:

$$\delta S_{ab}^{cd}(\theta, \lambda) = \frac{\partial S_{ab}^{cd}(\theta, \lambda = 0)}{\partial \theta} \delta \theta + \lambda \left. \frac{\partial S_{ab}^{cd}(\theta, \lambda)}{\partial \lambda} \right|_{\lambda=0}$$

where

$$\delta \theta = - \frac{m_a \delta m_a + m_a \delta m_a + (m_b \delta m_a + m_a \delta m_b) \cosh \theta}{m_a m_b \sinh \theta}$$

is the shift of the rapidity variable induced by the mass corrections given by eqn. (2.29).

It is also possible to calculate the (partial) decay width of particles [92], but we do not need it here.

We can use the above results to calculate diagonal matrix elements involving one particle. For simplicity we present the derivation for a theory with a single particle species. Let us start with the one-particle case. The variation of the energy of a stationary one-particle state with respect to the vacuum (i.e. the finite volume particle mass) can be expressed as the difference between the first order perturbative results for the one-particle and vacuum states in volume L :

$$\Delta m(L) = \lambda L (\langle \{0\} | \Psi | \{0\} \rangle_L - \langle 0 | \Psi | 0 \rangle_L) \quad (2.31)$$

On the other hand, using Lüscher's results [5] it only differs from the infinite volume mass in terms exponentially falling with L . Using eqn. (2.29)

$$\Delta m(L) = \frac{\lambda}{m} F^\Psi(i\pi, 0) + O(e^{-\mu L})$$

Similarly, the vacuum expectation value receives only corrections falling off exponentially with L . Therefore we obtain

$$\langle \{0\} | \Psi | \{0\} \rangle_L = \frac{1}{mL} (F^\Psi(i\pi, 0) + mL \langle 0 | \Psi | 0 \rangle) + \dots$$

with the ellipsis denoting residual finite size corrections. Note that the factor mL is just the one-particle Bethe-Yang Jacobian $\rho_1(\theta) = mL \cosh \theta$ evaluated for a stationary particle $\theta = 0$.

We can extend the above result to moving particles in the following way. Up to residual finite size corrections, the one-particle energy is given by

$$E(L) = \sqrt{m^2 + p^2}$$

with

$$p = \frac{2\pi I}{L}$$

where I is the Lorentz spin (which is identical to the particle momentum quantum number). Therefore

$$E \Delta E = m \Delta m$$

whereas perturbation theory gives:

$$\Delta E = \lambda L (\langle \{I\} | \Psi | \{I\} \rangle_L - \langle 0 | \Psi | 0 \rangle_L)$$

and so we obtain

$$\langle \{I\} | \Psi | \{I\} \rangle_L = \frac{1}{\rho_1(\tilde{\theta})} \left(F^\Psi(i\pi, 0) + \rho_1(\tilde{\theta}) \langle 0 | \Psi | 0 \rangle \right) + \dots \quad (2.32)$$

where

$$\sinh \tilde{\theta} = \frac{2\pi I}{mL} \Rightarrow \rho_1(\tilde{\theta}) = \sqrt{m^2 L^2 + 4\pi^2 I^2}$$

One can use a similar argument to evaluate diagonal two-particle matrix elements in finite volume. The energy levels can be calculated from the relevant Bethe-Yang equations

$$\begin{aligned} m_{i_1} L \sinh \tilde{\theta}_1 + \delta(\tilde{\theta}_1 - \tilde{\theta}_2) &= 2\pi I_1 \\ m_{i_2} L \sinh \tilde{\theta}_2 + \delta(\tilde{\theta}_2 - \tilde{\theta}_1) &= 2\pi I_2 \end{aligned}$$

and (up to residual finite size corrections)

$$E_2(L) = E_{2pt}(L) - E_0(L) = m_{i_1} \cosh \tilde{\theta}_1 + m_{i_2} \cosh \tilde{\theta}_2$$

where i_1 and i_2 label the particle species. After a somewhat tedious, but elementary calculation the variation of this energy difference with respect to λ can be determined, using (2.29) and (2.30):

$$\begin{aligned} \Delta E_2(L) &= \lambda \frac{L}{\rho_{i_1 i_2}(\tilde{\theta}_1, \tilde{\theta}_2)} \left(F_4^\Psi(\tilde{\theta}_2 + i\pi, \tilde{\theta}_1 + i\pi, \tilde{\theta}_1, \tilde{\theta}_2) \right)_{i_2 i_1 i_1 i_2} + m_{i_1} L \cosh \tilde{\theta}_1 F_2^\Psi(i\pi, 0)_{i_2 i_2} \\ &\quad + m_{i_2} L \cosh \tilde{\theta}_2 F_2^\Psi(i\pi, 0)_{i_1 i_1} \end{aligned}$$

where all quantities (such as Bethe-Yang rapidities $\tilde{\theta}_i$, masses m_i and the two-particle state density ρ_2) are in terms of the $\lambda = 0$ theory. This result expresses the fact that there are two sources for the variation of two-particle energy levels: one is the mass shift of the individual particles, and the second is due to the variation in the interaction. On the other hand, in analogy with (2.31) we have

$$\Delta E_2(L) = \lambda L ({}_{i_1 i_2} \langle \{I_1, I_2\} | \Psi | \{I_1, I_2\} \rangle_{i_1 i_2, L} - \langle 0 | \Psi | 0 \rangle_L)$$

and so we obtain the following relation:

$$\begin{aligned} {}_{i_1 i_2} \langle \{I_1, I_2\} | \Psi | \{I_1, I_2\} \rangle_{i_1 i_2, L} &= \frac{1}{\rho_{i_1 i_2}(\tilde{\theta}_1, \tilde{\theta}_2)} \left(F_4^\Psi(\tilde{\theta}_2 + i\pi, \tilde{\theta}_1 + i\pi, \tilde{\theta}_1, \tilde{\theta}_2) \right)_{i_2 i_1 i_1 i_2} \\ &\quad + m_{i_1} L \cosh \tilde{\theta}_1 F_2^\Psi(i\pi, 0)_{i_2 i_2} \\ &\quad + m_{i_2} L \cosh \tilde{\theta}_2 F_2^\Psi(i\pi, 0)_{i_1 i_1} + \langle 0 | \Psi | 0 \rangle + \dots \end{aligned} \quad (2.33)$$

where the ellipsis again indicate residual finite size effects. The above argument is a generalization of the derivation of the mini-Hamiltonian coefficient C in Appendix C of [8].

We wish to remark that the result (2.33) extends to two-particle states in non-integrable models below the inelastic threshold, as the Bethe-Yang equations remain valid in this case [5].

2.3.2 Generalization to higher number of particles

Let us now introduce some more convenient notations. Given a state

$$|\{I_1 \dots I_n\}\rangle_{i_1 \dots i_n}$$

we denote

$$\rho(\{k_1, \dots, k_r\})_L = \rho_{i_{k_1} \dots i_{k_r}}(\tilde{\theta}_{k_1}, \dots, \tilde{\theta}_{k_r}) \quad (2.34)$$

where $\tilde{\theta}_l$, $l = 1, \dots, n$ are the solutions of the n -particle Bethe-Yang equations (2.11) at volume L with quantum numbers I_1, \dots, I_n and $\rho(\{k_1, \dots, k_r\}, L)$ is the r -particle Bethe-Yang Jacobi determinant (2.15) involving only the r -element subset $1 \leq k_1 < \dots < k_r \leq n$ of the n particles, evaluated with rapidities $\tilde{\theta}_{k_1}, \dots, \tilde{\theta}_{k_r}$. Let us further denote

$$\mathcal{F}(\{k_1, \dots, k_r\})_L = F_{2r}^s(\tilde{\theta}_{k_1}, \dots, \tilde{\theta}_{k_r})_{i_{k_1} \dots i_{k_r}}$$

where

$$F_{2n}^s(\theta_1, \dots, \theta_n)_{i_1 \dots i_n} = \lim_{\epsilon \rightarrow 0} F_{2n}^\Psi(\theta_n + i\pi + \epsilon, \dots, \theta_1 + i\pi + \epsilon, \theta_1, \dots, \theta_n)_{i_1 \dots i_n i_n \dots i_1} \quad (2.35)$$

is the so-called symmetric evaluation of diagonal n -particle matrix elements, which we analyze more closely in the next subsection. Note that the exclusion property mentioned at the end of subsection 2.1 carries over to the symmetric evaluation too: (2.35) vanishes whenever the rapidities of two particles of the same species coincide.

Based on the above results, we conjecture that the general rule for a diagonal matrix element takes the form of a sum over all bipartite divisions of the set of the n particles involved (including the trivial ones when A is the empty set or the complete set $\{1, \dots, n\}$):

$$i_1 \dots i_n \langle \{I_1 \dots I_n\} | \Psi | \{I_1 \dots I_n\} \rangle_{i_1 \dots i_n, L} = \frac{1}{\rho(\{1, \dots, n\})_L} \times \sum_{A \subset \{1, 2, \dots, n\}} \mathcal{F}(A)_L \rho(\{1, \dots, n\} \setminus A)_L + O(e^{-\mu L}) \quad (2.36)$$

2.3.3 Diagonal matrix elements in terms of connected form factors

Here we discuss diagonal matrix elements in terms of connected form factors. The results will be used in the following subsection to prove that a conjecture made by Saleur in [31] exactly coincides with our eqn. (2.36). To simplify notations we omit the particle species labels; they can be restored easily if needed.

Relation between connected and symmetric matrix elements

The purpose of this discussion is to give a treatment of the ambiguity inherent in diagonal matrix elements. Due to the existence of kinematical poles (2.5) the expression

$$F_{2n}(\theta_1 + i\pi, \theta_2 + i\pi, \dots, \theta_n + i\pi, \theta_n, \dots, \theta_2, \theta_1)$$

which is relevant for diagonal multi-particle matrix elements, is not well-defined. Let us consider the regularized version

$$F_{2n}(\theta_1 + i\pi + \epsilon_1, \theta_2 + i\pi + \epsilon_2, \dots, \theta_n + i\pi + \epsilon_n, \theta_n, \dots, \theta_2, \theta_1)$$

It was first observed in [91] that the singular parts of this expression drop when taking the limits $\epsilon_i \rightarrow 0$ simultaneously; however, the end result depends on the direction of the limit, i.e. on the ratio of the ϵ_i parameters. The terms that are relevant in the limit can be written in the following general form:

$$F_{2n}(\theta_1 + i\pi + \epsilon_1, \theta_2 + i\pi + \epsilon_2, \dots, \theta_n + i\pi + \epsilon_n, \theta_n, \dots, \theta_2, \theta_1) = \quad (2.37)$$

$$\prod_{i=1}^n \frac{1}{\epsilon_i} \cdot \sum_{i_1=1}^n \sum_{i_2=1}^n \dots \sum_{i_n=1}^n a_{i_1 i_2 \dots i_n}(\theta_1, \dots, \theta_n) \epsilon_{i_1} \epsilon_{i_2} \dots \epsilon_{i_n} + \dots$$

where $a_{i_1 i_2 \dots i_n}$ is a completely symmetric tensor of rank n and the ellipsis denote terms that vanish when taking $\epsilon_i \rightarrow 0$ simultaneously.

In our previous considerations we used the symmetric limit, which is defined by taking all ϵ_i equal:

$$F_{2n}^s(\theta_1, \theta_2, \dots, \theta_n) = \lim_{\epsilon \rightarrow 0} F_{2n}(\theta_1 + i\pi + \epsilon, \theta_2 + i\pi + \epsilon, \dots, \theta_n + i\pi + \epsilon, \theta_n, \dots, \theta_2, \theta_1)$$

It is symmetric in all the variables $\theta_1, \dots, \theta_n$. There is another evaluation with this symmetry property, namely the so-called connected form factor, which is defined as the ϵ_i independent part of eqn. (2.37), i.e. the part which does not diverge whenever any of the ϵ_i is taken to zero:

$$F_{2n}^c(\theta_1, \theta_2, \dots, \theta_n) = n! a_{12\dots n} \quad (2.38)$$

where the appearance of the factor $n!$ is simply due to the permutations of the ϵ_i .

The relation for $n \leq 3$

We now spell out the relation between the symmetric and connected evaluations for $n = 1, 2$ and 3 .

The $n = 1$ case is simple, since the two-particle form factor $F_2(\theta_1, \theta_2)$ has no singularities at $\theta_1 = \theta_2 + i\pi$ and therefore

$$F_2^s(\theta) = F_2^c(\theta) = F_2(i\pi, 0) \quad (2.39)$$

It is independent of the rapidities and will be denoted F_2^c in the sequel.

For $n = 2$ we need to consider

$$F_4(\theta_1 + i\pi + \epsilon_1, \theta_2 + i\pi + \epsilon_2, \theta_2, \theta_1) \approx \frac{a_{11}\epsilon_1^2 + 2a_{12}\epsilon_1\epsilon_2 + a_{22}\epsilon_2^2}{\epsilon_1\epsilon_2} \quad (2.40)$$

which gives

$$\begin{aligned} F_4^s(\theta_1, \theta_2) &= a_{11} + 2a_{12} + a_{22} \\ F_4^c(\theta_1, \theta_2) &= 2a_{12} \end{aligned}$$

The terms a_{11} and a_{22} can be expressed using the two-particle form factor. Taking an infinitesimal, but fixed $\epsilon_2 \neq 0$

$$\text{Res}_{\epsilon_1=0} F_4(\theta_1 + i\pi + \epsilon_1, \theta_2 + i\pi + \epsilon_2, \theta_2, \theta_1) = a_{22}\epsilon_2$$

whereas according to (2.6)

$$\text{Res}_{\epsilon_1=0} F_4(\theta_1 + i\pi + \epsilon_1, \theta_2 + i\pi + \epsilon_2, \theta_2, \theta_1) = i(1 - S(\theta_1 - \theta_2)S(\theta_1 - \theta_2 - i\pi - \epsilon_2)) F_2(\theta_2 + i\pi + \epsilon_2, \theta_2)$$

To first order in ϵ_2

$$S(\theta_1 - \theta_2 - i\pi - \epsilon_2) = S(\theta_2 - \theta_1 + \epsilon_2) = S(\theta_2 - \theta_1)(1 + i\varphi(\theta_2 - \theta_1)\epsilon_2 + \dots)$$

where

$$\varphi(\theta) = -i \frac{d}{d\theta} \log S(\theta)$$

is the derivative of the two-particle phase shift defined before. Therefore we obtain

$$a_{22} = \varphi(\theta_2 - \theta_1) F_2^c$$

and similarly

$$a_{11} = \varphi(\theta_1 - \theta_2) F_2^c$$

and so

$$F_4^s(\theta_1, \theta_2) = F_4^c(\theta_1, \theta_2) + 2\varphi(\theta_1 - \theta_2) F_2(i\pi, 0) \quad (2.41)$$

In the case of the trace of the energy-momentum tensor Θ the following expressions are known [34]

$$\begin{aligned} F_2^\Theta &= 2\pi m^2 \\ F_4^{\Theta,s} &= 8\pi m^2 \varphi(\theta_1 - \theta_2) \cosh^2 \left(\frac{\theta_1 - \theta_2}{2} \right) \\ F_4^{\Theta,c} &= 4\pi m^2 \varphi(\theta_1 - \theta_2) \cosh(\theta_1 - \theta_2) \end{aligned}$$

and they are in agreement with (2.41).

For $n = 3$, a procedure similar to the above gives the following relation:

$$\begin{aligned} F_6^s(\theta_1, \theta_2, \theta_3) &= F_6^c(\theta_1, \theta_2, \theta_3) + [F_4^c(\theta_1, \theta_2)(\varphi(\theta_1 - \theta_3) + \varphi(\theta_2 - \theta_3)) + \text{permutations}] \\ &\quad + 3F_2^c[\varphi(\theta_1 - \theta_2)\varphi(\theta_1 - \theta_3) + \text{permutations}] \end{aligned} \quad (2.42)$$

where we omitted terms that only differ by permutation of the particles.

Relation between the connected and symmetric evaluation in the general case

Our goal is to compute the general expression

$$F_{2n}(\theta_1, \dots, \theta_n | \epsilon_1, \dots, \epsilon_n) = F_{2n}(\theta_1 + i\pi + \epsilon_1, \theta_2 + i\pi + \epsilon_2, \dots, \theta_n + i\pi + \epsilon_n, \theta_n, \dots, \theta_2, \theta_1) \quad (2.43)$$

Let us take n vertices labeled by the numbers $1, 2, \dots, n$ and let G be the set of the directed graphs G_i with the following properties:

- G_i is tree-like.
- For each vertex there is at most one outgoing edge.

For an edge going from i to j we use the notation E_{ij} .

Theorem 1 (2.43) can be evaluated as a sum over all graphs in G , where the contribution of a graph G_i is given by the following two rules:

- Let $A_i = \{a_1, a_2, \dots, a_m\}$ be the set of vertices from which there are no outgoing edges in G_i . The form factor associated to G_i is

$$F_{2m}^c(\theta_{a_1}, \theta_{a_2}, \dots, \theta_{a_m}) \quad (2.44)$$

- For each edge E_{jk} the form factor above has to be multiplied by

$$\frac{\epsilon_j}{\epsilon_k} \varphi(\theta_j - \theta_k)$$

Note that since cannot contain cycles, the product of the ϵ_i/ϵ_j factors will never be trivial (except for the empty graph with no edges).

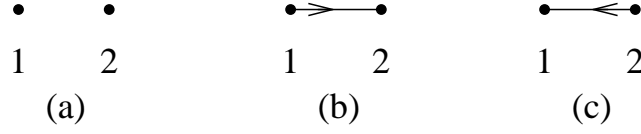
Proof The proof goes by induction in n . For $n = 1$ we have

$$F_2^s(\theta_1) = F_2^c(\theta_1) = F_2(i\pi, 0)$$

This is in accordance with the theorem, because for $n = 1$ there is only the trivial graph which contains no edges and a single node.

Now assume that the theorem is true for $n - 1$ and let us take the case of n particles. Consider the residue of the matrix element (2.43) at $\epsilon_n = 0$ while keeping all the ϵ_i finite

$$R = \operatorname{Res}_{\epsilon_n=0} F_{2n}(\theta_1 \dots \theta_n | \epsilon_1 \dots \epsilon_n)$$

Figure 2.1: The graphs relevant for $n = 2$

According to the theorem the graphs contributing to this residue are exactly those for which the vertex n has an outgoing edge and no incoming edges. Let R_j be sum of the diagrams where the outgoing edge is E_{nj} for some $j = 1, \dots, n - 1$, and so

$$R = \sum_{j=1}^{n-1} R_j$$

The form factors appearing in R_j do not depend on θ_n . Therefore we get exactly the diagrams that are needed to evaluate $F_{2(n-1)}(\theta_1 \dots \theta_{n-1} | \epsilon_1 \dots \epsilon_{n-1})$, apart from the proportionality factor associated to the link E_{nj} and so

$$R_j = \frac{\epsilon_j}{\epsilon_n} \varphi(\theta_j - \theta_n) F_{2(n-1)}(\theta_1 \dots \theta_{n-1} | \epsilon_1 \dots \epsilon_{n-1})$$

and summing over j gives

$$R = (\epsilon_1 \varphi(\theta_1 - \theta_n) + \epsilon_2 \varphi(\theta_2 - \theta_n) + \dots + \epsilon_{n-1} \varphi(\theta_{n-1} - \theta_n)) F_{2(n-1)}(\theta_1 \dots \theta_{n-1} | \epsilon_1 \dots \epsilon_{n-1}) \quad (2.45)$$

In order to prove the theorem, we only need to show that the residue indeed takes this form. On the other hand, the kinematical residue axiom (2.5) gives

$$R = i \left(1 - \prod_{j=1}^{n-1} S(\theta_n - \theta_j) S(\theta_n - \theta_j - i\pi - \epsilon_j) \right) F_{2(n-1)}(\theta_1 \dots \theta_{n-1} | \epsilon_1 \dots \epsilon_{n-1})$$

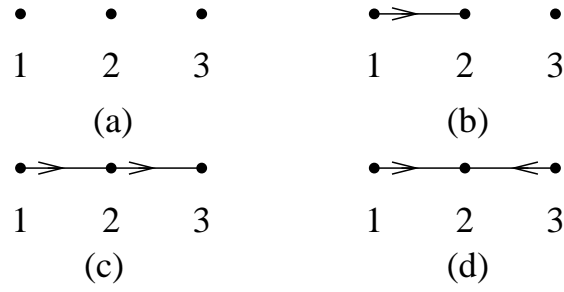
which is exactly the same as eqn. (2.45) when expanded to first order in ϵ_j .

We thus checked that the theorem gives the correct result for the terms that include a $1/\epsilon_n$ singularity. Using symmetry in the rapidity variables this is true for all the terms that include at least one $1/\epsilon_i$ for an arbitrary i . There is only one diagram that cannot be generated by the inductive procedure, namely the empty graph. However, there are no singularities ($1/\epsilon_i$ factors) associated to it, and it gives $F_{2n}^c(\theta_1, \dots, \theta_n)$ by definition. *Qed.*

We now illustrate how the theorem works. For $n = 2$, there are only three graphs, depicted in figure 2.1. Applying the rules yields

$$F_4(\theta_1, \theta_2 | \epsilon_1, \epsilon_2) = F_4^c(\theta_1, \theta_2) + \varphi(\theta_1 - \theta_2) \left(\frac{\epsilon_1}{\epsilon_2} + \frac{\epsilon_2}{\epsilon_1} \right) F_2^c$$

which gives back (2.41) upon putting $\epsilon_1 = \epsilon_2$. For $n = 3$ there are 4 different kinds of graphs, the representatives of which are shown in figure 2.2; all other graphs can be obtained by permuting the node labels 1, 2, 3. The contributions of these graphs are

Figure 2.2: The graphs relevant for $n = 3$

$$\begin{aligned}
(a) & : F_6^c(\theta_1, \theta_2, \theta_3) \\
(b) & : \frac{\epsilon_2}{\epsilon_1} \varphi(\theta_1 - \theta_2) F_4^c(\theta_2, \theta_3) \\
(c) & : \frac{\epsilon_2 \epsilon_3}{\epsilon_1 \epsilon_2} \varphi(\theta_1 - \theta_2) \varphi(\theta_2 - \theta_3) F_2^c = \frac{\epsilon_3}{\epsilon_1} \varphi(\theta_1 - \theta_2) \varphi(\theta_2 - \theta_3) F_2^c \\
(d) & : \frac{\epsilon_2 \epsilon_2}{\epsilon_1 \epsilon_3} \varphi(\theta_1 - \theta_2) \varphi(\theta_3 - \theta_2) F_2^c
\end{aligned}$$

Adding up all the contributions and putting $\epsilon_1 = \epsilon_2 = \epsilon_3$ we recover eqn. (2.42).

2.3.4 Consistency with Saleur's proposal

Saleur proposed an expression for diagonal matrix elements in terms of connected form factors in [31], which is partially based on earlier work by Balog [93] and also on the determinant formula for normalization of states in the framework of algebraic Bethe Ansatz, derived by Gaudin, and also by Korepin (see [94] and references therein). To describe it, we must extend the normalization of finite volume states defined previously to the case when the particle rapidities form a proper subset of some multi-particle Bethe-Yang solution.

It was shown in subsection 2.2.2 that the normalization of a finite volume state is given by

$$|\{I_1, \dots, I_n\}\rangle_L = \frac{1}{\sqrt{\rho_n(\tilde{\theta}_1, \dots, \tilde{\theta}_n)}} |\tilde{\theta}_1, \dots, \tilde{\theta}_n\rangle$$

We again omit the particle species labels, and also denote the n -particle determinant by ρ_n . Let us take a subset of particle indices $A \in \{1, \dots, n\}$ and define the corresponding sub-determinant by

$$\tilde{\rho}_n(\tilde{\theta}_1, \dots, \tilde{\theta}_n|A) = \det \mathcal{J}_A^{(n)}$$

where $\mathcal{J}_A^{(n)}$ is the sub-matrix of the matrix $\mathcal{J}^{(n)}$ defined in eqn. (2.15) which is given by choosing the elements whose indices belong to A . The full matrix can be written explicitly

as

$$\mathcal{J}^{(n)} = \begin{pmatrix} E_1 L + \varphi_{12} + \cdots + \varphi_{1n} & -\varphi_{12} & \cdots & -\varphi_{1n} \\ -\varphi_{12} & E_2 L + \varphi_{21} + \varphi_{23} + \cdots + \varphi_{2n} & \cdots & -\varphi_{2n} \\ \vdots & \vdots & \ddots & \vdots \\ -\varphi_{1n} & -\varphi_{2n} & \cdots & E_n L + \varphi_{1n} + \cdots + \varphi_{n-1,n} \end{pmatrix}$$

where the following abbreviations were used: $E_i = m_i \cosh \theta_i$, $\varphi_{ij} = \varphi_{ji} = \varphi(\theta_i - \theta_j)$. Note that $\tilde{\rho}_n$ depends on all the rapidities, not just those which correspond to elements of A . It is obvious that

$$\rho_n(\tilde{\theta}_1, \dots, \tilde{\theta}_n) \equiv \tilde{\rho}_n(\tilde{\theta}_1, \dots, \tilde{\theta}_n | \{1, \dots, n\})$$

Saleur proposed the definition

$$\langle \{\tilde{\theta}_k\}_{k \in A} | \{\tilde{\theta}_k\}_{k \in A} \rangle_L = \tilde{\rho}_n(\tilde{\theta}_1, \dots, \tilde{\theta}_n | A) \quad (2.46)$$

where

$$|\{\tilde{\theta}_k\}_{k \in A}\rangle_L$$

is a ‘‘partial state’’ which contains only the particles with index in A , but with rapidities that solve the Bethe-Yang equations for the full n -particle state. Note that this is not a proper state in the sense that it is not an eigenstate of the Hamiltonian since the particle rapidities do not solve the Bethe-Yang equations relevant for a state consisting of $|A|$ particles (where $|A|$ denotes the cardinal number – i.e. number of elements – of the set A). The idea behind this proposal is that the density of these partial states in rapidity space depends on the presence of the other particles which are not included, and indeed it is easy to see that it is given by $\tilde{\rho}_n(\tilde{\theta}_1, \dots, \tilde{\theta}_n | A)$.

In terms of the above definitions, Saleur’s conjecture for the diagonal matrix element is

$${}_{i_1 \dots i_n} \langle \{I_1 \dots I_n\} | \Psi | \{I_1 \dots I_n\} \rangle_{i_1 \dots i_n, L} = \frac{1}{\rho_n(\tilde{\theta}_1, \dots, \tilde{\theta}_n)} \times \sum_{A \subset \{1, 2, \dots, n\}} F_{2|A|}^c(\{\tilde{\theta}_k\}_{k \in A}) \tilde{\rho}(\tilde{\theta}_1, \dots, \tilde{\theta}_n | A) + O(e^{-\mu L}) \quad (2.47)$$

which is just the standard representation of the full matrix element as the sum of all the connected contributions provided we accept eqn. (2.46). The full amplitude is obtained by summing over all possible bipartite divisions of the particles, where the division is into particles that are connected to the local operator, giving the connected form factor F^c and into those that simply go directly from the initial to the final state which contribute the norm of the corresponding partial multi-particle state.

Using the results of the previous subsection, it is easy to check explicitly that our rule for the diagonal matrix elements as given in eqn. (2.36) is equivalent to eqn. (2.47). We now give a complete proof for the general case.

Theorem 2

$$\sum_{A \subset N} F_{2|A|}^c(\{\theta_k\}_{k \in A}) \tilde{\rho}(\theta_1, \dots, \theta_n | A) = \sum_{A \subset N} F_{2|A|}^s(\{\theta_k\}_{k \in A}) \rho(\{\theta_k\}_{k \in N \setminus A}) \quad (2.48)$$

where we denoted $N = \{1, 2, \dots, n\}$.

Proof The two sides of eqn. (2.48) differ in two ways:

- The form factors on the right hand side are evaluated according to the „symmetric” prescription, and in addition to the connected part also they contain extra terms, which are proportional to connected form factors with fewer particles.
- The densities $\tilde{\rho}$ on the left hand side are not determinants of the form (2.15) written down in terms of the particles contained in $N \setminus A$: they contain additional terms due to the presence of the particles in A as well.

Here we show that eqn. (2.48) is merely a reorganization of these terms.

For simplicity consider first the term on the left hand side which corresponds to $A = \{m+1, m+2, \dots, n\}$, i.e.

$$F_{2m}^c(\theta_{m+1}, \dots, \theta_n) \tilde{\rho}(\theta_1, \dots, \theta_n | A)$$

We expand $\tilde{\rho}$ in terms of the physical multi-particle densities ρ . In order to accomplish this, it is useful to rewrite the sub-matrix $\mathcal{J}_{N \setminus A}^n$ as

$$\mathcal{J}^{(n)}|_{N \setminus A} = \mathcal{J}^m(\theta_1, \dots, \theta_m) + \begin{pmatrix} \sum_{i=m+1}^n \varphi_{1i} & & & \\ & \sum_{i=m+1}^n \varphi_{2i} & & \\ & & \ddots & \\ & & & \sum_{i=m+1}^n \varphi_{mi} \end{pmatrix}$$

where \mathcal{J}^m is the m -particle Jacobian matrix which does not contain any terms depending on the particles in A . The determinant of $\mathcal{J}_{N \setminus A}^n$ can be written as a sum over the subsets of $N \setminus A$. For a general subset $B \subset N \setminus A$ let us use the notation $B = \{b_1, b_2, \dots, b_{|B|}\}$. We can then write

$$\tilde{\rho}(\theta_1, \dots, \theta_n | A) = \det \mathcal{J}^{(n)}|_{N \setminus A} = \sum_B \left[\rho(N \setminus (A \cup B)) \prod_{i=1}^{|B|} \left(\sum_{c_i=m+1}^n \varphi_{b_i, c_i} \right) \right] \quad (2.49)$$

where $\rho(N \setminus (A \cup B))$ is the ρ -density (2.15) written down with the particles in $N \setminus (A \cup B)$.

Applying a suitable permutation of variables we can generalize eqn. (2.49) to an arbitrary subset $A \subset N$:

$$\tilde{\rho}(\theta_1, \dots, \theta_n | A) = \det \mathcal{J}^{(n)}|_{N \setminus A} = \sum_B \rho(N \setminus (A \cup B)) \sum_C \left(\prod_{i=1}^{|B|} \varphi_{b_i, c_i} \right) \quad (2.50)$$

where the second summation goes over all the sets $C = \{c_1, c_2, \dots, c_{|B|}\}$ with $|C| = |B|$ and $c_i \in A$. The left hand side of eqn. (2.48) can thus be written as

$$\sum_{A \subset N} F_{2|A|}^c(\{\theta_k\}_{k \in A}) \tilde{\rho}(\theta_1, \dots, \theta_n | A) = \sum_{\substack{A, B \subset N \\ A \cap B = \emptyset}} \rho(N \setminus (A \cup B)) \sum_C F_{(A, B, C)} \quad (2.51)$$

$$\text{where} \quad F_{(A, B, C)} = F_{2|A|}^c(\{\theta_k\}_{k \in A}) \prod_{i=1}^{|B|} \varphi_{b_i, c_i}$$

We now show that there is a one-to-one correspondence between all the terms in (2.51) and those on the right hand side of (2.48) if the symmetric evaluations F_{2k}^s are expanded according to Theorem 1. To each triplet (A, B, C) let us assign the graph $G_{(A, B, C)}$ defined as follows:

- The vertices of the graph are the elements of the set $A \cup B$.
- There are exactly $|B|$ edges in the graph, which start at b_i and end at c_i with $i = 1, \dots, |B|$.

The contribution of $G_{(A, B, C)}$ to $F_{2(|A|+|B|)}^s(\{\theta_k\}_{k \in A \cup B})$ is nothing else than $F_{(A, B, C)}$ which can be proved by applying the rules of Theorem 1. Note that all the possible diagrams with at most n vertices are contained in the above list of the $G_{(A, B, C)}$, because a general graph G satisfying the conditions in Theorem 1 can be characterized by writing down the set of vertices with and without outgoing edges (in this case B and A) and the endpoints of the edges (in this case C).

It is easy to see that the factors $\rho(N \setminus (A \cup B))$ multiplying the $F_{(A, B, C)}$ in (2.51) are also the correct ones: they are just the density factors multiplying $F_{2(|A|+|B|)}^s(\{\theta_k\}_{k \in A \cup B})$ on the right hand side of (2.48). *Qed.*

2.4 Zero-momentum particles

2.4.1 Theories with one particle species

In theories with only a single particle species, there can only be a single particle of zero momentum in a multi-particle state due to the exclusion principle. For the momentum to

be exactly zero in finite volume it is necessary that all the other particles should come with quantum numbers in pairs of opposite sign, which means that the state must have $2n + 1$ particles in a configuration

$$|\{I_1, \dots, I_n, 0, -I_n, \dots, -I_1\}\rangle_L$$

Therefore we consider matrix elements of the form

$$\langle \{I'_1, \dots, I'_k, 0, -I'_k, \dots, -I'_1\} | \Phi | \{I_1, \dots, I_l, 0, -I_l, \dots, -I_1\} \rangle_L$$

(with $k = 0$ or $l = 0$ corresponding to a state containing a single stationary particle). We also suppose that the two sets $\{I_1, \dots, I_k\}$ and $\{I'_1, \dots, I'_l\}$ are not identical, otherwise we have the case of diagonal matrix elements treated in section 2.3.

We need to examine form factors of the form

$$F_{2k+2l+2}(i\pi + \theta'_1, \dots, i\pi + \theta'_k, i\pi - \theta'_k, \dots, i\pi - \theta'_1, i\pi + \theta, 0, \theta_1, \dots, \theta_l, -\theta_l, \dots, -\theta_1)$$

where the particular ordering of the rapidities was chosen to ensure that no additional S matrix factors appear in the disconnected terms of the crossing relation (2.2). Using the singularity axiom (2.5), plus unitarity and crossing symmetry of the S -matrix it is easy to see that the residue of the above function at $\theta = 0$ vanishes, and so it has a finite limit as $\theta \rightarrow 0$. However, this limit depends on direction just as in the case of the diagonal matrix elements considered in section 4. Therefore we must specify the way it is taken, and just as previously we use a prescription that is maximally symmetric in all variables: we choose to shift all rapidities entering the left hand state with the same amount to define

$$\begin{aligned} \mathcal{F}_{k,l}(\theta'_1, \dots, \theta'_k | \theta_1, \dots, \theta_l) = \\ \lim_{\epsilon \rightarrow 0} F_{2k+2l+2}(i\pi + \theta'_1 + \epsilon, \dots, i\pi + \theta'_k + \epsilon, i\pi - \theta'_k + \epsilon, \dots, i\pi - \theta'_1 + \epsilon, \\ i\pi + \epsilon, 0, \theta_1, \dots, \theta_l, -\theta_l, \dots, -\theta_1) \end{aligned} \quad (2.52)$$

Using the above definition, by analogy to (2.36) we conjecture that

$$\begin{aligned} \langle \{I'_1, \dots, I'_k, 0, -I'_k, \dots, -I'_1\} | \Phi | \{I_1, \dots, I_l, 0, -I_l, \dots, -I_1\} \rangle_L = \\ \frac{1}{\sqrt{\rho_{2k+1}(\tilde{\theta}'_1, \dots, \tilde{\theta}'_k, 0, -\tilde{\theta}'_k, \dots, -\tilde{\theta}'_1) \rho_{2l+1}(\tilde{\theta}_1, \dots, \tilde{\theta}_l, 0, -\tilde{\theta}_l, \dots, -\tilde{\theta}_1)}} \times \\ \left(\mathcal{F}_{k,l}(\tilde{\theta}'_1, \dots, \tilde{\theta}'_k | \tilde{\theta}_1, \dots, \tilde{\theta}_l) + mL F_{2k+2l}(i\pi + \tilde{\theta}'_1, \dots, i\pi + \tilde{\theta}'_k, \right. \\ \left. i\pi - \tilde{\theta}'_k, \dots, i\pi - \tilde{\theta}'_1, \tilde{\theta}_1, \dots, \tilde{\theta}_l, -\tilde{\theta}_l, \dots, -\tilde{\theta}_1) \right) + O(e^{-\mu L}) \end{aligned} \quad (2.53)$$

where $\tilde{\theta}$ denote the solutions of the appropriate Bethe-Yang equations at volume L , ρ_n is a shorthand notation for the n -particle Bethe-Yang density (2.15) and equality is understood

up to phase factors. We recall from section 2.2.1 that relative phases of multi-particle states are in general fixed differently in the form factor bootstrap and in numerical methods (TCSA). Also note that reordering particles gives phase factors on the right hand side according to the exchange axiom (2.3). This issue is obviously absent in the case of diagonal matrix elements treated in the previous section, since any such phase factor cancels out between the state and its conjugate. Such phases do not affect correlation functions, or as a consequence, any physically relevant quantities since they can all be expressed in terms of correlators.

There is some argument that can be given in support of eqn. (2.53). Note that the zero-momentum particle occurs in both the left and right states, which actually makes it unclear how to define a density similar to $\tilde{\rho}$ in (2.46). Such a density would take into account the interaction with the other particles. However, the nonzero rapidities entering of the two states are different and therefore there is no straightforward way to apply Saleur's recipe (2.47) here. Using the maximally symmetric definition (2.52) the shift ϵ can be equally put on the right hand side rapidities as well, and therefore we expect that the density factor multiplying the term F_{2k+2l} in (2.53) would be the one-particle state density in which none of the other rapidities appear, which is exactly mL for a stationary particle. This is a natural guess from eqn. (2.36) which states that when diagonal matrix elements are expressed using the symmetric evaluation, only densities of the type ρ appear.

Another argument can be formulated using the observation that eqn. (2.53) is only valid if $\mathcal{F}_{k,l}$ is defined as in (2.52); all other possible ways to take the limit can be related in a simple way to this definition and so the rule (2.53) can be rewritten appropriately. Let us consider two other natural choices

$$\begin{aligned} \mathcal{F}_{k,l}^+(\theta'_1, \dots, \theta'_k | \theta_1, \dots, \theta_l) &= \\ \lim_{\epsilon \rightarrow 0} F_{2k+2l+2}(i\pi + \theta'_1, \dots, i\pi + \theta'_k, i\pi - \theta'_k, \dots, i\pi - \theta'_1, i\pi, \epsilon, \theta_1, \dots, \theta_l, -\theta_l, \dots, -\theta_1) \\ \mathcal{F}_{k,l}^-(\theta'_1, \dots, \theta'_k | \theta_1, \dots, \theta_l) &= \\ \lim_{\epsilon \rightarrow 0} F_{2k+2l+2}(i\pi + \theta'_1, \dots, i\pi + \theta'_k, i\pi - \theta'_k, \dots, i\pi - \theta'_1, i\pi + \epsilon, 0, \theta_1, \dots, \theta_l, -\theta_l, \dots, -\theta_1) \end{aligned}$$

in which the shift is put only on the zero-momentum particle on the right/left, respectively. Using the kinematical residue axiom (2.5), \mathcal{F}^\pm can be related to \mathcal{F} via

$$\begin{aligned} \mathcal{F}_{k,l}(\theta'_1, \dots, \theta'_k | \theta_1, \dots, \theta_l) &= \mathcal{F}_{k,l}^+(\theta'_1, \dots, \theta'_k | \theta_1, \dots, \theta_l) \\ &+ 2 \sum_{i=1}^l \varphi(\theta_i) F_{2k+2l}(i\pi + \theta'_1, \dots, i\pi + \theta'_k, i\pi - \theta'_k, \dots, i\pi - \theta'_1, \theta_1, \dots, \theta_l, -\theta_l, \dots, -\theta_1) \\ \mathcal{F}_{k,l}(\theta'_1, \dots, \theta'_k | \theta_1, \dots, \theta_l) &= \mathcal{F}_{k,l}^-(\theta'_1, \dots, \theta'_k | \theta_1, \dots, \theta_l) \\ &- 2 \sum_{i=1}^k \varphi(\theta'_i) F_{2k+2l}(i\pi + \theta'_1, \dots, i\pi + \theta'_k, i\pi - \theta'_k, \dots, i\pi - \theta'_1, \theta_1, \dots, \theta_l, -\theta_l, \dots, -\theta_1) \end{aligned}$$

With the help of the above relations eqn. (2.53) can also be rewritten in terms of \mathcal{F}^\pm . The way \mathcal{F} and therefore also eqn. (2.53) are expressed in terms of \mathcal{F}^\pm shows a remarkable and natural symmetry under the exchange of the left and right state (and correspondingly \mathcal{F}^+ with \mathcal{F}^-), which provides a further support to our conjecture.

The above two arguments cannot be considered as a proof; we do not have a proper derivation of relation (2.53). On the other hand, as we show in section 3.7 it agrees very well with numerical data which would be impossible if there were some additional φ terms present; such terms, as shown in section 2.2.1 would contribute corrections of order $1/l$ in terms of the dimensionless volume parameter $l = mL$.

2.4.2 Generalization to more than one particle species

In a general diagonal scattering theory, there can be more than one particles of zero momentum in a multi-particle state. This can occur if the following two conditions hold:

- The sets of the rapidities are “parity-symmetric” for each particle species separately, ie. for every particle with non-zero rapidity θ there is a particle of the same species with rapidity $-\theta$. The same holds for the momentum quantum numbers. It is convenient to denote such a state with $2n + m$ particles by

$$|\{I_1, -I_1, I_2, -I_2, \dots, I_n, -I_n, 0, 0, \dots, 0\}\rangle_{i_1 i_1 i_2 i_2 \dots i_n i_n \ j_1 \dots j_m, L}$$

- The scattering phases between the zero-momentum particles satisfy

$$\prod_{\substack{l=1 \dots m \\ l \neq k}} S_{j_k j_l}(0) = 1 \quad k = 1 \dots m$$

This condition is necessary for the Bethe-Yang equations to hold.

Here we consider matrix elements between two different states $|\varphi\rangle$ and $|\varphi'\rangle$ which satisfy the previous two conditions. The generalization of (2.53) is straightforward: one has to include a disconnected term for every proper subset of those zero-momentum particles, which are present in both states. To precisely formulate this rule, once again (and in this section for the last time \smile) we need to introduce new notations. We wish to remark that the result presented below is unpublished material.

Let $|\psi\rangle$ and $|\psi'\rangle$ be a scattering state with $n + o$ and $n' + o$ particles, respectively, where o denotes the number of those zero-momentum particles which are present in both states. The sets of the remaining particles consist of “parity-symmetric” pairs or they may also contain zero-momentum particles that are not present in the other state. For the rapidities of these particles we use the standard notation $\theta_1 \dots \theta_n$ and $\theta'_1 \dots \theta'_{n'}$, and in the following we do not distinguish whether a particular rapidity belongs to a pair or is

zero. Particle types of these first n and n' particles are denoted by i_1, \dots, i_n and $i'_1, \dots, i'_{n'}$, whereas for the remaining o particles we use j_1, \dots, j_o .

For every subset $A \subset \{j_1, \dots, j_o\}$ we define

$$\mathcal{F}_{nn'}^o(A) = \lim_{\varepsilon \rightarrow 0} F_{n+n'+2|A|}(i\pi + \theta_1 + \varepsilon, \dots, i\pi + \theta_n + \varepsilon, \underbrace{i\pi + \varepsilon, \dots, i\pi + \varepsilon}_{|A| \text{ times}}, \underbrace{0, \dots, 0}_{|A| \text{ times}}, \theta'_1, \dots, \theta'_{n'})_B$$

where the label of particle types is given by

$$B = \{i_1 \dots i_n\} A \bar{A} \{i'_1 \dots i'_{n'}\}$$

with \bar{A} consisting of the elements of A listed in reverse order.

With these notations, the conjectured general formula reads

$$\langle \psi | \Phi | \psi' \rangle_L = \frac{1}{\sqrt{\rho_{n+o}(\theta_1, \dots, \theta_n, 0, \dots, 0) \rho_{n'+o}(\theta'_1, \dots, \theta'_{n'}, 0, \dots, 0)}} \times \sum_{A \subset \{j_1, \dots, j_o\}} \mathcal{F}_{nn'}^o(A) \prod_{j \in B} (m_j L) + \mathcal{O}(e^{-\mu L}) \quad (2.54)$$

where $B = \{j_1, \dots, j_o\} \setminus A$. Note, that an exchange of any two rapidities in $\theta_1 \dots \theta_n$ or $\theta'_1 \dots \theta'_{n'}$ yields the same phase factor in each term; the expression (2.54) is therefore well-defined and is to be understood up to an overall phase factor, similar to (2.53) and (2.18).

Chapter 3

Finite Volume Form Factors – Numerical analysis

Here we compare the analytic predictions of the previous chapter to numerical data obtained by the Truncated Conformal Space Approach (TCSA).

In 3.1 we explain in detail the methods we used to numerically determine the finite volume matrix elements in the Lee-Yang model and in the Ising model in a magnetic field. In sections 3.2-3.5 we present results on form factors without disconnected terms. The special cases of diagonal matrix elements and form factors with zero-momentum particles are investigated in 3.6 and 3.7, respectively.

3.1 Form factors from truncated conformal space

3.1.1 Truncated conformal space approach for scaling Lee-Yang model

We use the truncated conformal space approach (TCSA) developed by Yurov and Zamolodchikov in [86].

Due to translational invariance of the Hamiltonian (1.20), the conformal Hilbert space \mathcal{H} can be split into sectors characterized by the eigenvalues of the total spatial momentum

$$P = \frac{2\pi}{L} (L_0 - \bar{L}_0)$$

the operator $L_0 - \bar{L}_0$ generates Lorentz transformations and its eigenvalue is called Lorentz spin. For a numerical evaluation of the spectrum, the Hilbert space is truncated by imposing a cut in the conformal energy. The truncated conformal space corresponding to a given truncation and fixed value s of the Lorentz spin reads

$$\mathcal{H}_{\text{TCS}}(s, e_{\text{cut}}) = \left\{ |\psi\rangle \in \mathcal{H} \mid (L_0 - \bar{L}_0) |\psi\rangle = s |\psi\rangle, \left(L_0 + \bar{L}_0 - \frac{c}{12} \right) |\psi\rangle = e |\psi\rangle : e \leq e_{\text{cut}} \right\}$$

On this subspace, the dimensionless Hamiltonian matrix can be written as

$$h_{ij} = \frac{2\pi}{l} \left(L_0 + \bar{L}_0 - \frac{c}{12} + i \frac{\kappa l^{2-2\Delta}}{(2\pi)^{1-2\Delta}} G^{(s)-1} B^{(s)} \right) \quad (3.1)$$

where energy is measured in units of the particle mass m , $l = mL$ is the dimensionless volume parameter,

$$G_{ij}^{(s)} = \langle i|j \rangle \quad (3.2)$$

is the conformal inner product matrix and

$$B_{ij}^{(s)} = \langle i|\Phi(z, \bar{z})|j \rangle|_{z=\bar{z}=1} \quad (3.3)$$

is the matrix element of the operator Φ at the point $z = \bar{z} = 1$ on the complex plane between vectors $|i\rangle$, $|j\rangle$ from $\mathcal{H}_{\text{TCS}}(s, e_{\text{cut}})$. The natural basis provided by the action of Virasoro generators is not orthonormal and therefore $G^{(s)-1}$ must be inserted to transform the left vectors to the dual basis. The Hilbert space and the matrix elements are constructed using an algorithm developed by Kausch et al. and first used in [95].

Diagonalizing the matrix h_{ij} we obtain the energy levels as functions of the volume, with energy and length measured in units of m . The maximum value of the cutoff e_{cut} we used was 30, in which case the Hilbert space contains around one thousand vectors, slightly depending on the spin.

3.1.2 Exact form factors of the primary field Φ in the Lee-Yang model

Form factors of the trace of the stress-energy tensor Θ were computed by Al.B. Zamolodchikov in [19], and using the relation

$$\Theta = i\lambda\pi(1 - \Delta)\Phi \quad (3.4)$$

we can rewrite them in terms of Φ . They have the form

$$F_n(\theta_1, \dots, \theta_n) = \langle \Phi \rangle H_n Q_n(x_1, \dots, x_n) \prod_{i=1}^n \prod_{j=i+1}^n \frac{f(\theta_i - \theta_j)}{x_i + x_j} \quad (3.5)$$

with the notations

$$\begin{aligned} f(\theta) &= \frac{\cosh \theta - 1}{\cosh \theta + 1/2} v(i\pi - \theta) v(-i\pi + \theta) \\ v(\theta) &= \exp \left(2 \int_0^\infty dt \frac{\sinh \frac{\pi t}{2} \sinh \frac{\pi t}{3} \sinh \frac{\pi t}{6}}{t \sinh^2 \pi t} e^{i\theta t} \right) \\ x_i &= e^{\theta_i} \quad , \quad H_n = \left(\frac{3^{1/4}}{2^{1/2} v(0)} \right)^n \end{aligned}$$

The mass-gap of the theory is related to the coupling constant as

$$\lambda = 0.09704845636 \cdots \times m^{12/5} \quad (3.6)$$

The exact vacuum expectation value of the field Φ is

$$\langle \Phi \rangle = 1.239394325 \cdots \times i m^{-2/5}$$

which can be readily obtained using (3.6, 3.4) and also the known vacuum expectation value of Θ [19]

$$\langle \Theta \rangle = -\frac{\pi m^2}{4\sqrt{3}}$$

The functions Q_n are symmetric polynomials in the variables x_i . Defining the elementary symmetric polynomials of n variables by the relations

$$\prod_{i=1}^n (x + x_i) = \sum_{i=0}^n x^{n-i} \sigma_i^{(n)}(x_1, \dots, x_n) \quad , \quad \sigma_i^{(n)} = 0 \text{ for } i > n$$

they can be constructed as

$$\begin{aligned} Q_1 &= 1 \quad , \quad Q_2 = \sigma_1^{(2)} \quad , \quad Q_3 = \sigma_1^{(3)} \sigma_2^{(3)} \\ Q_n &= \sigma_1^{(n)} \sigma_{n-1}^{(n)} P_n \quad , \quad n > 3 \\ P_n &= \det \mathcal{M}^{(n)} \quad \text{where} \quad \mathcal{M}_{ij}^{(n)} = \sigma_{3i-2j+1}^{(n)} \quad , \quad i, j = 1, \dots, n-3 \end{aligned}$$

Note that the one-particle form factor is independent of the rapidity:

$$F_1^\Phi = 1.0376434349 \cdots \times i m^{-2/5} \quad (3.7)$$

3.1.3 Truncated fermionic space approach for the Ising model

The conformal Ising model can be represented as the theory of a massless Majorana fermion with the action

$$\mathcal{A}_{Ising} = \frac{1}{2\pi} \int d^2z (\bar{\psi} \partial \bar{\psi} + \psi \bar{\partial} \psi)$$

On the conformal plane the model has two sectors, with the mode expansions

$$\psi(z) = \begin{cases} \sum_{r \in \mathbb{Z} + \frac{1}{2}} b_r z^{-r-1/2} & \text{Neveu-Schwarz (NS) sector} \\ \sum_{r \in \mathbb{Z}} b_r z^{-r-1/2} & \text{Ramond (R) sector} \end{cases}$$

and similarly for the anti-holomorphic field $\bar{\psi}$. The Hilbert space is the direct sum of a certain projection of the NS and R sectors, with the Virasoro content

$$\mathcal{H}_{Ising} = \bigoplus_{h=0, \frac{1}{2}, \frac{1}{16}} \mathcal{V}_h \otimes \bar{\mathcal{V}}_h$$

The spin field σ connects the NS and R sectors, and its matrix elements $B_{ij}^{(s)}$ in the sector with a given conformal spin s (cf. eqn. (3.3)) can be most conveniently computed in the fermionic basis using the work of Yurov and Zamolodchikov [96], who called this method the truncated fermionic space approach. The fermionic basis can easily be chosen orthonormal, and thus in this case the metrics $G^{(s)}$ on the spin subspaces (cf. eqn. (3.2)) are all given by unit matrices of appropriate dimension. Apart from the choice of basis all the calculation proceeds very similarly to the case of the Lee-Yang model. Energy and volume is measured in units of the lowest particle mass $m = m_1$ and using relation (1.25) one can write the dimensionless Hamiltonian in the form (3.1). The highest cutoff we use is $e_{\text{cut}} = 30$, in which case the Hilbert space contains around three thousand vectors (slightly depending on the value of the spin chosen).

We remark that the energy density operator can be represented in the fermionic language as

$$\epsilon = \bar{\psi}\psi$$

which makes the evaluation of its matrix elements in the fermionic basis extremely simple.

3.1.4 Ising model – Form factors of the energy density operator

The form factors of the operator ϵ in the E_8 model were first calculated in [97] and their determination was carried further in [92]. The exact vacuum expectation value of the field ϵ is given by [98]

$$\langle \epsilon \rangle = \epsilon_h |h|^{8/15} \quad , \quad \epsilon_h = 2.00314 \dots$$

or in terms of the mass scale $m = m_1$

$$\langle \epsilon \rangle = 0.45475 \dots \times m \tag{3.8}$$

The form factors are not known for the general n -particle case in a closed form, i.e. no formula similar to that in (3.5) exists. They can be evaluated by solving the appropriate polynomial recursion relations derived from the form-factor axioms. We do not present explicit formulae here; instead we refer to the above papers. For practical calculations we used the results computed by Delfino, Grinza and Mussardo, which can be downloaded from the Web in `Mathematica` format [99].

3.1.5 Evaluating matrix elements of a local operator \mathcal{O} in TCSA

Identification of multi-particle states

Diagonalizing the TCSA Hamiltonian (3.1) yields a set of eigenvalues and eigenvectors at each value of the volume, but it is not immediately obvious how to select the same

state at different values of the volume. Therefore in order to calculate form factors it is necessary to identify the states with the corresponding many-particle interpretation.

Finding the vacuum state is rather simple since it is the lowest lying state in the spin-0 sector and its energy is given by

$$E_0(L) = BL + \dots$$

where the ellipsis indicate residual finite size effects decaying exponentially fast with volume L and B is the bulk energy density which in the models we consider is exactly known (1.22, 1.26). One-particle states can be found using that their energies can be expressed as

$$E_i^{(s)}(L) = BL + \sqrt{\left(\frac{2\pi s}{L}\right)^2 + m_i^2} + \dots$$

again up to residual finite size effects where s is the spin of the sector considered and i is the species label (every sector contains a single one-particle state for each species).

Higher multi-particle states can be identified by comparing the measured eigenvalues to the levels predicted by the Bethe-Yang equations. Fixing species labels i_1, \dots, i_n and momentum quantum numbers I_1, \dots, I_n , eqns. (2.11) can be solved to give the rapidities $\tilde{\theta}_1, \dots, \tilde{\theta}_n$ of the particles as function of the dimensionless volume parameter $l = mL$. Then the energy of the multi-particle state in question is

$$E_{i_1 \dots i_n}^{(I_1 \dots I_n)}(L) = BL + \sum_{k=1}^n m_{i_k} \cosh \tilde{\theta}_k + \dots$$

which can be compared to the spectrum.

For each state there exists a range of the volume, called the *scaling region*, where L is large enough so that the omitted residual finite size effects can be safely neglected and small enough so that the truncation errors are also negligible. More precisely, the scaling region for any quantity depending on the volume can be defined as the volume range in which the residual finite size corrections and the truncation errors are of the same order of magnitude; since both sources of error show a dependence on the state and the particular quantity considered (as well as on the value of the cutoff), so does the exact position of the scaling region itself.

In the scaling region, we can use a comparison between the Bethe-Yang predictions and the numerical energy levels to sort the states and label them by multi-particle quantum numbers. An example is shown in figure 3.1, where we plot the first few states in the spin-0 sector of the scaling Lee-Yang model and their identification in terms of multi-particle states is given. In this case, the agreement with the predicted bulk energy density and the Bethe-Yang levels in the scaling region is better than one part in 10^4 for every state shown (with the TCSA cutoff taken at $e_{\text{cut}} = 30$).

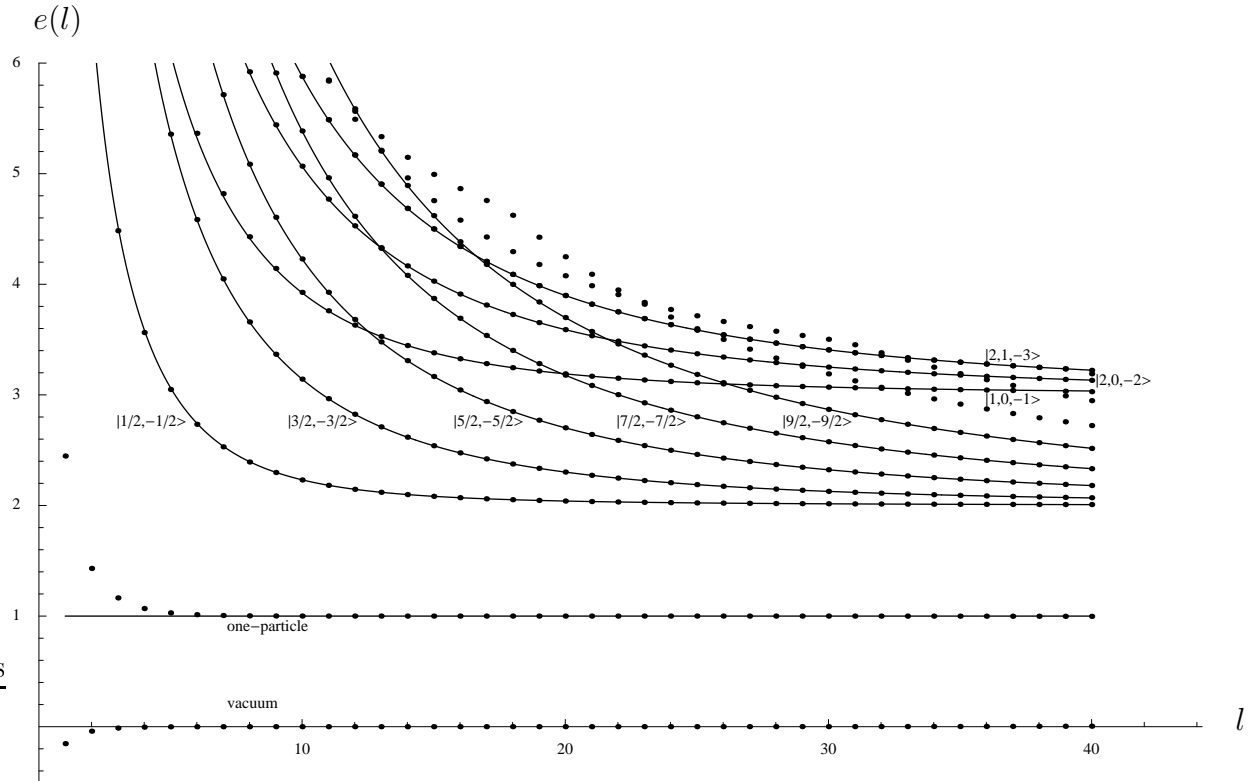


Figure 3.1: The first 13 states in the finite volume spectrum of scaling Lee-Yang model. We plot the energy in units of m (with the bulk subtracted): $e(l) = (E(L) - BL)/m$, against the dimensionless volume variable $l = mL$. n -particle states are labeled by $|I_1, \dots, I_n\rangle$, where the I_k are the momentum quantum numbers. The state labeled $|2, 1, -3\rangle$ is actually two-fold degenerate because of the presence of $|-2, -1, 3\rangle$ (up to a splitting which vanishes as e^{-l} , cf. the discussion in subsection 3.3). The dots are the TCSA results and the continuous lines are the predictions of the Bethe-Yang equations (2.11). The points not belonging to any of the Bethe-Yang lines drawn are two- and three-particle states which are only partly contained in the first 13 levels due to line crossings, whose presence is a consequence of the integrability of the model.

Evaluation of matrix elements

Suppose that we computed two Hamiltonian eigenvectors as functions of the volume L (labeled by their quantum numbers in the Bethe-Yang description (2.11), omitting the particle species labels for brevity):

$$\begin{aligned} |\{I_1, \dots, I_n\}\rangle_L &= \sum_i \Psi_i(I_1, \dots, I_n; L) |i\rangle \\ |\{I'_1, \dots, I'_k\}\rangle_L &= \sum_j \Psi_j(I'_1, \dots, I'_k; L) |j\rangle \end{aligned}$$

in the sector with spin s and spin s' , respectively. Let the inner products of these vectors with themselves be given by

$$\begin{aligned} \mathcal{N} &= \sum_{i,j} \Psi_i(I_1, \dots, I_n; L) G_{ij}^{(s)} \Psi_j(I_1, \dots, I_n; L) \\ \mathcal{N}' &= \sum_{i,j} \Psi_i(I'_1, \dots, I'_k; L) G_{ij}^{(s')} \Psi_j(I'_1, \dots, I'_k; L) \end{aligned}$$

It is important that the components of the left eigenvector are not complex conjugated. In the Ising model we work in a basis where all matrix and vector components are naturally real. In the Lee-Yang model, the TCSA eigenvectors are chosen so that all of their components Ψ_i are either purely real or purely imaginary depending on whether the basis vector $|i\rangle$ is an element of the $h = \bar{h} = 0$ or the $h = \bar{h} = -1/5$ component in the Hilbert space. It is well-known that the Lee-Yang model is non-unitary, which is reflected in the presence of complex structure constants as indicated in (1.19). This particular convention for the structure constants forces upon us the above inner product, because it is exactly the one under which TCSA eigenvectors corresponding to different eigenvalues are orthogonal. We remark that by redefining the structure constants and the conformal inner product it is also possible to use a manifestly real representation for the Lee-Yang TCSA (up to some truncation effects that lead to complex eigenvalues in the vicinity of level crossings [86]). Note that the above conventions mean that the phases of the eigenvectors are fixed up to a sign.

Let us consider a spinless primary field \mathcal{O} with scaling weights $\Delta_{\mathcal{O}} = \bar{\Delta}_{\mathcal{O}}$, which can be described as the matrix

$$O_{ij}^{(s',s)} = \langle i | \mathcal{O}(z, \bar{z}) | j \rangle \Big|_{z=\bar{z}=1} \quad , \quad |i\rangle \in \mathcal{H}_{\text{TCS}}(s', e_{\text{cut}}) \quad , \quad |j\rangle \in \mathcal{H}_{\text{TCS}}(s, e_{\text{cut}})$$

between the two truncated conformal space sectors. Then the matrix element of \mathcal{O} can be computed as

$$\begin{aligned} m^{-2\Delta_{\mathcal{O}}} \langle \{I'_1, \dots, I'_k\} | \mathcal{O}(0,0) | \{I_1, \dots, I_n\} \rangle_L = \\ \left(\frac{2\pi}{mL} \right)^{2\Delta_{\mathcal{O}}} \frac{1}{\sqrt{\mathcal{N}}} \frac{1}{\sqrt{\mathcal{N}'}} \sum_{j,l} \Psi_j(I'_1, \dots, I'_k; L) O_{jl}^{(s',s)} \Psi_l(I_1, \dots, I_n; L) \end{aligned} \quad (3.9)$$

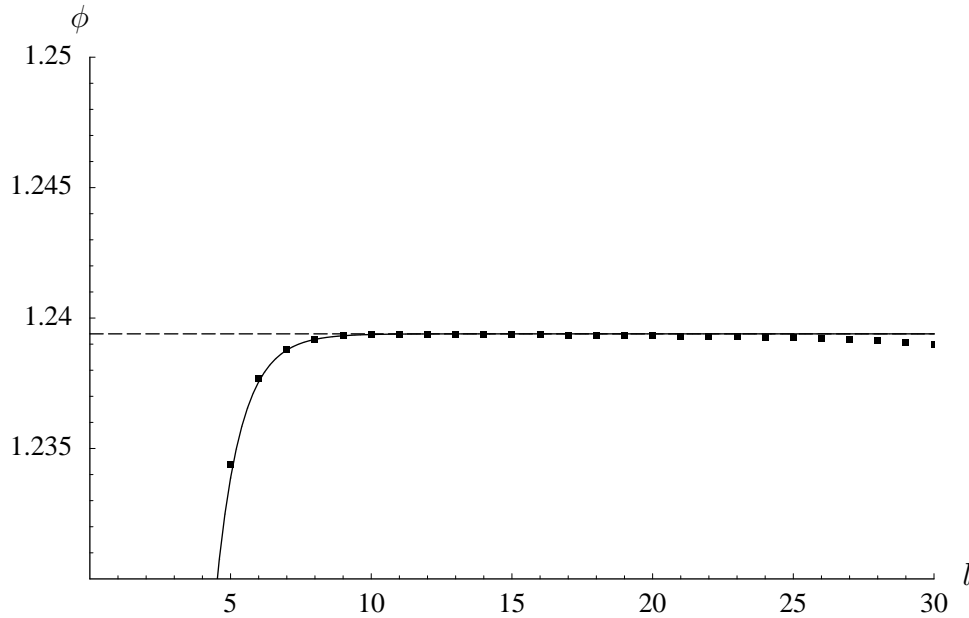


Figure 3.2: The vacuum expectation value of Φ in finite volume. The dashed line shows the exact infinite volume value, while the continuous line corresponds to eqn. (3.10).

where the volume dependent pre-factor comes from the transformation of the primary field \mathcal{O} under the exponential map (1.15) and we wrote the equation in a dimensionless form using the mass scale m . The above procedure is a generalization of the one used by Guida and Magnoli to evaluate vacuum expectation values in [100]; it was extended to one-particle form factors in the context of the tricritical Ising model by Fioravanti et al. in [101].

3.2 Vacuum expectation values and one-particle form factors

3.2.1 Scaling Lee-Yang model

Before the one-particle form factor we discuss the vacuum expectation value. Let us define the dimensionless function

$$\phi(l) = -im^{2/5} \langle 0 | \Phi | 0 \rangle_L$$

where the finite volume expectation value is evaluated from TCSA using (3.9). We performed measurement of ϕ as a function of both the cutoff $e_{\text{cut}} = 21 \dots 30$ and the volume $l = 1 \dots 30$ and then extrapolated the cutoff dependence fitting a function

$$\phi(l, e_{\text{cut}}) = \phi(l) + A(l)e_{\text{cut}}^{-12/5}$$

(where the exponent was chosen by verifying that it provides an optimal fit to the data). The data corresponding to odd and even values of the cutoff must be extrapolated separately [8], therefore one gets two estimates for the result, but they only differ by a very small amount (of order 10^{-5} at $l = 30$ and even less for smaller volumes). The theoretical prediction for $\phi(l)$ is

$$\phi(l) = 1.239394325 \dots + O(e^{-l})$$

The numerical result (after extrapolation) is shown in figure 3.2 from which it is clear that there is a long scaling region. Estimating the infinite volume value from the flattest part of the extrapolated curve (at l around 12) we obtain the following measured value

$$\phi(l = \infty) = 1.23938 \dots$$

where the numerical errors from TCSA are estimated to affect only the last displayed digit, which corresponds to an agreement within one part in 10^5 .

There is also a way to compute the leading exponential correction, which was derived by Delfino [33]:

$$\langle \Phi \rangle_L = \langle \Phi \rangle + \frac{1}{\pi} \sum_i F_2(i\pi, 0)_{ii} K_0(m_i r) + \dots \quad (3.10)$$

where

$$K_0(x) = \int_0^\infty d\theta \cosh \theta e^{-x \cosh \theta}$$

is the modified Bessel-function, and the summation is over the particle species i (there is only a single term in the scaling Lee-Yang model). This agrees very well with the numerical data, as demonstrated in table 3.1 and also in figure 3.2. Using Lüscher's finite-volume perturbation theory introduced in [4], the correction term can be interpreted as the sum of Feynman diagrams where there is exactly one propagator that winds around the cylinder, and therefore eqn. (3.10) can be represented graphically as shown in figure 3.3. On the other hand, by Euclidean invariance this finite size correction coincides with the first term in the low-T expansion for one-point functions at finite temperature (see subsections 5.1.1 and 5.2.2).

To measure the one-particle form factor we use the correspondence (2.16) between the finite and infinite volume form factors to define the dimensionless function

$$\tilde{f}_1^s(l) = -im^{2/5} (l^2 + (2\pi s)^2)^{1/4} \langle 0 | \Phi | \{s\} \rangle_L$$

where $|\{s\}\rangle_L$ is the finite volume one-particle state with quantum number $I = s$ i.e. from the spin- s sector. The theoretical prediction for this quantity is

$$\tilde{f}_1^s(l) = 1.0376434349 \dots + O(e^{-l}) \quad (3.11)$$

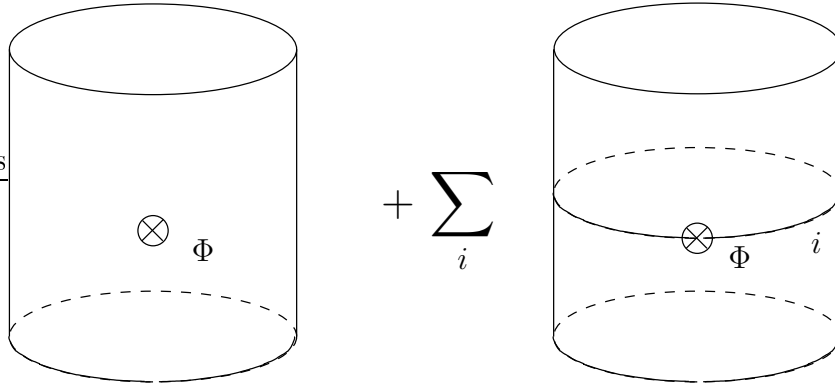


Figure 3.3: Graphical representation of eqn. (3.10).

| l | $\phi(l)$ (predicted) | $\phi(l)$ (TCSA) |
|-----|-----------------------|------------------|
| 2 | 1.048250 | 1.112518 |
| 3 | 1.184515 | 1.195345 |
| 4 | 1.222334 | 1.224545 |
| 5 | 1.233867 | 1.234396 |
| 6 | 1.237558 | 1.237698 |
| 7 | 1.238774 | 1.238811 |
| 8 | 1.239182 | 1.239189 |
| 9 | 1.239321 | 1.239317 |
| 10 | 1.239369 | 1.239360 |
| 11 | 1.239385 | 1.239373 |
| 12 | 1.239391 | 1.239375 |

Table 3.1: Comparison of eqn. (3.10) to TCSA data

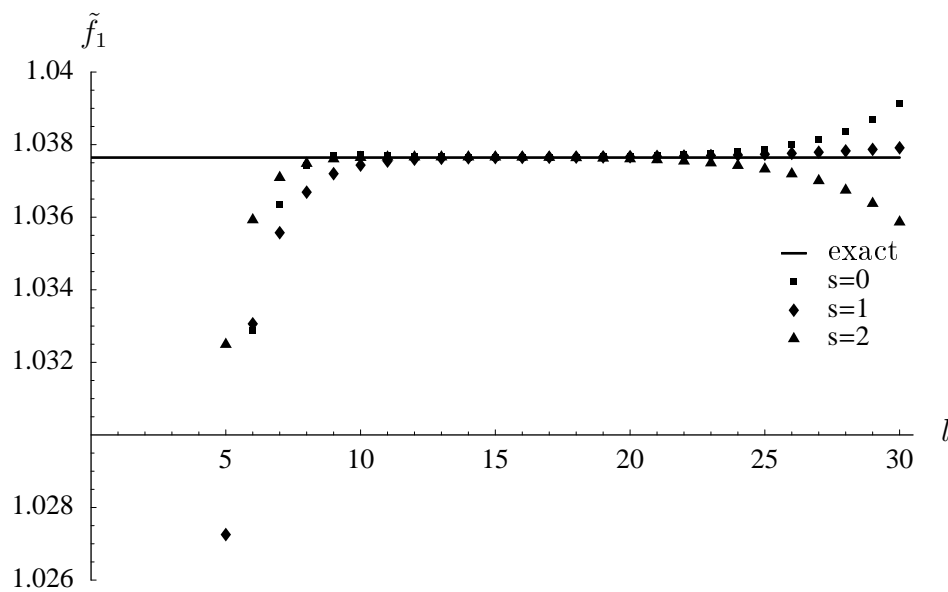


Figure 3.4: One-particle form factor from sectors with spin $s = 0, 1, 2$. The continuous line shows the exact infinite volume prediction.

The numerical results (after extrapolation in the cutoff) are shown in figure 3.4. The scaling region gives the following estimates for the infinite volume limit:

$$\begin{aligned}\tilde{f}_1^0(l = \infty) &= 1.037654\dots \\ \tilde{f}_1^1(l = \infty) &= 1.037650\dots \\ \tilde{f}_1^2(l = \infty) &= 1.037659\dots\end{aligned}$$

which show good agreement with eqn. (3.11) (the relative deviation is again around 10^{-5} , as for the vacuum expectation value).

3.2.2 Ising model in magnetic field

For the Ising model, we again start with checking the dimensionless vacuum expectation value for which, using eqn. (3.8) we have the prediction

$$\phi(l) = \frac{1}{m} \langle \epsilon \rangle_L = 0.45475\dots + O(e^{-l})$$

where $m = m_1$ is the mass of the lightest particle and $l = mL$ as before. The TCSA data are shown in figure 3.5. Note that there is substantial dependence on the cutoff e_{cut} and also that extrapolation in e_{cut} is really required to achieve good agreement with the infinite volume limit. Reading off the plateau value from the extrapolated data gives the estimate

$$\frac{1}{m} \langle \epsilon \rangle = 0.4544\dots$$

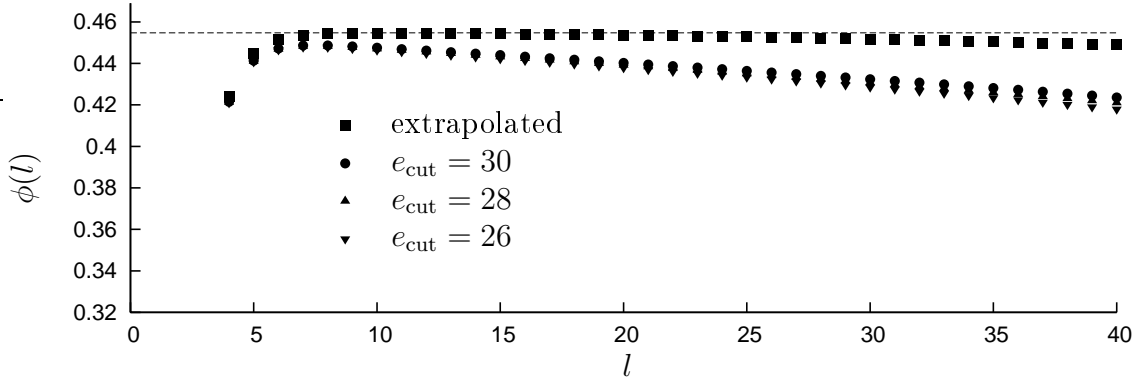


Figure 3.5: Measuring the vacuum expectation value of ϵ in the Ising model

for the infinite volume vacuum expectation value, which has $8 \cdot 10^{-4}$ relative deviation from the exact result. Our first numerical comparison thus already tells us that we can expect much larger truncation errors than in the Lee-Yang case. It is also clear from figure 3.5 that in order to attain suitable precision in the Ising model extrapolation in the cutoff is very important.

Defining the function

$$\bar{\phi}(l) = \langle \epsilon \rangle_L / \langle \epsilon \rangle$$

we can calculate the leading exponential correction using eqn. (3.10) and the exact two-particle form factors from [99]. It only makes sense to include particles $i = 1, 2, 3$ since the contribution of the fourth particle is sub-leading with respect to two-particle terms from the lightest particle due to $m_4 > 2m_1$. The result is shown in figure 3.6; we do not give the data in numerical tables, but we mention that the relative deviation between the predicted and measured value is better than 10^{-3} in the range $5 < l < 10$.

From now on we normalize all form factors of the operator ϵ by the infinite volume vacuum expectation value (3.8), i.e. we consider form factors of the operator

$$\Psi = \epsilon / \langle \epsilon \rangle \quad (3.12)$$

which conforms with the conventions used in [92, 99]. We define the dimensionless one-particle form factor functions as

$$\tilde{f}_i^s(l) = \left(\left(\frac{m_i l}{m_1} \right)^2 + (2\pi s)^2 \right)^{1/4} \langle 0 | \Psi | \{s\} \rangle_{i,L}$$

In the plots of figure 3.7 we show how these functions measured from TCSA compare to predictions from the exact form factors for particles $i = 1, 2, 3$ and spins $s = 0, 1, 2, 3$.

It is evident that the scaling region sets in much later than for the Lee-Yang model; therefore for the Ising model we do not plot data for low values of the volume (all plots

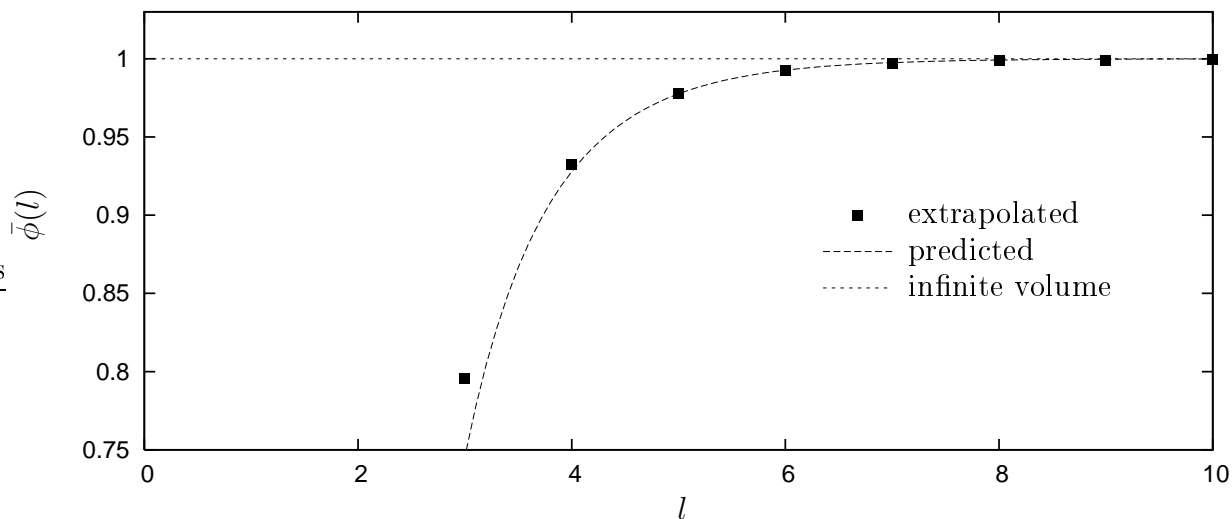


Figure 3.6: The volume dependence of the vacuum expectation value of ϵ in the Ising model, showing the extrapolated value and the prediction from eqn. (3.10), normalized by the value in the infinite volume limit.

start from $l \sim 10 \dots 15$). This also means that truncation errors in the scaling region are also much larger than in the scaling Lee-Yang model; we generally found errors larger by an order of magnitude after extrapolation in the cutoff. We remark that extrapolation improves the precision by an order of magnitude compared to the raw data at the highest value of the cutoff.

Note the rather large finite size correction in the case of A_3 . This can be explained rather simply as the presence of a μ -term. Based on Lüscher's finite-volume perturbation theory [4] it is expected, that similar to the μ -term for the masses of stable particles (1.11), the leading contribution (which is associated to the diagram depicted in figure 3.8) has the volume dependence

$$e^{-\mu_{311}L} \quad , \quad \mu_{311} = \sqrt{m_1^2 - \frac{m_3^2}{4}} = 0.10453 \dots \times m_1$$

Therefore we can expect a contribution suppressed only by $e^{-0.1l}$. A numerical fit of the l -dependence in the $s = 0$ case is perfectly consistent with this expectation. As a result, no scaling region can be found, because truncation errors are too large in the volume range where the exponential correction is suitably small. We do not elaborate on this issue further here: chapter 4 is devoted to the study of exponential corrections.

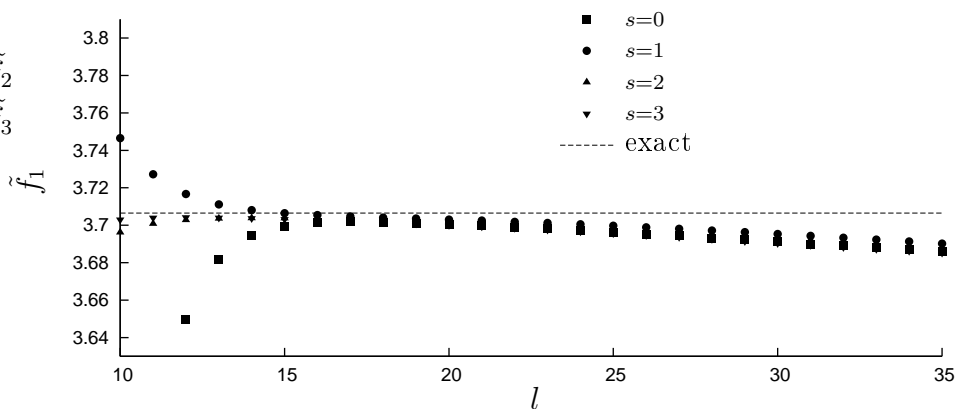
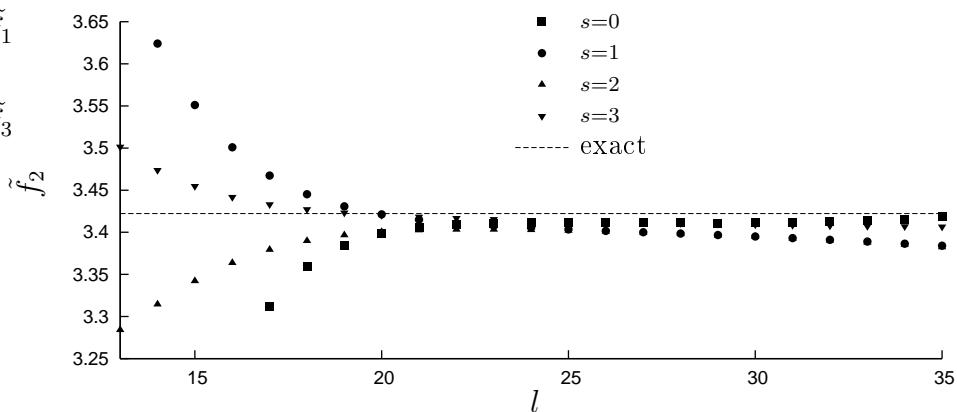
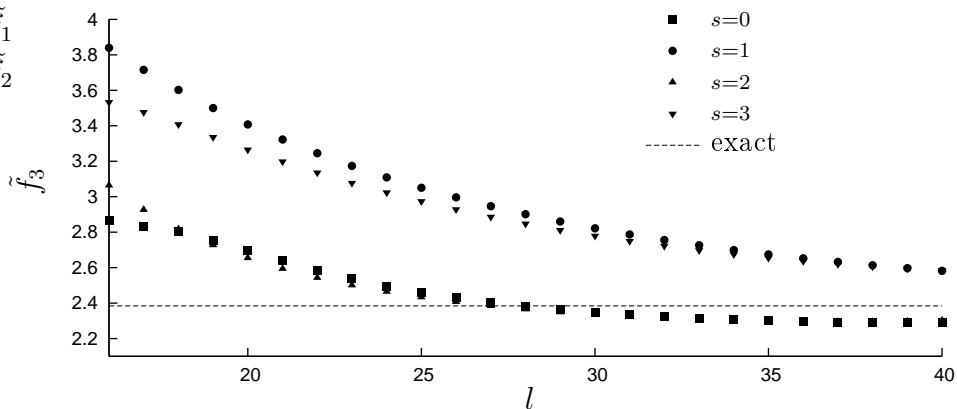
(a) A_1 (b) A_2 (c) A_3

Figure 3.7: One-particle form factors measured from TCSA (dots) compared to the infinite-volume prediction from exact form factors. All numerical data have been extrapolated to $e_{\text{cut}} = \infty$ and s denotes the Lorentz spin of the state considered. The relative deviation in the scaling region is around 10^{-3} for A_1 and A_2 ; there is no scaling region for A_3 (see the discussion in the main text).

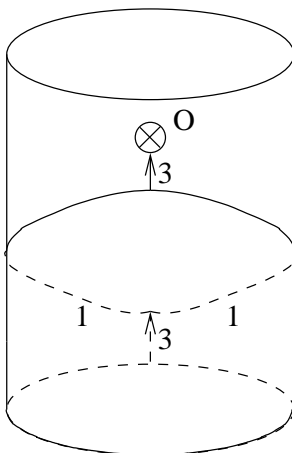


Figure 3.8: Leading finite size correction (a so-called μ -term) to the one-particle form factor of A_3 , which results from the process of splitting up into two copies of A_1 which then wind around the cylinder once before recombining into A_3 again.

3.3 Two-particle form factors

3.3.1 Scaling Lee-Yang model

Following the ideas in the previous subsection, we can again define a dimensionless function for each two-particle state as follows:

$$f_2(l)_{I_1 I_2} = -im^{2/5} \langle 0 | \Phi | \{I_1, I_2\} \rangle_L \quad , \quad l = mL$$

Relation (2.16) gives the following prediction in terms of the exact form-factors:

$$f_2(l)_{I_1 I_2} = \frac{-im^{2/5}}{\sqrt{\rho_{11}(\tilde{\theta}_1(l), \tilde{\theta}_2(l))}} F_2^\Phi(\tilde{\theta}_1(l), \tilde{\theta}_2(l)) + O(e^{-l}) \quad (3.13)$$

where $\tilde{\theta}_1(l)$, $\tilde{\theta}_2(l)$ solve the Bethe-Yang equations

$$\begin{aligned} l \sinh \tilde{\theta}_1 + \delta(\tilde{\theta}_1 - \tilde{\theta}_2) &= 2\pi I_1 \\ l \sinh \tilde{\theta}_2 + \delta(\tilde{\theta}_2 - \tilde{\theta}_1) &= 2\pi I_2 \end{aligned}$$

and the density of states is given by

$$\rho_{11}(\theta_1, \theta_2) = l^2 \cosh \theta_1 \cosh \theta_2 + l \cosh \theta_1 \varphi(\theta_2 - \theta_1) + l \cosh \theta_2 \varphi(\theta_1 - \theta_2)$$

the phase shift δ is defined according to eqn. (1.24) and

$$\varphi(\theta) = \frac{d\delta(\theta)}{d\theta}$$

There is a further issue to take into account: the relative phases of the multi-particle states are a matter of convention and the choice made in subsection 3.1.5 for the TCSA eigenvectors may differ from the convention adapted in the form factor bootstrap. Therefore in the numerical work we compare the absolute values of the functions $f_2(l)$ computed from TCSA with those predicted from the exact form factors. Note that this issue is present for any non-diagonal matrix element, and was in fact tacitly dealt with in the case of one-particle matrix elements treated in subsection 3.2.1.

The prediction (3.13) for the finite volume two-particle form factors is compared with spin-0 states graphically in figure 3.9 and numerically in table 3.2, while the spin-1 and spin-2 case is presented in figure 3.10 and in table 3.3. These contain no more than a representative sample of our data: we evaluated similar matrix elements for a large number of two-particle states for values of the volume parameter l running from 1 to 30. The behaviour of the relative deviation is consistent with the presence of a correction of e^{-l} type up to $l \sim 9 \dots 10$ (i.e. the logarithm of the deviation is very close to being a linear function of l), and after $l \sim 16 \dots 18$ it starts to increase due to truncation errors. This is demonstrated in figure 3.11 using the data presented in table 3.3 for spin-1 and spin-2 states¹, but it is equally valid for all the other states we examined. In the intermediate region $l \sim 10 \dots 16$ the two sources of numerical deviation are of the same order, and so that range can be considered as the optimal scaling region: according to the data in the tables agreement there is typically around 10^{-4} (relative deviation). It is also apparent that scaling behaviour starts at quite low values of the volume (around $l \sim 4$ the relative deviation is already down to around 1%).

It can be verified by explicit evaluation that in the scaling region the Bethe-Yang density of states (ρ) given in (2.15) differs by corrections of relative magnitude $10^{-1} - 10^{-2}$ (analytically: of order $1/l$) from the free density of states (ρ^0) in (2.14), and therefore without using the proper interacting density of states it is impossible to obtain the precision agreement we demonstrated. In fact the observed 10^{-4} relative deviation corresponds to corrections of order l^{-4} at $l = 10$, but it is of the order of estimated truncation errors².

These results are very strong evidence for the main statement in (3.13) (and thus also (2.16)), namely, that all $1/L$ corrections are accounted by the proper interacting state density factor and that all further finite size corrections are just residual finite size effects decaying exponentially in L . In section 3.4 we show that data from higher multi-particle form factors fully support the above conclusions drawn from the two-particle form factors.

¹Note that the dependence of the logarithm of the deviation on the volume is not exactly linear because the residual finite size correction can also contain a factor of some power of l , and so it is expected that a $\log l$ contribution is also present in the data plotted in figure 3.11.

²Truncation errors can be estimated by examining the dependence of the extracted data on the cutoff e_{cut} , as well as by comparing TCSA energy levels to the Bethe-Yang predictions.

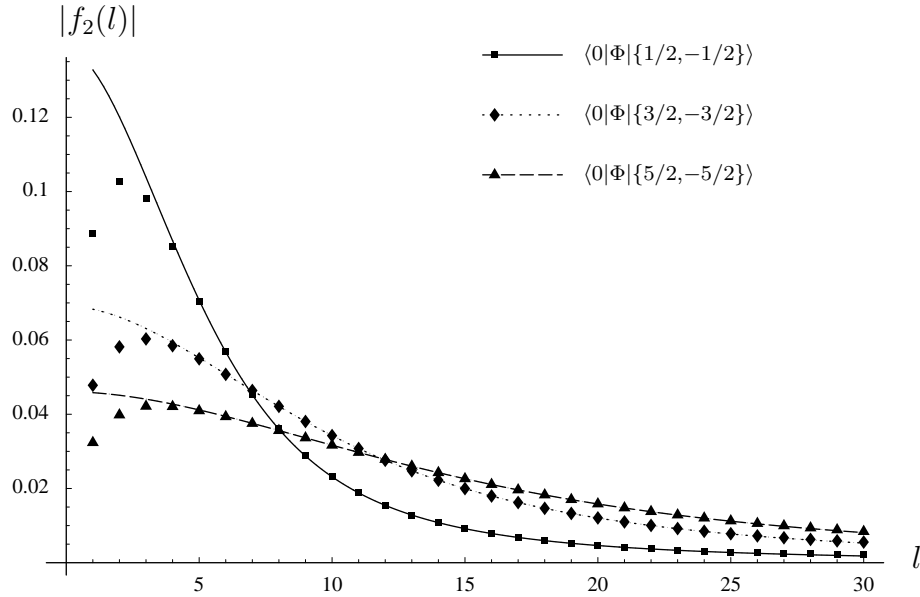


Figure 3.9: Two-particle form factors in the spin-0 sector. Dots correspond to TCSA data, while the lines show the corresponding form factor prediction.

| | $I_1 = 1/2, I_2 = -1/2$ | | $I_1 = 3/2, I_2 = -3/2$ | | $I_1 = 5/2, I_2 = -5/2$ | |
|-----|-------------------------|----------|-------------------------|----------|-------------------------|----------|
| l | TCSA | FF | TCSA | FF | TCSA | FF |
| 2 | 0.102780 | 0.120117 | 0.058158 | 0.066173 | 0.039816 | 0.045118 |
| 4 | 0.085174 | 0.086763 | 0.058468 | 0.059355 | 0.042072 | 0.042729 |
| 6 | 0.056828 | 0.056769 | 0.050750 | 0.050805 | 0.039349 | 0.039419 |
| 8 | 0.036058 | 0.035985 | 0.042123 | 0.042117 | 0.035608 | 0.035614 |
| 10 | 0.023168 | 0.023146 | 0.034252 | 0.034248 | 0.031665 | 0.031664 |
| 12 | 0.015468 | 0.015463 | 0.027606 | 0.027604 | 0.027830 | 0.027828 |
| 14 | 0.010801 | 0.010800 | 0.022228 | 0.022225 | 0.024271 | 0.024267 |
| 16 | 0.007869 | 0.007867 | 0.017976 | 0.017972 | 0.021074 | 0.021068 |
| 18 | 0.005950 | 0.005945 | 0.014652 | 0.014645 | 0.018268 | 0.018258 |
| 20 | 0.004643 | 0.004634 | 0.012061 | 0.012050 | 0.015844 | 0.015827 |

Table 3.2: Two-particle form factors $|f_2(l)|$ in the spin-0 sector

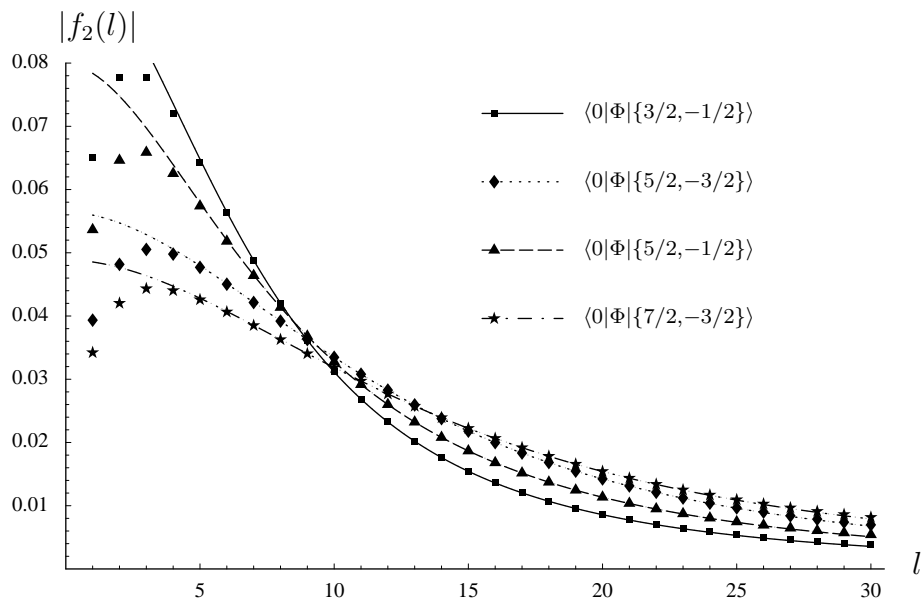


Figure 3.10: Two-particle form factors in the spin-1 and spin-2 sectors. Dots correspond to TCSA data, while the lines show the corresponding form factor prediction.

| l | $I_1 = 3/2, I_2 = -1/2$ | | $I_1 = 5/2, I_2 = -3/2$ | | $I_1 = 5/2, I_2 = -1/2$ | | $I_1 = 7/2, I_2 = -3/2$ | |
|-----|-------------------------|----------|-------------------------|----------|-------------------------|----------|-------------------------|----------|
| | TCSA | FF | TCSA | FF | TCSA | FF | TCSA | FF |
| 2 | 0.077674 | 0.089849 | 0.048170 | 0.054711 | 0.064623 | 0.074763 | 0.042031 | 0.047672 |
| 4 | 0.072104 | 0.073571 | 0.049790 | 0.050566 | 0.062533 | 0.063932 | 0.044034 | 0.044716 |
| 6 | 0.056316 | 0.056444 | 0.045031 | 0.045100 | 0.051828 | 0.052009 | 0.040659 | 0.040724 |
| 8 | 0.042051 | 0.042054 | 0.039191 | 0.039193 | 0.041370 | 0.041394 | 0.036284 | 0.036287 |
| 10 | 0.031146 | 0.031144 | 0.033469 | 0.033467 | 0.032757 | 0.032759 | 0.031850 | 0.031849 |
| 12 | 0.023247 | 0.023245 | 0.028281 | 0.028279 | 0.026005 | 0.026004 | 0.027687 | 0.027684 |
| 14 | 0.017619 | 0.017616 | 0.023780 | 0.023777 | 0.020802 | 0.020799 | 0.023941 | 0.023936 |
| 16 | 0.013604 | 0.013599 | 0.019982 | 0.019977 | 0.016808 | 0.016802 | 0.020659 | 0.020652 |
| 18 | 0.010717 | 0.010702 | 0.016831 | 0.016822 | 0.013735 | 0.013724 | 0.017835 | 0.017824 |
| 20 | 0.008658 | 0.008580 | 0.014249 | 0.014227 | 0.011357 | 0.011337 | 0.015432 | 0.015413 |

Table 3.3: Two-particle form factors $|f_2(l)|$ in the spin-1 and spin-2 sectors

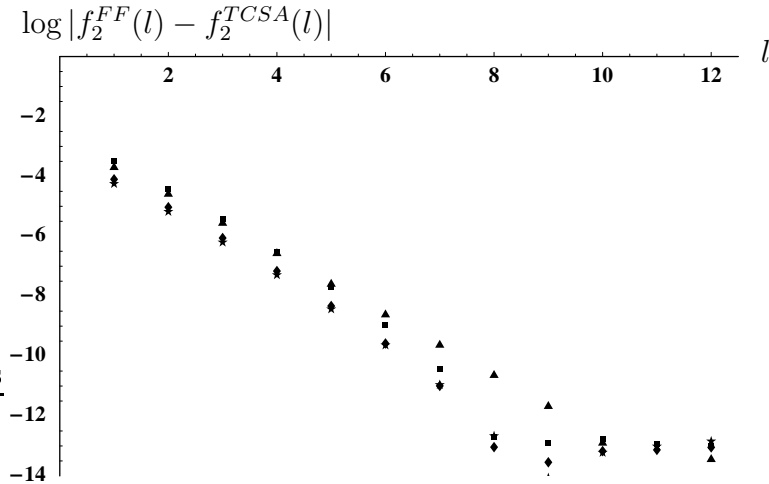


Figure 3.11: Estimating the error term in (3.13) using the data in table 3.3. The various plot symbols correspond to the same states as specified in figure 3.10.

3.3.2 Ising model in magnetic field

In this case, there is some further subtlety to be solved before proceeding to the numerical comparison. Namely, there are spin-0 states which are parity reflections of each other, but are degenerate according to the Bethe-Yang equations. An example is the state $|\{1, -1\}\rangle_{12}$ in figure 3.12 (b), which is degenerate with $|\{-1, 1\}\rangle_{12}$ to all orders in $1/L$. In general the degeneracy of these states is lifted by residual finite size effects (more precisely by quantum mechanical tunneling – a detailed discussion of this mechanism was given in the framework of the k -folded sine-Gordon model in [102]). Since the finite volume spectrum is parity symmetric, the TCSA eigenvectors correspond to the states

$$|\{1, -1\}\rangle_{12,L}^{\pm} = \frac{1}{\sqrt{2}} (|\{1, -1\}\rangle_{12,L} \pm |\{-1, 1\}\rangle_{12,L})$$

Because the Hilbert space inner product is positive definite, the TCSA eigenvectors $|\{1, -1\}\rangle_{12}^{\pm}$ can be chosen orthonormal and the problem can be resolved by calculating the form factor matrix element using the two-particle state vectors

$$\frac{1}{\sqrt{2}} (|\{1, -1\}\rangle_{12,L}^{+} \pm |\{1, -1\}\rangle_{12,L}^{-})$$

Because the Ising spectrum is much more complicated than that of the scaling Lee-Yang model (and truncation errors are larger as well), we only identified two-particle states containing two copies of A_1 , or an A_1 and an A_2 . The numerical results are plotted in figures 3.12 (a) and (b), respectively. The finite volume form factor functions of the operator Ψ (3.12) are defined as

$$\bar{f}_{11}(l)_{I_1 I_2} = \sqrt{\rho_{11}(\tilde{\theta}_1(l), \tilde{\theta}_2(l))} \langle 0 | \Psi | \{I_1, I_2\} \rangle_{11}$$

where

$$\begin{aligned} l \sinh \tilde{\theta}_1 + \delta_{11}(\tilde{\theta}_1 - \tilde{\theta}_2) &= 2\pi I_1 \\ l \sinh \tilde{\theta}_2 + \delta_{11}(\tilde{\theta}_2 - \tilde{\theta}_1) &= 2\pi I_2 \\ \rho_{11}(\theta_1, \theta_2) &= l^2 \cosh \theta_1 \cosh \theta_2 + l \cosh \theta_1 \varphi_{11}(\theta_2 - \theta_1) + l \cosh \theta_2 \varphi_{11}(\theta_1 - \theta_2) \\ \varphi_{11}(\theta) &= \frac{d\delta_{11}(\theta)}{d\theta} \end{aligned}$$

and

$$\bar{f}_{12}(l)_{I_1 I_2} = \sqrt{\rho_{11}(\tilde{\theta}_1, \tilde{\theta}_2)} \langle 0 | \Psi | \{I_1, I_2\} \rangle_{12}$$

with

$$\begin{aligned} l \sinh \tilde{\theta}_1 + \delta_{12}(\tilde{\theta}_1 - \tilde{\theta}_2) &= 2\pi I_1 \\ \frac{m_2}{m_1} l \sinh \tilde{\theta}_2 + \delta_{12}(\tilde{\theta}_2 - \tilde{\theta}_1) &= 2\pi I_2 \\ \rho_{12}(\theta_1, \theta_2) &= \frac{m_2}{m_1} l^2 \cosh \theta_1 \cosh \theta_2 + l \cosh \theta_1 \varphi_{12}(\theta_2 - \theta_1) + \frac{m_2}{m_1} l \cosh \theta_2 \varphi_{12}(\theta_1 - \theta_2) \\ \varphi_{12}(\theta) &= \frac{d\delta_{12}(\theta)}{d\theta} \end{aligned}$$

and are compared against the form factor functions

$$F_2^\Psi(\tilde{\theta}_1(l), \tilde{\theta}_2(l))_{11}$$

and

$$F_2^\Psi(\tilde{\theta}_1(l), \tilde{\theta}_2(l))_{12}$$

respectively.

Although (as we already noted) truncation errors in the Ising model are much larger than in the Lee-Yang case, extrapolation in the cutoff improves them by an order of magnitude compared to the evaluation at the highest cutoff (in our case 30). After extrapolation, deviations in the scaling region become less than 1% (with a minimum of around 10^{-3} in the $A_1 A_1$, and 10^{-4} in the $A_1 A_2$ case), and even better for states with nonzero total spin. As noted in the previous subsection this means that the numerics is really sensitive to the dependence of the particle rapidities and state density factors on the interaction between the particles; generally the truncation errors in the extrapolated data are about two orders of magnitude smaller than the interaction corrections.

It is a general tendency that the agreement is better in the sectors with nonzero spin, and the scaling region starts at smaller values of the volume. This is easy to understand for the energy levels, since for low-lying states nonzero spin generally means higher particle momenta. The higher the momenta of the particles, the more the Bethe-Yang contributions dominate over the residual finite size effects. This is consistent with the results of Rummukainen and Gottlieb in [103] where it was found that resonance phase shifts can be more readily extracted from sectors with nonzero momentum; our data show that this observation carries over to general matrix elements as well.

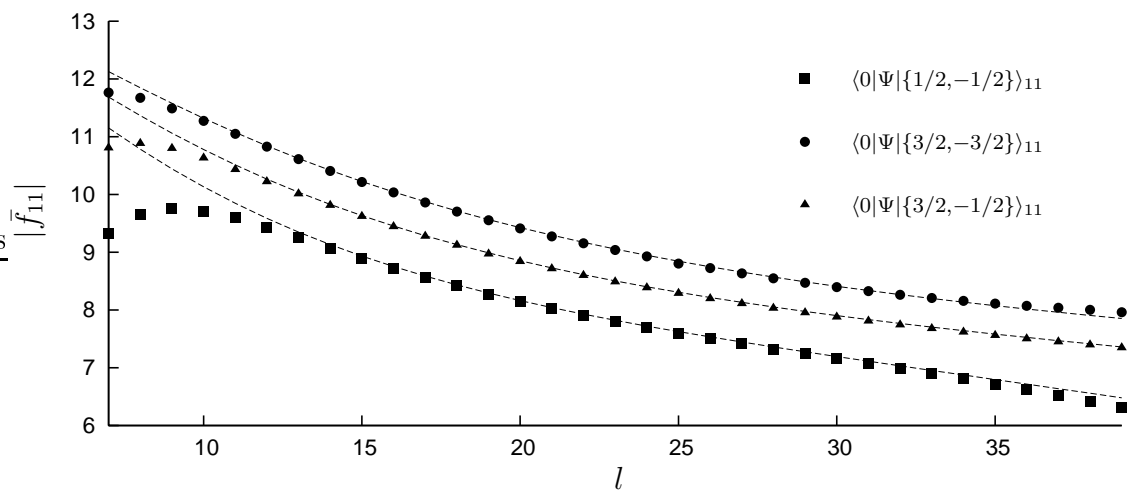
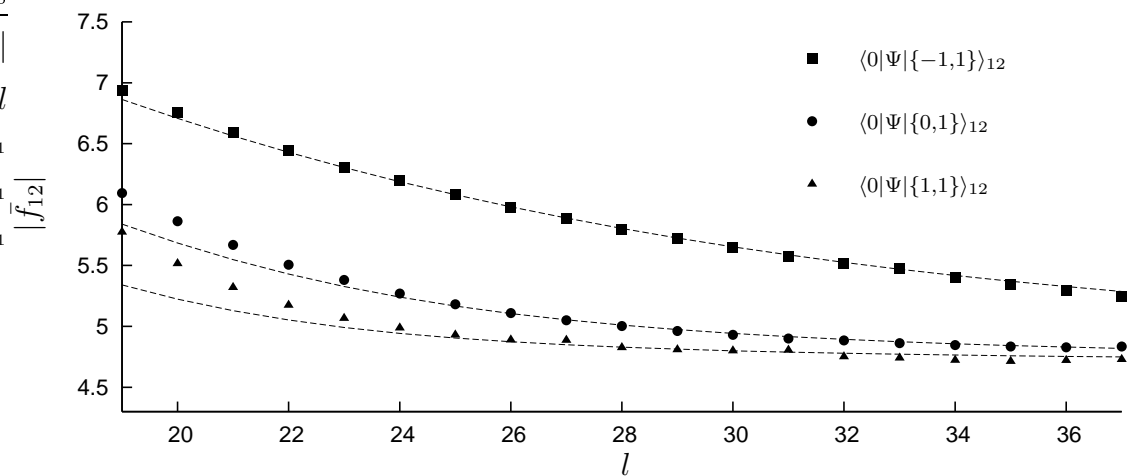
(a) $A_1 A_1$ (b) $A_1 A_2$

Figure 3.12: Two-particle form factors in the Ising model. Dots correspond to TCSA data, while the lines show the corresponding form factor prediction.

3.4 Many-particle form factors

3.4.1 Scaling Lee-Yang model

We also performed numerical evaluation of three and four-particle form factors in the scaling Lee-Yang model; some of the results are presented in figures 3.13 and 3.14, respectively. For the sake of brevity we refrain from presenting explicit numerical tables; we only mention that the agreement between the numerical TCSA data and the prediction from the exact form factor solution is always better than 10^{-3} in the scaling region. For better visibility we plotted the functions

$$\tilde{f}_k(l)_{I_1 \dots I_k} = -im^{2/5} \sqrt{\rho_k(\tilde{\theta}_1, \dots, \tilde{\theta}_k)} \langle 0 | \Phi | \{I_1, \dots, I_k\} \rangle_L \quad , \quad l = mL$$

for which relation (2.16) gives:

$$\tilde{f}_k(l)_{I_1 \dots I_k} = -im^{2/5} F_k^\Phi(\tilde{\theta}_1, \dots, \tilde{\theta}_k) + O(e^{-l}) \quad (3.14)$$

Due to the fact that in the Lee-Yang model there is only a single particle species, we introduced the simplified notation ρ_n for the n -particle Jacobi determinant.

The complication noted in subsection 3.2.2 for the Ising state $|\{1, -1\}\rangle_{12}$ is present in the Lee-Yang model as well. The Bethe-Yang equations give degenerate energy values for the states $|\{I_1, \dots, I_k\}\rangle_L$ and $|\{-I_k, \dots, -I_1\}\rangle_L$ (as noted before, the degeneracy is lifted by quantum mechanical tunneling). For states with nonzero spin this causes no problem, because these two states are in sectors of different spin (their spins differ by a sign) and similarly there is no difficulty when the two quantum number sets are identical, i.e.

$$\{I_1, \dots, I_k\} = \{-I_1, \dots, -I_k\}$$

since then there is a single state. However, there are states in the zero spin sector (i.e. with $\sum_k I_k = 0$) for which

$$\{I_1, \dots, I_k\} \neq \{-I_1, \dots, -I_k\}$$

We use two such pairs of states in our data here: the three-particle states $|\{3, -1, -2\}\rangle_L$, $|\{2, 1, -3\}\rangle_L$ and the four-particle states $|\{7/2, 1/2, -3/2, -5/2\}\rangle_L$, $|\{5/2, 3/2, -1/2, -7/2\}\rangle_L$. Again, the members of such pairs are related to each other by spatial reflection, which is a symmetry of the exact finite-volume Hamiltonian and therefore (supposing that the eigenvectors are orthonormal) the finite volume eigenstates correspond to

$$|\{I_1, \dots, I_k\}\rangle_L^\pm = \frac{1}{\sqrt{2}} (|\{I_1, \dots, I_k\}\rangle_L \pm |\{-I_k, \dots, -I_1\}\rangle_L)$$

and this must be taken into account when evaluating the form factor matrix elements. In the Lee-Yang case, however, the inner product is not positive definite (and some nonzero

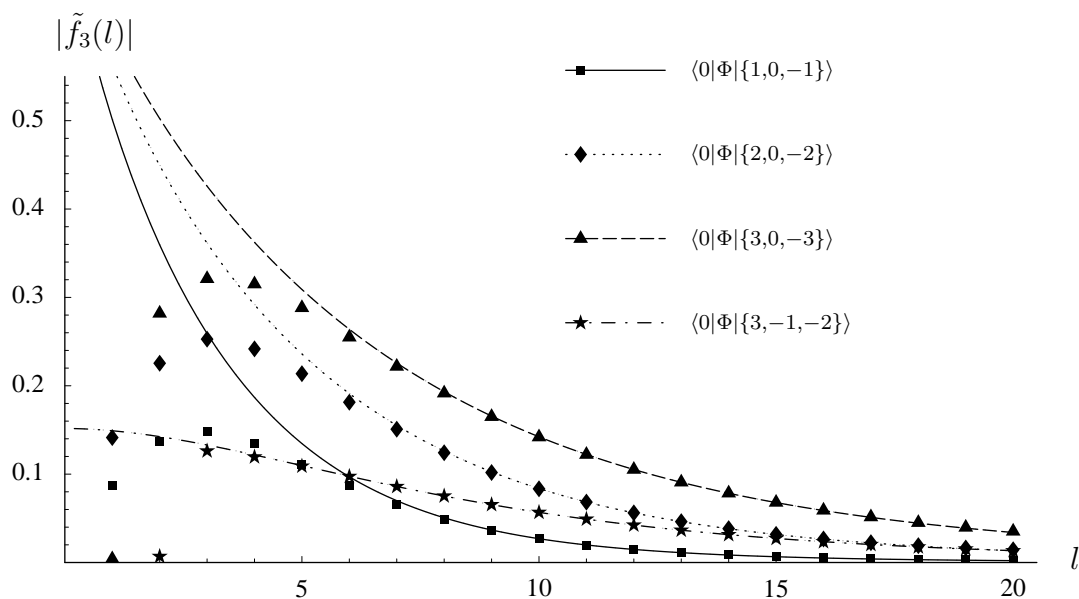


Figure 3.13: Three-particle form factors in the spin-0 sector. Dots correspond to TCSA data, while the lines show the corresponding form factor prediction.

vectors may have zero “length”, although this does not happen for TCSA eigenvectors, because they are orthogonal to each other and the inner product is non-degenerate), but there is a simple procedure that can be used in the general case. Suppose the two TCSA eigenvectors corresponding to such a pair are v_1 and v_2 . Then we can define their inner product matrix as

$$g_{ij} = v_i G^{(0)} v_j$$

using the TCSA inner product (3.2). The appropriate basis vectors of this two-dimensional subspace, which can be identified with $|\{I_1, \dots, I_k\}\rangle_L$ and $|\{-I_k, \dots, -I_1\}\rangle_L$, can be found by solving the two-dimensional generalized eigenvalue problem

$$g \cdot w = \lambda P \cdot w$$

for the vector (w_1, w_2) describing orientation in the subspace, with

$$P = \begin{pmatrix} 0 & 1 \\ 1 & 0 \end{pmatrix}$$

This procedure has the effect of rotating from the basis of parity eigenvectors to basis vectors which are taken into each other by spatial reflection.

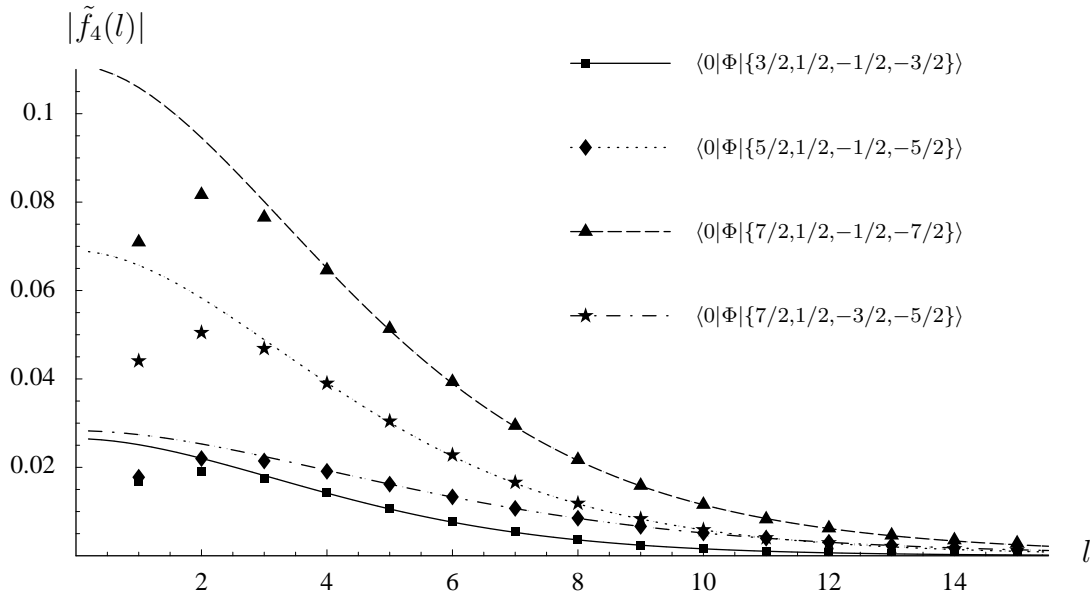


Figure 3.14: Four-particle form factors in the spin-0 sector. Dots correspond to TCSA data, while the lines show the corresponding form factor prediction.

3.4.2 Ising model in a magnetic field

As we already noted, it is much harder to identify³ higher states in the Ising model due to the complexity of the spectrum, and so we only performed an analysis of states containing three A_1 particles. We define

$$\tilde{f}_{111}(l)_{I_1 I_2 I_3} = \sqrt{\rho_{111}(\tilde{\theta}_1(l), \tilde{\theta}_2(l), \tilde{\theta}_3(l))} \langle 0 | \Psi | \{I_1, I_2, I_3\} \rangle_{111}$$

where $\tilde{\theta}_i(l)$ are the solutions of the three-particle Bethe-Yang equations in (dimensionless) volume l and ρ_{111} is the appropriate 3-particle determinant. The results of the comparison can be seen in figure 3.15. The numerical precision indicated for two-particle form factors at the end of subsection 3.2.2, as well as the remarks made there on the spin dependence apply here as well; we only wish to emphasize that for $A_1 A_1 A_1$ states with nonzero total spin the agreement between the extrapolated TCSA data and the form factor prediction in the optimal part of the scaling region is within 2×10^{-4} .

³To identify $A_1 A_1 A_1$ states it is necessary to use at least $e_{\text{cut}} = 22$ or 24 and even then the agreement with the Bethe-Yang prediction is still only within 20%, but the identification can be made for the first few $A_1 A_1 A_1$ states using data up to $e_{\text{cut}} = 30$. Truncation errors are substantially decreased by extrapolation to $e_{\text{cut}} = \infty$.

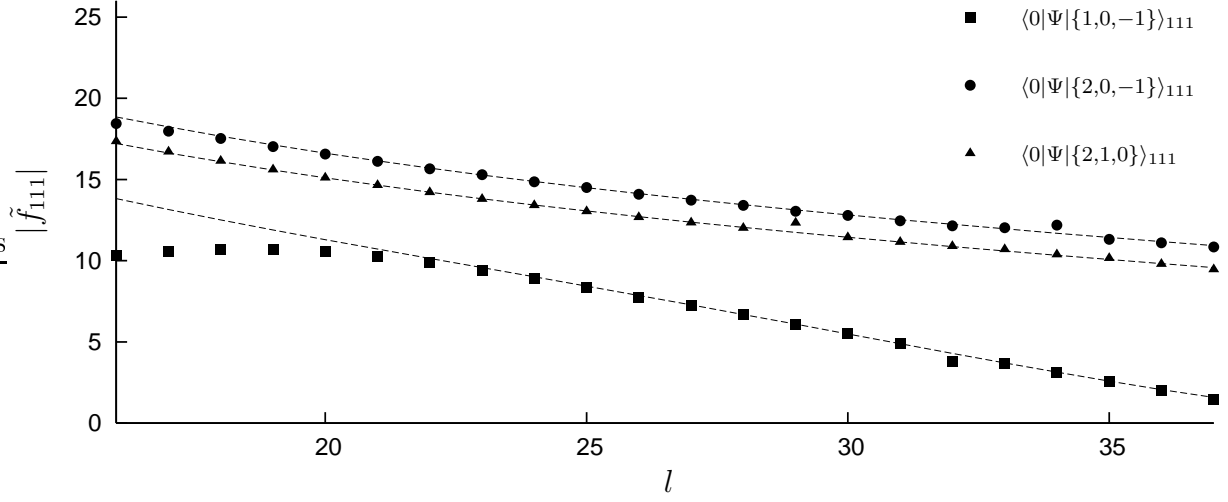


Figure 3.15: Three-particle form factors in the Ising model. Dots correspond to TCSA data, while the lines show the corresponding form factor prediction.

3.5 General form factors without disconnected pieces

3.5.1 Scaling Lee-Yang model

In this model there is a single particle species, so we can introduce the following notations:

$$f_{kn}(l)_{I_1, \dots, I_n}^{I'_1, \dots, I'_k} = -im^{2/5} \langle \{I'_1, \dots, I'_k\} | \Phi(0, 0) | \{I_1, \dots, I_n\} \rangle_L$$

and also

$$\tilde{f}_{kn}(l)_{I_1, \dots, I_n}^{I'_1, \dots, I'_k} = -im^{2/5} \sqrt{\rho_k(\tilde{\theta}'_1, \dots, \tilde{\theta}'_k)} \sqrt{\rho_n(\tilde{\theta}_1, \dots, \tilde{\theta}_n)} \langle \{I'_1, \dots, I'_k\} | \Phi(0, 0) | \{I_1, \dots, I_n\} \rangle_L$$

for which relation (2.18) yields

$$\begin{aligned} f_{kn}(l)_{I_1, \dots, I_n}^{I'_1, \dots, I'_k} &= -im^{2/5} \frac{F_{k+n}^\Phi(\tilde{\theta}'_k + i\pi, \dots, \tilde{\theta}'_1 + i\pi, \tilde{\theta}_1, \dots, \tilde{\theta}_n)}{\sqrt{\rho_n(\tilde{\theta}_1, \dots, \tilde{\theta}_n) \rho_k(\tilde{\theta}'_1, \dots, \tilde{\theta}'_k)}} + O(e^{-l}) \\ \tilde{f}_{kn}(l)_{I_1, \dots, I_n}^{I'_1, \dots, I'_k} &= -im^{2/5} F_{k+n}^\Phi(\tilde{\theta}'_k + i\pi, \dots, \tilde{\theta}'_1 + i\pi, \tilde{\theta}_1, \dots, \tilde{\theta}_n) + O(e^{-l}) \end{aligned} \quad (3.15)$$

For the plots we chose to display f or \tilde{f} depending on which one gives a better visual picture. The numerical results shown here are just a fraction of the ones we actually obtained, but all of them show an agreement with precision $10^{-4} - 10^{-3}$ in the scaling region (the volume range corresponding to the scaling region typically varies depending on the matrix element considered due to variation in the residual finite size corrections and truncation effects).

The simplest cases involve one and two-particle states: the one-particle–one-particle data in figure 3.16 actually test the two-particle form factor F_2^Φ , while the one-particle–two-particle plot 3.17 corresponds to F_3^Φ (we obtained similar results on F_4^Φ using matrix

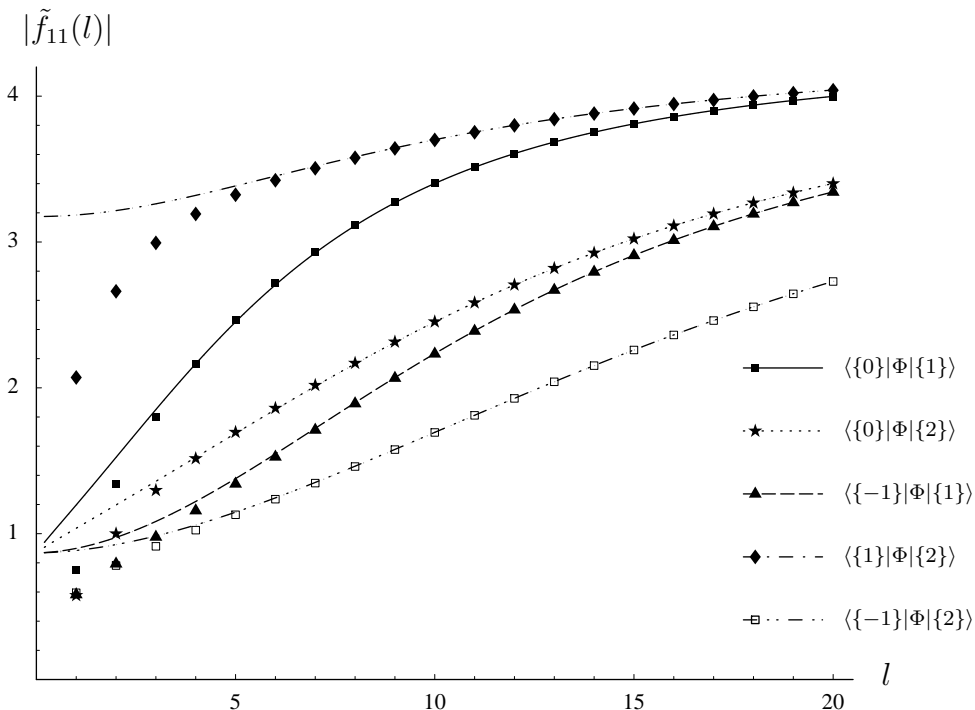


Figure 3.16: One-particle–one-particle form factors in Lee-Yang model. Dots correspond to TCSA data, while the lines show the corresponding form factor prediction.

elements f_{22}). Note that in contrast to the comparisons performed in subsections 3.2 and 3.3, these cases involve the form factor solutions (3.5) at complex values of the rapidities. In general, all tests performed with TCSA can test form factors at rapidity arguments with imaginary parts 0 or π , which are the only parts of the complex rapidity plane where form factors eventually correspond to physical matrix elements.

One-particle–three-particle and one-particle–four-particle matrix elements f_{13} and f_{14} contribute another piece of useful information. We recall that there are pairs of parity-related states in the spin-0 factors which we cannot distinguish in terms of their elementary form factors. In subsection 3.3 we showed the example of the three-particle states

$$|\{3, -1, -2\}\rangle_L \text{ and } |\{2, 1, -3\}\rangle_L$$

and the four-particle states

$$|\{7/2, 1/2, -3/2, -5/2\}\rangle_L \text{ and } |\{5/2, 3/2, -1/2, -7/2\}\rangle_L$$

In fact it is only true that they cannot be distinguished if the left state is parity-invariant. However, using a one-particle state of nonzero spin on the left it is possible to distinguish and appropriately label the two states, as shown in figures 3.18 and 3.19. This can also be done using matrix elements with two-particle states of nonzero spin: the two-particle–three-particle case f_{23} is shown in 3.20 (similar results were obtained for f_{24}). Examining

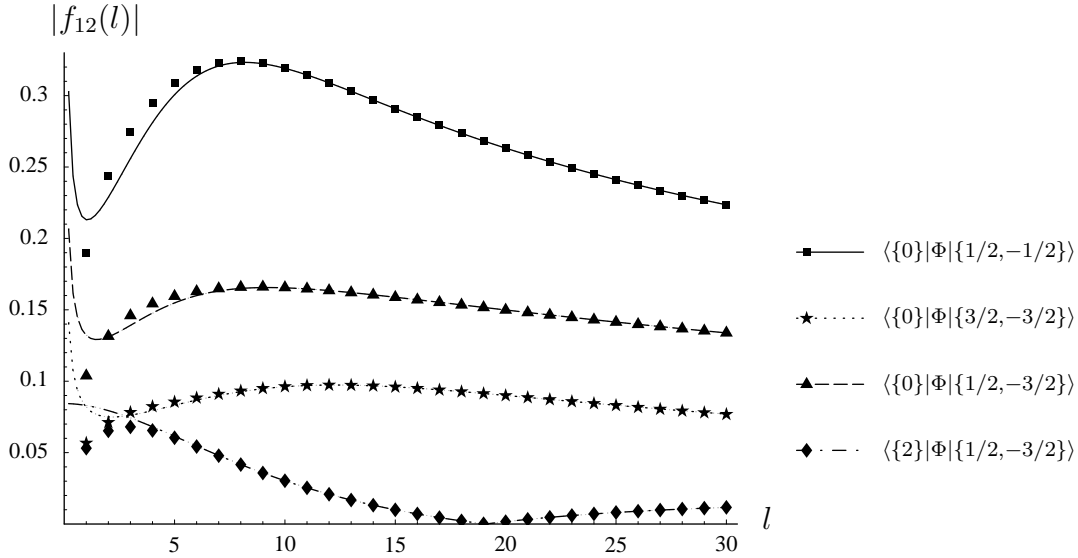


Figure 3.17: One-particle–two-particle form factors in Lee-Yang model. Dots correspond to TCSA data, while the lines show the corresponding form factor prediction.

the data in detail shows that the identifications provided using different states on the left are all consistent with each other.

It is also interesting to note that the f_{14} (figure 3.19) and f_{23} data (figure 3.20) provide a test for the five-particle form factor solutions F_5 . This is important since it is progressively harder to identify many-particle states in the TCSA spectrum for two reasons. First, the spectrum itself becomes more and more dense as we look for higher levels; second, the truncation errors grow as well. Both of these make the identification of the energy levels by comparison with the predictions of the Bethe-Yang equations more difficult; in the Lee-Yang case we stopped at four-particle levels. However, using general matrix elements and the relations (3.15) we can even get data for form factors up to 8 particles, a sample of which is shown in figures 3.21 (f_{33} and f_{44} , corresponding to 6 and 8 particle form-factors) and 3.22 (f_{34} which corresponds to 7 particle form factors).

3.5.2 Ising model in magnetic field

In the case of the Ising model, we define the functions

$$\tilde{f}_{j_1 \dots j_m; i_1 \dots i_n}(l) = \sqrt{\rho_{i_1 \dots i_n}(\tilde{\theta}_1, \dots, \tilde{\theta}_n) \rho_{j_1 \dots j_m}(\tilde{\theta}'_1, \dots, \tilde{\theta}'_m)} \times_{j_1 \dots j_m} \langle \{I'_1, \dots, I'_m\} | \Psi | \{I_1, \dots, I_n\} \rangle_{i_1 \dots i_n, L}$$

which are compared against form factors

$$F_{m+n}^\Psi(\tilde{\theta}'_m + i\pi, \dots, \tilde{\theta}'_1 + i\pi, \tilde{\theta}_1, \dots, \tilde{\theta}_n)_{j_m \dots j_1 i_1 \dots i_n}$$

where $\tilde{\theta}_i$ and $\tilde{\theta}'_j$ denote the rapidities obtained as solutions of the appropriate Bethe-Yang equations at the given value of the volume. We chose states for which the necessary form

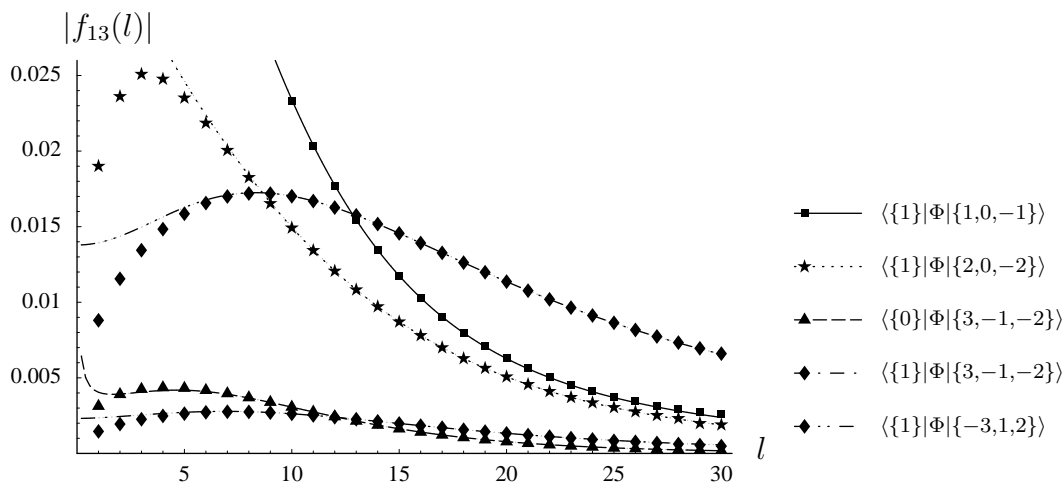


Figure 3.18: One-particle–three-particle form factors in Lee-Yang model. Dots correspond to TCSA data, while the lines show the corresponding form factor prediction.

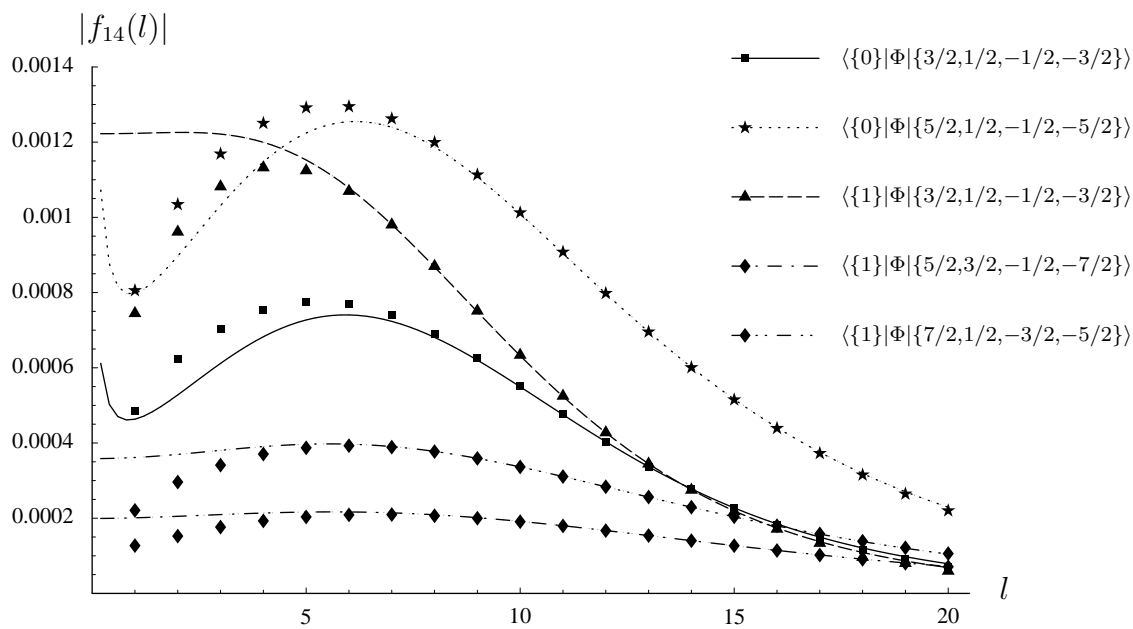


Figure 3.19: One-particle–four-particle form factors in Lee-Yang model. Dots correspond to TCSA data, while the lines show the corresponding form factor prediction.

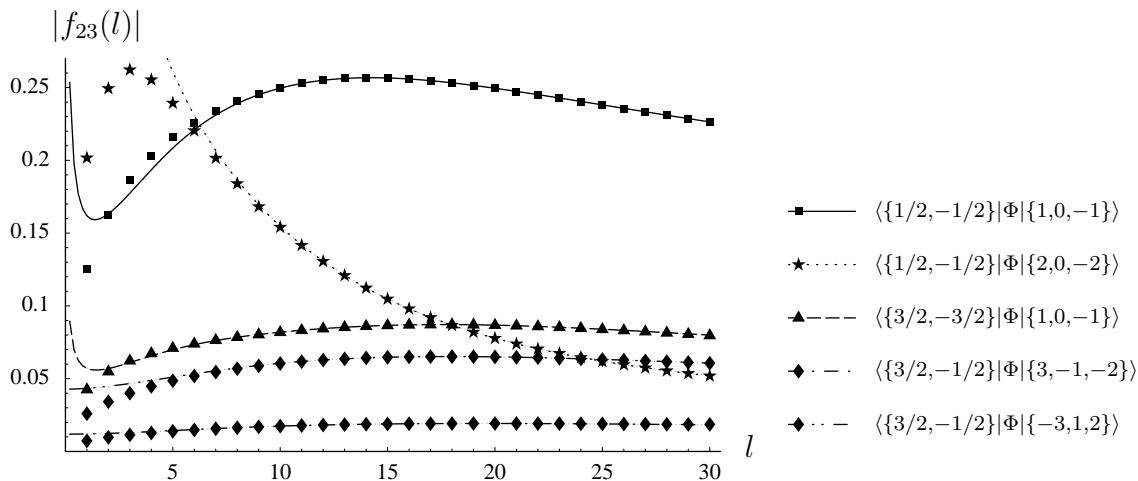


Figure 3.20: Two-particle–three-particle form factors in Lee-Yang model. Dots correspond to TCSA data, while the lines show the corresponding form factor prediction.

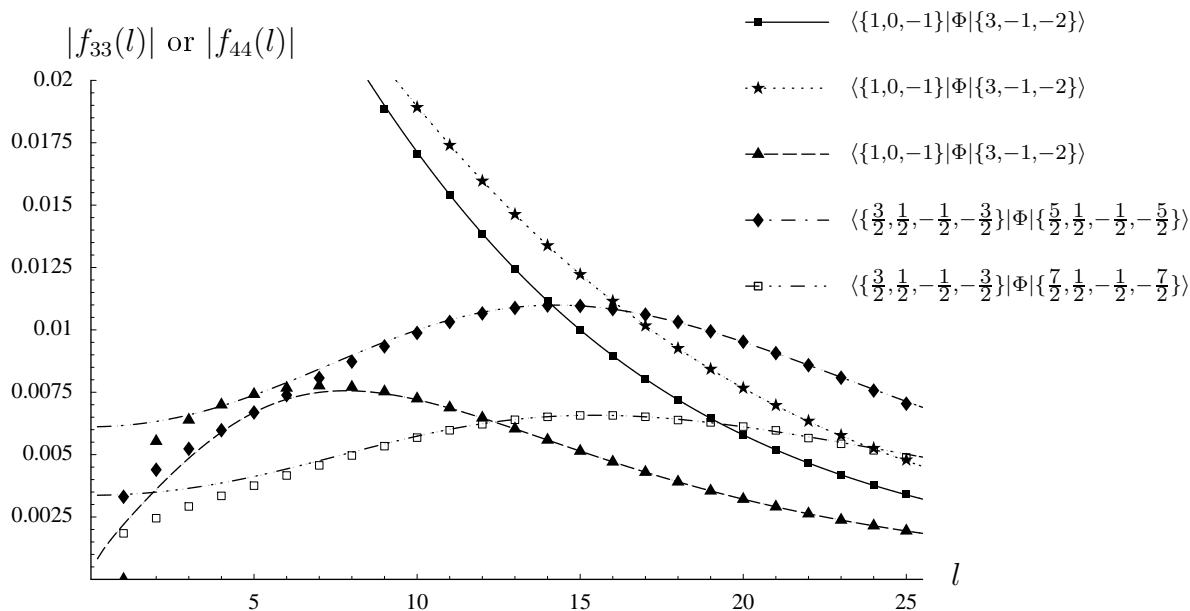


Figure 3.21: Three-particle–three-particle and four-particle–four-particle form factors in Lee-Yang model. Dots correspond to TCSA data, while the lines show the corresponding form factor prediction.

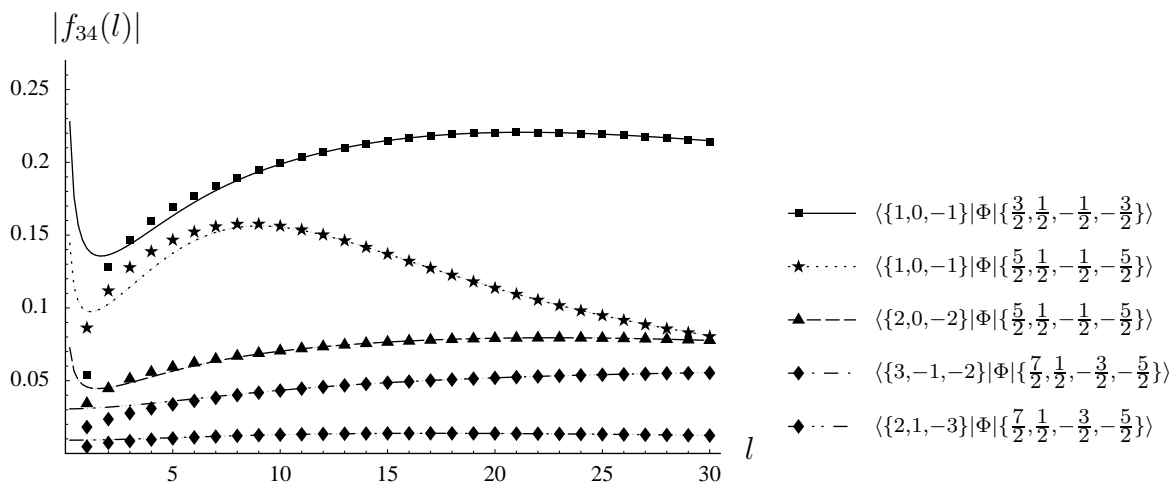


Figure 3.22: Three-particle–four-particle form factors in Lee-Yang model. Dots correspond to TCSA data, while the lines show the corresponding form factor prediction.

factor solution was already known (and given in [99]) i.e. we did not construct new form factor solutions ourselves.

One-particle–one-particle form factors are shown in figure 3.23; these provide another numerical test for the two-particle form factors examined previously in subsection 3.2.2. One-particle–two-particle form factors, besides testing again the three-particle form factor $A_1 A_1 A_1$ (figure 3.24 (a)) also provide information on $A_1 A_1 A_2$ (figure 3.24 (b)).

Finally, one-particle–three-particle and two-particle–two-particle matrix elements can be compared to the $A_1 A_1 A_1 A_1$ form factor, which again shows that by considering general matrix elements we can go substantially higher in the form factor tree than using only elementary form factors.

We remark that the cusps on the horizontal axis in the form factor plots correspond to zeros where the form factors change sign; they are artifacts introduced by taking the absolute value of the matrix elements. The pattern of numerical deviations between TCSA data and exact form factor predictions is fully consistent with the discussion in the closing paragraphs of subsections 3.2.2 and 3.3.2. The deviations in the scaling region are around 1% on average, with agreement of the order of 10^{-3} in the optimal range.

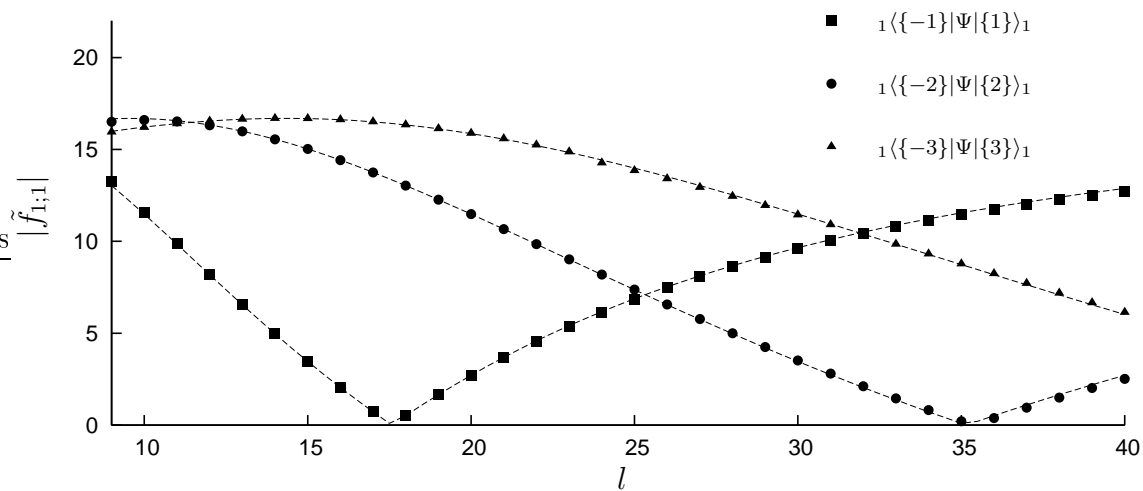
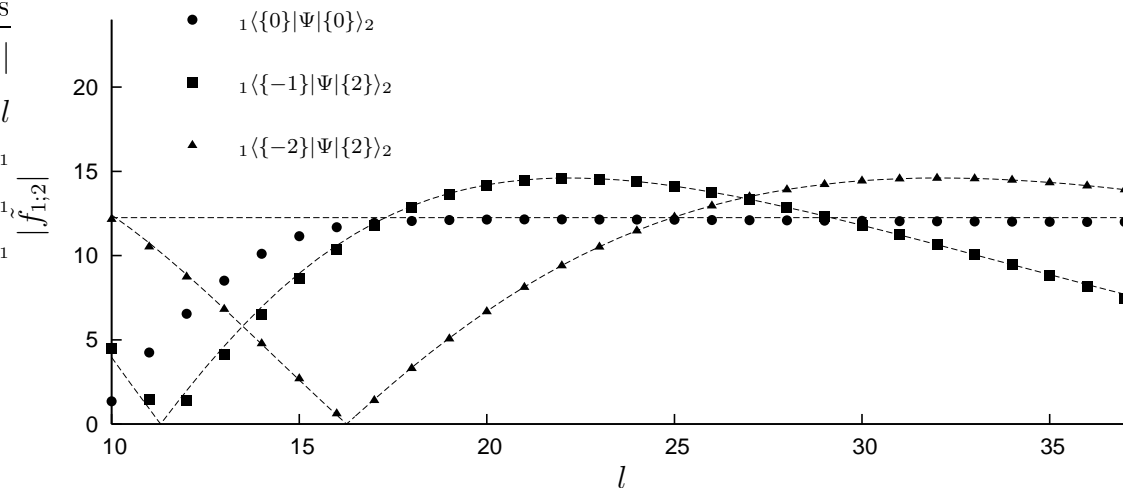
(a) $A_1 - A_1$ matrix elements(b) $A_1 - A_2$ matrix elements

Figure 3.23: One-particle-one-particle form factors in the Ising model. Dots correspond to TCSA data, while the lines show the corresponding form factor prediction.

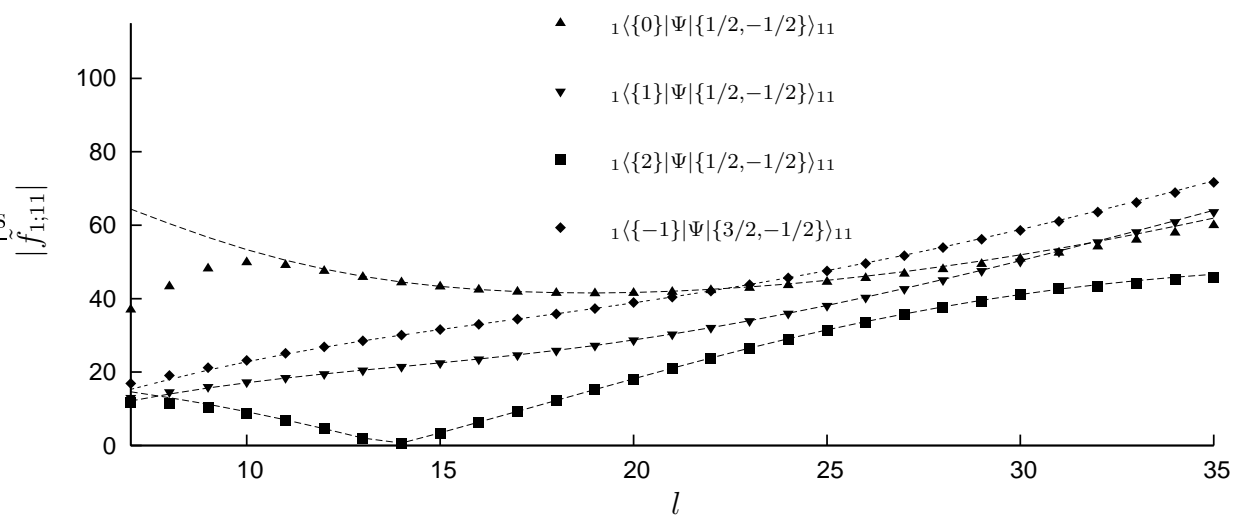
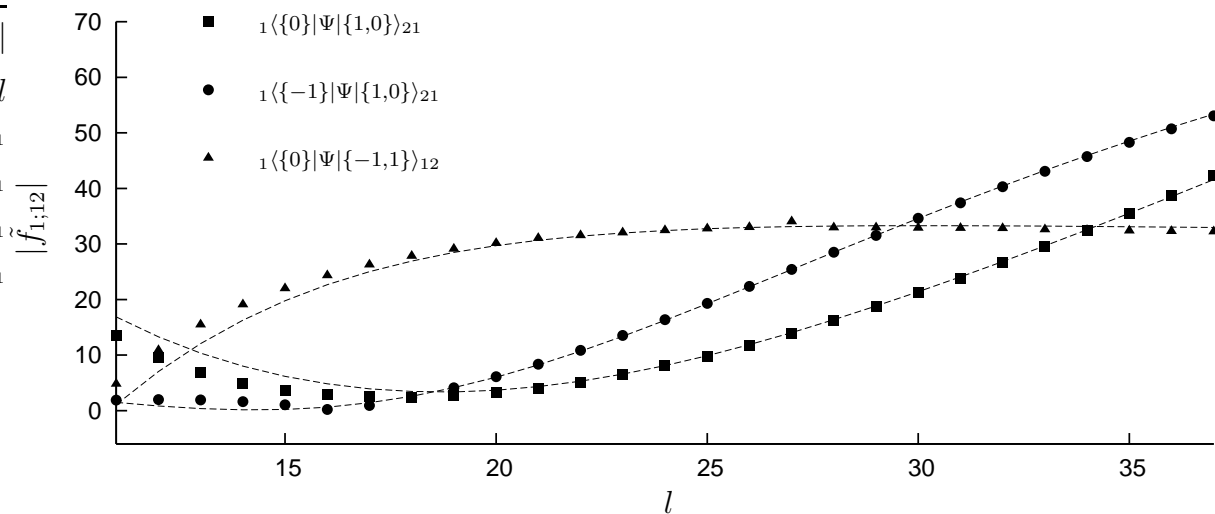
(a) $A_1 - A_1 A_1$ matrix elements(b) $A_1 - A_1 A_2$ matrix elements

Figure 3.24: One-particle-two-particle form factors in the Ising model. Dots correspond to TCSA data, while the lines show the corresponding form factor prediction.

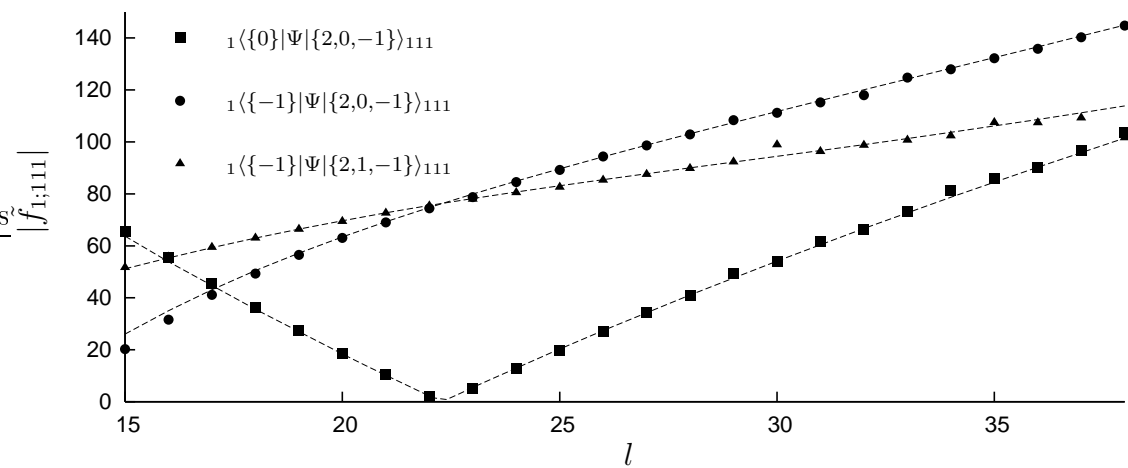
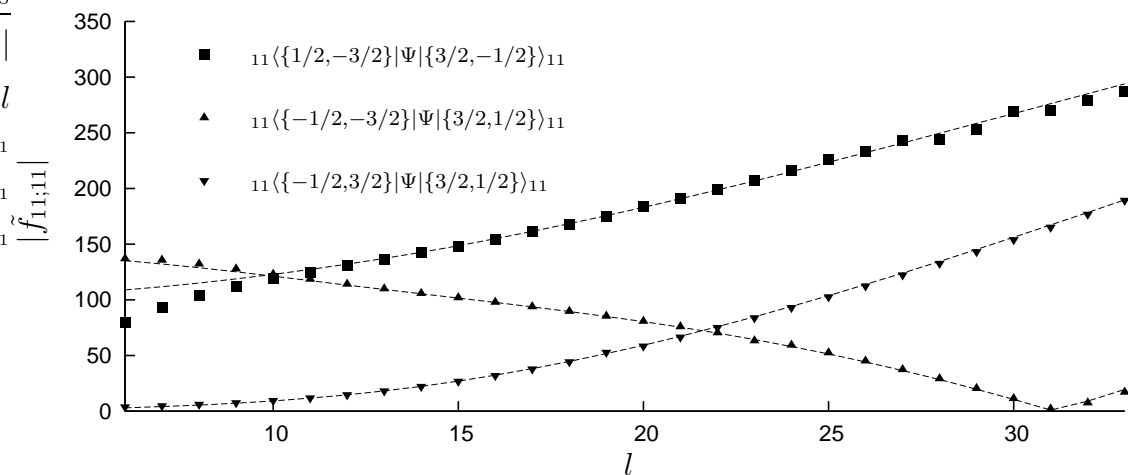
(a) $A_1 - A_1 A_1 A_1$ matrix elements(b) $A_1 A_1 - A_1 A_1$ matrix elements

Figure 3.25: One-particle–three-particle and two-particle–two-particle form factors in the Ising model. Dots correspond to TCSA data, while the lines show the corresponding form factor prediction.

3.6 Diagonal matrix elements

Here we compare the predictions of section 2.3 for the diagonal form factors to the numerical data obtained from TCSA.

3.6.1 Diagonal one-particle and two-particle form factors

Figure (3.26) shows the comparison of eqn. (2.32) to numerical data obtained from Lee-Yang TCSA: the matching is spectacular, especially in the so-called scaling region (the volume range where residual finite size corrections are of the order of truncation errors, cf. [104]) where the relative deviation is less than 10^{-4} . Diagonal one-particle matrix elements for the Ising model are shown in figure 3.27.

Formula (2.33) describing diagonal two-particle matrix elements is tested against numerical data in the Lee-Yang model in figure 3.28, and the agreement is as precise as it was for the one-particle case. Similar results can be found in the Ising case; they are shown in figure 3.29.

3.6.2 The general result

Formula 2.36 can be tested against matrix elements with $n = 3$ and $n = 4$ in the Lee-Yang model, which are displayed in figures 3.30 and 3.31, respectively. The agreement is excellent as before, with the relative deviation in the scaling region being of the order of 10^{-4} .

3.7 Zero-momentum particles

In this section we test the predictions of sec. 2.4 for disconnected pieces associated to zero-momentum particles.

3.7.1 Lee-Yang model

First we test eqn. (2.53) using low-lying symmetric states with a zero-momentum particle present. Data for matrix elements of the type

$$\langle \{0\} | \Phi | \{-I, 0, I\} \rangle_L \quad \text{and} \quad \langle \{-I', 0, I'\} | \Phi | \{-I, 0, I\} \rangle_L$$

are shown in figures 3.32 and 3.33, respectively. The agreement is precise as in all previous cases.

The support for eqn. (2.53) can be strengthened using 5-particle states. It is not easy to find them because they are high up in the spectrum, and identification using the

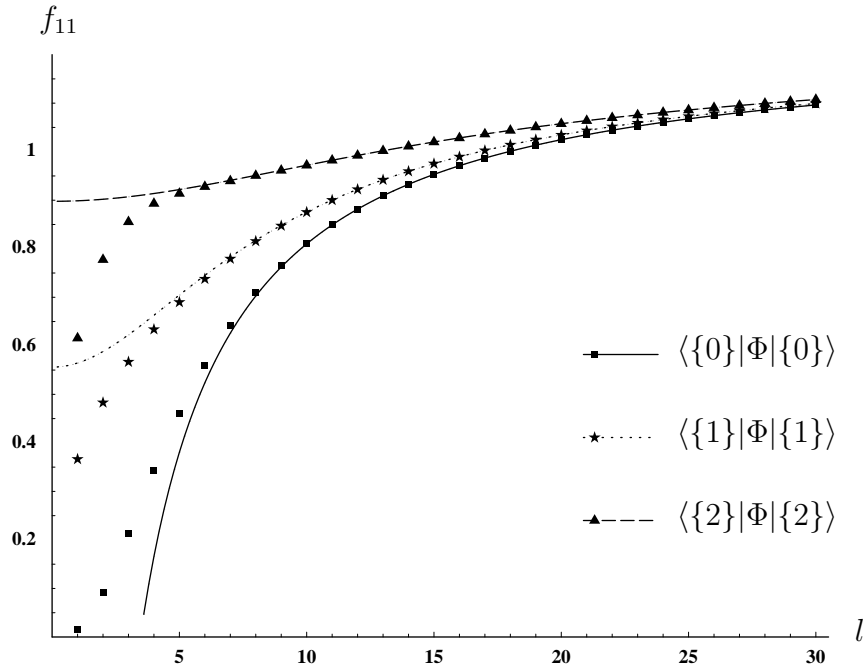


Figure 3.26: Diagonal 1-particle matrix elements in the scaling Lee-Yang model. The discrete points correspond to the TCSA data, while the continuous line corresponds to the prediction from exact form factors.

process of matching against Bethe-Yang predictions (as described in subsection 3.1.5) becomes ambiguous. We could identify the first 5-particle state by combining the Bethe-Yang matching with predictions for matrix elements with no disconnected pieces given by eqn. (2.18), as shown in figure 3.34. Some care must be taken in choosing the other state because many choices give matrix elements that are too small to be measured reliably in TCSA: since vector components and TCSA matrices are mostly of order 1 or slightly less, getting a result of order 10^{-4} or smaller involves a lot of cancellation between a large number of individual contributions, which inevitably leads to the result being dominated by truncation errors. Despite these difficulties, combining Bethe-Yang level matching with form factor evaluation we could identify the first five-particle level up to $l = 20$.

The simplest matrix element involving a five-particle state and zero-momentum disconnected pieces is the 1-5 one, but the prediction of eqn. (2.53) turns out to be too small to be usefully compared to TCSA. However, it is possible to find 3-5 matrix elements that are sufficiently large, and the data shown in figure 3.35 confirm our conjecture with a relative precision of somewhat better than 10^{-3} in the scaling region.

We close by noting that since the agreement is better than one part in 10^3 in the scaling region, which is typically found in the range of volume $l \sim 10 \dots 20$, and also this precision holds for quite a large number of independent matrix elements, the presence of

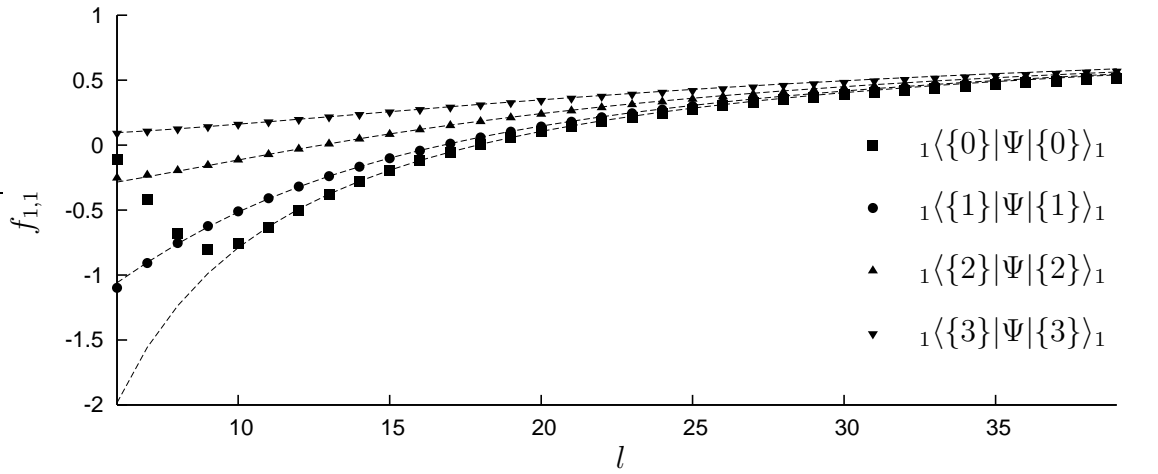
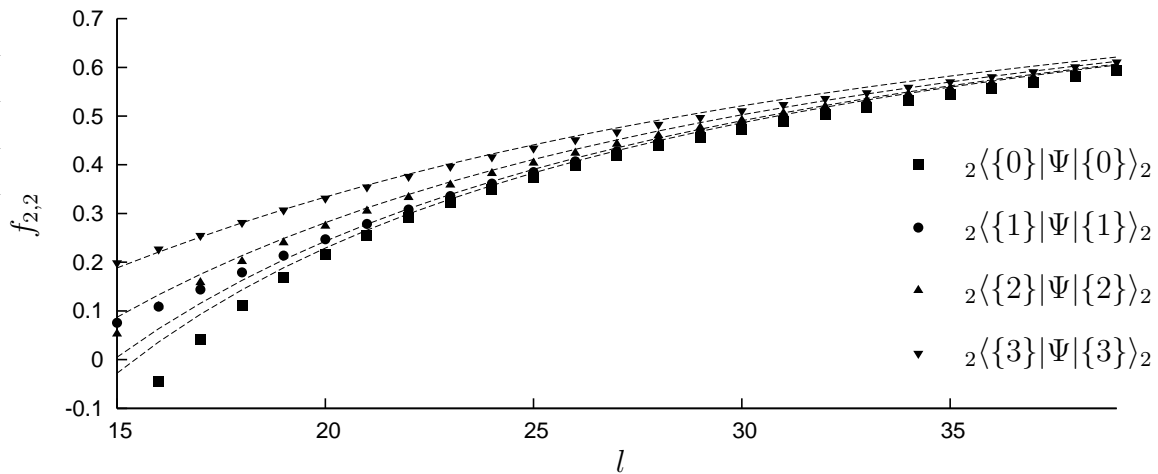
(a) A_1-A_1 (b) A_2-A_2

Figure 3.27: Diagonal 1-particle matrix elements in the Ising model. The discrete points correspond to the TCSA data, while the continuous line corresponds to the prediction from exact form factors.

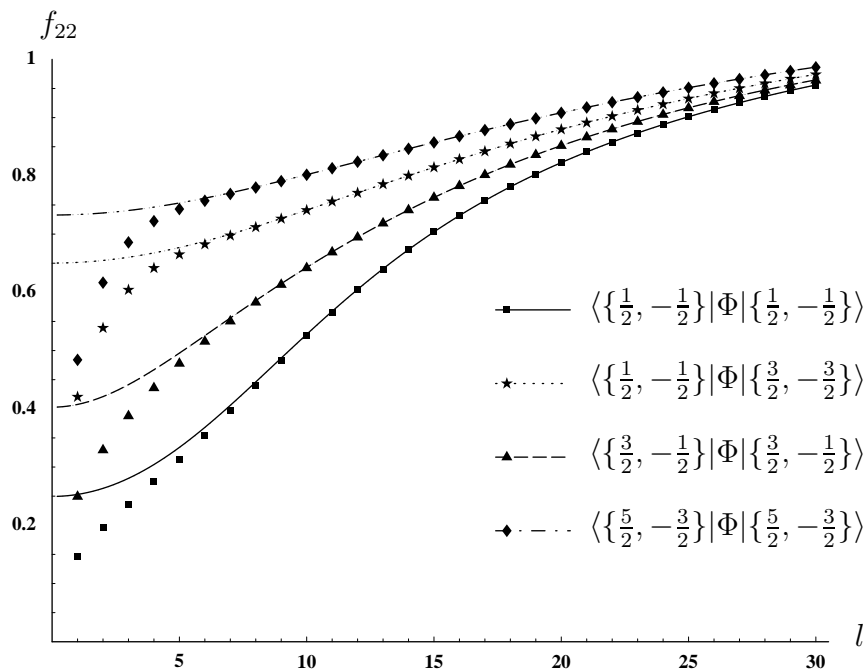


Figure 3.28: Diagonal 2-particle matrix elements in the scaling Lee-Yang model. The discrete points correspond to the TCSA data, while the continuous line corresponds to the prediction from exact form factors.

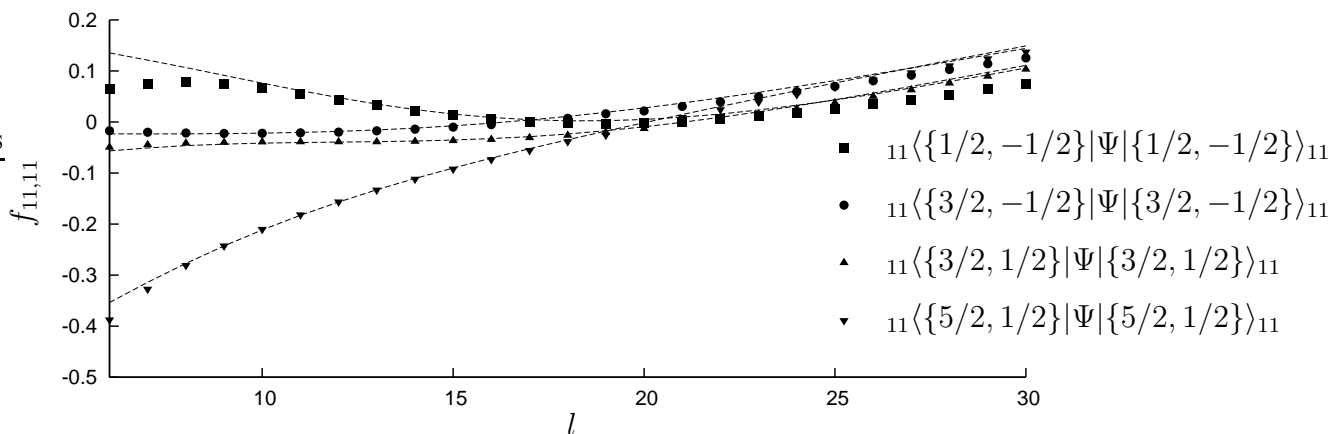


Figure 3.29: Diagonal 2-particle matrix elements in the Ising model. The discrete points correspond to the TCSA data, while the continuous line corresponds to the prediction from exact form factors.

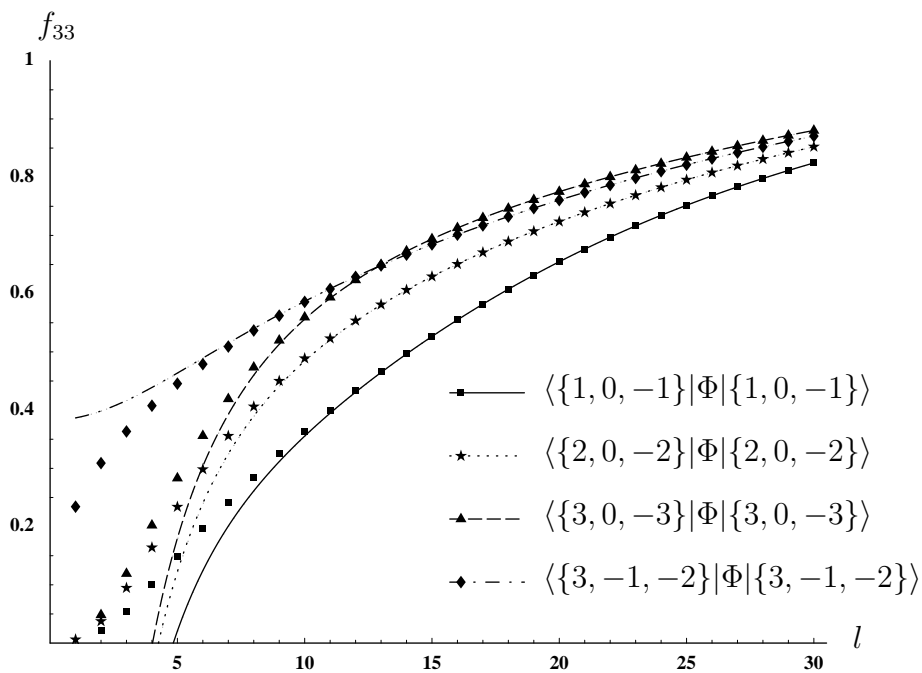


Figure 3.30: Diagonal 3-particle matrix elements in the scaling Lee-Yang model. The discrete points correspond to the TCSA data, while the continuous line corresponds to the prediction from exact form factors.

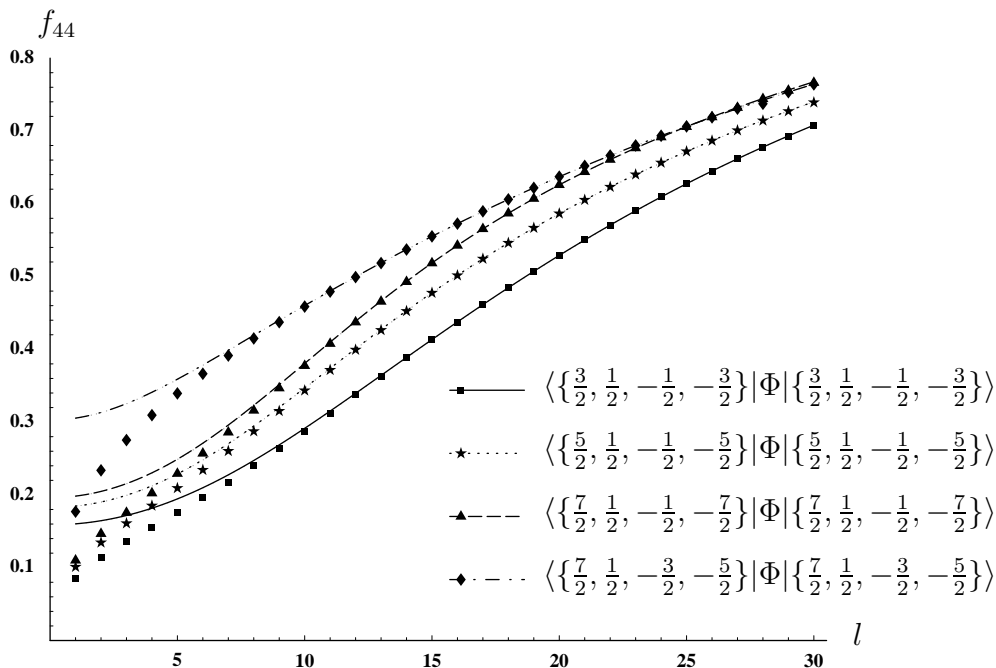


Figure 3.31: Diagonal 4-particle matrix elements in the scaling Lee-Yang model. The discrete points correspond to the TCSA data, while the continuous line corresponds to the prediction from exact form factors.

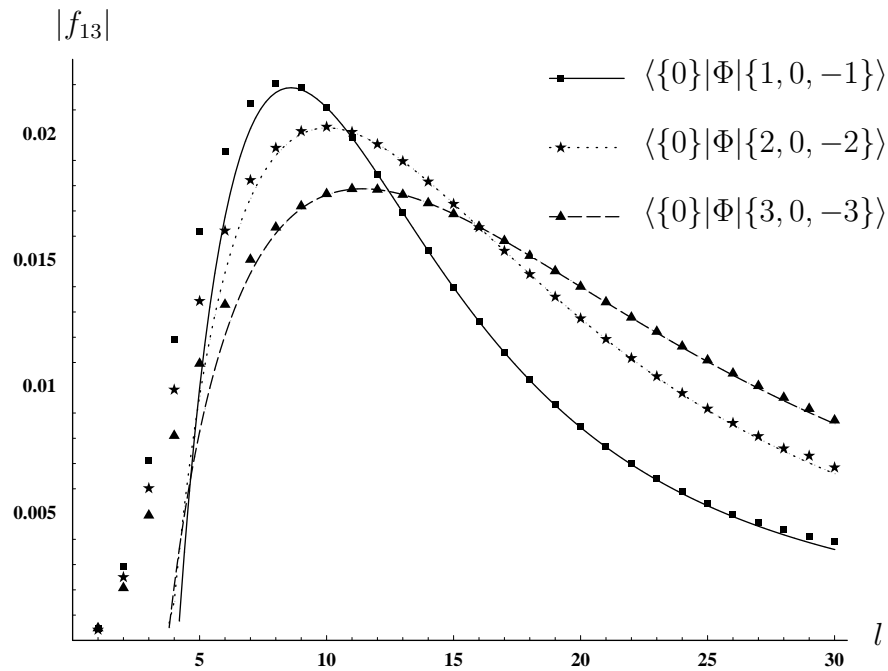


Figure 3.32: 1-particle–3-particle matrix elements in the scaling Lee-Yang model. The discrete points correspond to the TCSA data, while the continuous line corresponds to the prediction from exact form factors.

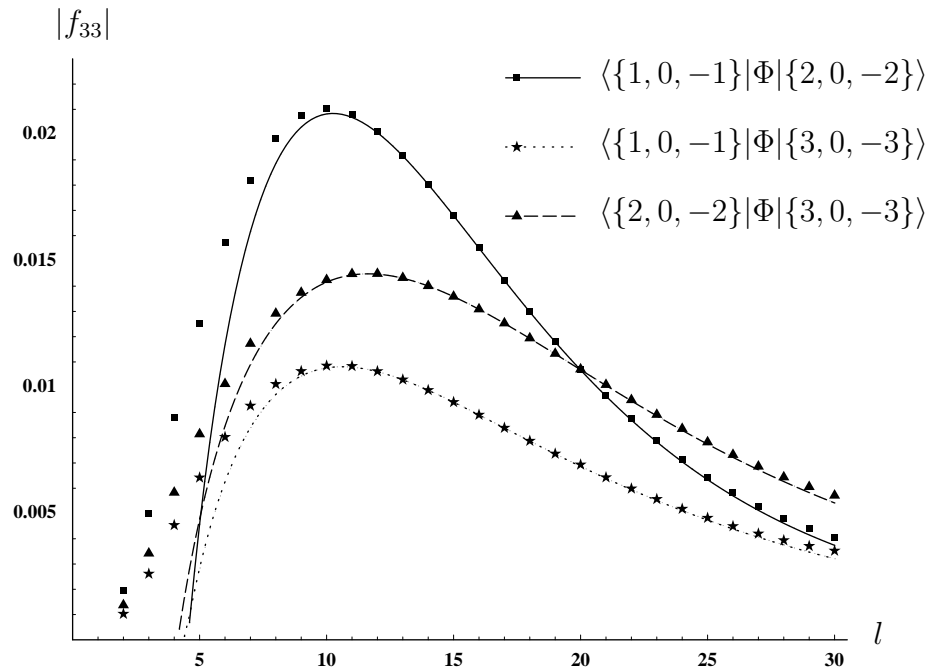


Figure 3.33: 3-particle–3-particle matrix elements in the scaling Lee-Yang model. The discrete points correspond to the TCSA data, while the continuous line corresponds to the prediction from exact form factors.

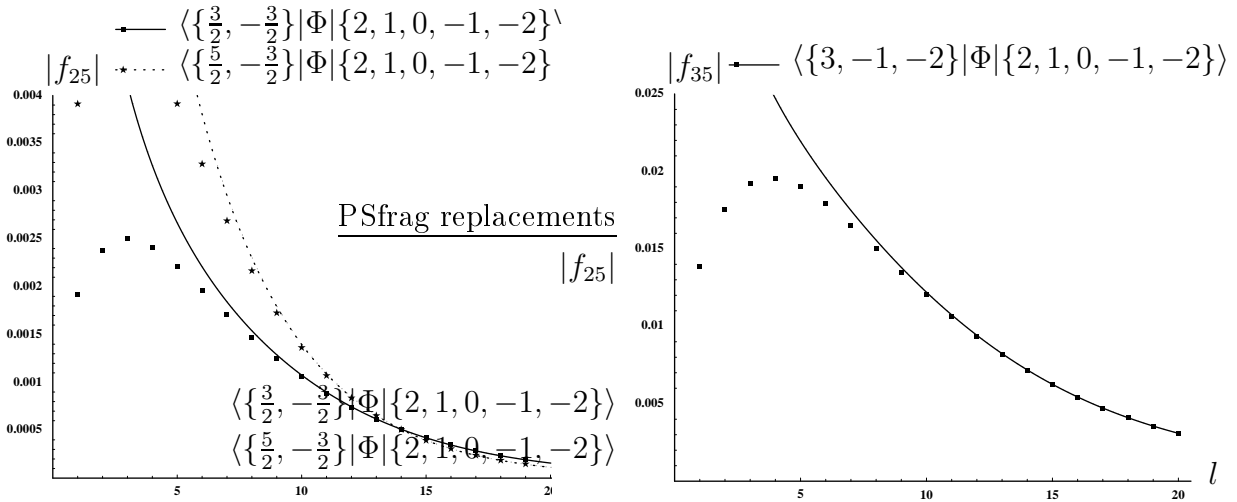


Figure 3.34: Identifying the 5-particle state using form factors. The discrete points correspond to the TCSA data, while the continuous line corresponds to the prediction from exact form factors.

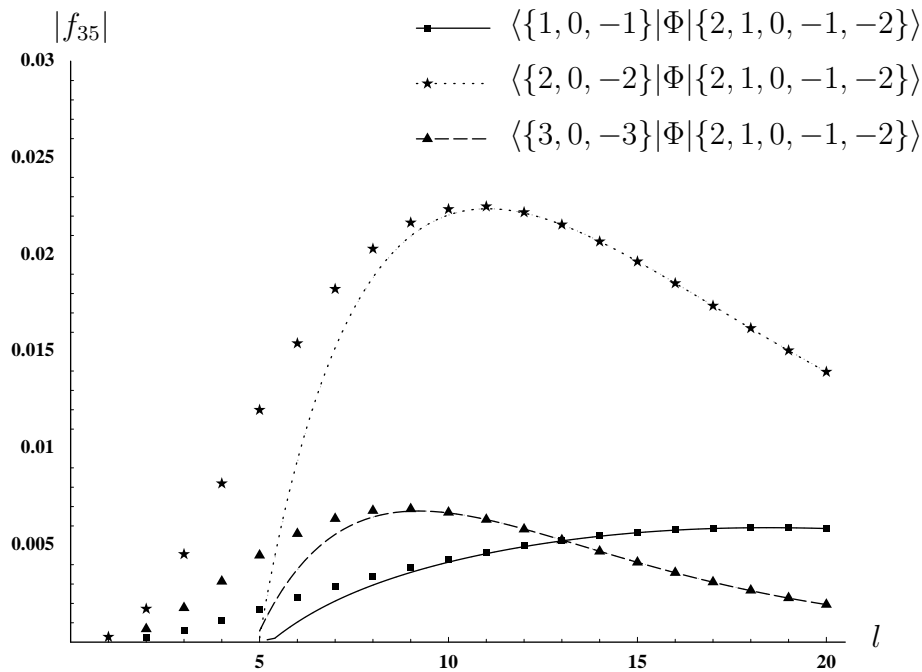


Figure 3.35: 3-particle–5-particle matrix elements in the scaling Lee-Yang model. The discrete points correspond to the TCSA data, while the continuous line corresponds to the prediction from exact form factors.

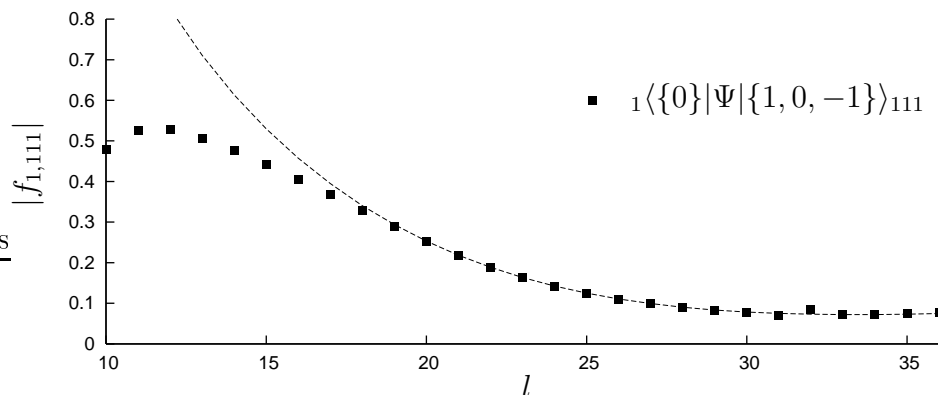


Figure 3.36: $A_1 - A_1 A_1 A_1$ matrix element in Ising model with a zero-momentum particle additional φ terms in eqn. (2.53) can be confidently excluded.

3.7.2 Ising model in magnetic field

We first test our analytic results on the example of the matrix element

$${}_1\langle\{0\}|\Phi|\{-1, 0, 1\}\rangle_{111,L}$$

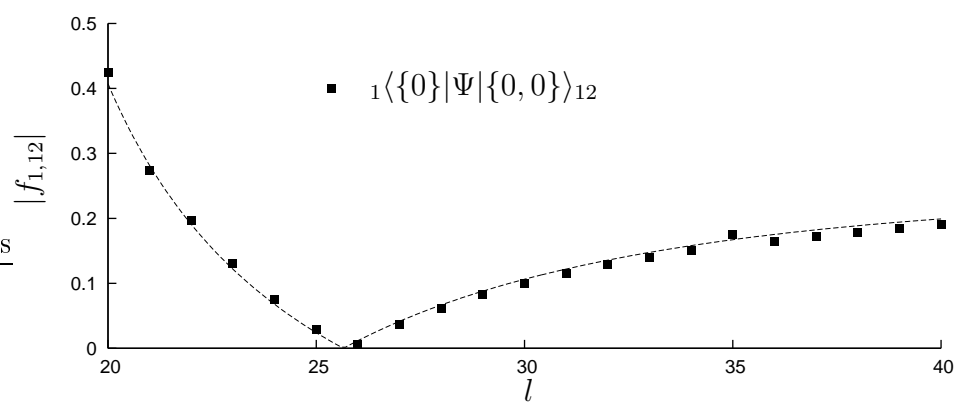
Since all particles are of species A_1 , formula (2.53) is applicable here. In figure 3.36 we plot the numerical results against the analytic prediction.

Due to the fact that the Ising model has more than one particle species, it is possible to have more than one stationary particles in the same state. Our TCSA data allow us to locate one such state, with a stationary A_1 and A_2 particle, for which we have the prediction

$$f_{1,12} = {}_1\langle\{0\}|\Psi|\{0, 0\}\rangle_{12} = \frac{1}{m_1 L \sqrt{m_2 L}} \left(\lim_{\epsilon \rightarrow 0} F_3(i\pi + \epsilon, 0, 0)_{112} + m_1 L F_1(0)_2 \right)$$

where $F_1(0)_2$ is the one-particle form factor corresponding to A_2 . This is compared to TCSA data in figure 3.37 and a convincing agreement is found.

Note that in both of figures 3.36 and 3.37 there is a point which obviously deviates from the prediction. This is a purely technical issue, and is due to the presence of a line crossing close to this particular value of the volume which makes the cutoff dependence more complicated and so slightly upsets the extrapolation in the cutoff.

Figure 3.37: $A_1 - A_1 A_2$ matrix element in Ising model with zero-momentum particle

Chapter 4

Residual finite size effects

The Bethe-Yang equations describe multi-particle energies in finite volume to all orders in $1/L$. The same holds for the results presented in section 2: formulas (2.18), (2.36) and (2.53) determine the finite volume form factors to all orders in $1/L$. The aim of this chapter is to derive the μ -term (which is the leading exponential correction) associated to moving one-particle states, generic multi-particle scattering states, and finite volume form factors.

The analytic results are derived using the principle of bound state quantization in finite volume. To confirm the calculations, all our formulas are tested against TCSA data.

We wish to remark, that there has been a recent interest in exponential corrections also in the framework of AdS/CFT correspondence. The μ -term and F-term for moving one-particle states was derived in [105] and [106], for multi-particle states in [107] and [108]. For the μ -term these results coincide with ours, but they can be considered as independent; they use completely different methods: generalizations of Lüscher's approach, summation of the vacuum fluctuations and calculations based on the TBA for excited states.

4.1 One-particle states

The energy of a moving one-particle state $|\{I\}\rangle_{c,L}$ is given to all orders by

$$E = \sqrt{m_c^2 + p_c^2} \quad \text{with} \quad p_c = \frac{2\pi I}{L} \quad (4.1)$$

Here we determine the leading μ -term associated to (4.1) Based on the description of mass corrections it is expected that this contribution is associated to the fusion $A_a A_b \rightarrow A_c$ with the smallest μ_{ab}^c . We assume that $a = b$, ie. the fusion in question is a symmetric one. This happens to be true for the lightest particle in models with the " Φ^3 -property" and for other low lying states in most known models. A possible extension to non-symmetric fusions has not yet been carried out, it is left for further research.

The (infinite volume) bootstrap principle for a symmetric fusion consists of the identification

$$|\theta\rangle_c \sim |\theta + i\bar{u}_{ac}^a, \theta - i\bar{u}_{ac}^a\rangle_{aa} \quad (4.2)$$

resulting in

$$m_c = 2m_a \cos(\bar{u}_{ac}^a) \quad (\mu_{aa}^c)^2 = m_a^2 - \frac{m_c^2}{4}$$

Smallness of μ_{aa}^c means that m_c is close to $2m_a$, in other words the binding energy is small.

For a moment let us lay aside the framework of QFT and consider quantum mechanics with an attractive potential. Bound states are described by wave functions

$$\Psi(x_1, x_2) = e^{iP(x_1+x_2)}\psi(x_1 - x_2)$$

where P is the total momentum and $\psi(x)$ is the appropriate solution of the Schrödinger equation in the relative coordinate. It is localized around $x = 0$ and shows exponential decay at infinity. Except for the region $x_1 \approx x_2$, the wave function can be approximated with a product of plane waves with imaginary momenta $p_{1,2} = P \pm ik$. The interaction results in the quantization of the allowed values of k .

The theory in finite volume is described along the same lines. There are however two differences:

- The total momentum gets quantized.
- $\psi(x)$ (and therefore k) obtains finite volume corrections.

This picture also applies to relativistic integrable theories. We consider A_c as a simple quantum mechanical bound state of two elementary particles and use the infinite volume scattering data to describe the interaction between the constituents. To develop these ideas, let us consider the spectrum of the theory defined on a circle with circumference L . We state the identification

$$|A_c(\theta)\rangle_L \sim |A_a(\theta_1)A_a(\theta_2)\rangle_L \quad (4.3)$$

where the $\theta_{1,2}$ are complex to describe a bound-state; this idea also appeared in [95, 109]. Relation (4.3) can be regarded as the finite volume realization of (4.2). The total energy and momentum of the bound state have to be purely real, constraining the rapidities to take the form

$$\theta_1 = \theta + iu, \quad \theta_2 = \theta - iu \quad (4.4)$$

where the dependence on L is suppressed. Energy and momentum are calculated as

$$E = 2m_a \cos(u) \cosh(\theta) \quad p = 2m_a \cos(u) \sinh(\theta) \quad (4.5)$$

The quantization condition for an n -particle state is given by the Bethe-Yang equations

$$e^{ip_j L} \prod_{\substack{k=1 \\ k \neq j}}^n S_{i_j i_k}(\theta_j - \theta_k) = 1, \quad j = 1 \dots n$$

To quantize the bound state in finite volume, an appropriate analytic continuation of the above equations with $n = 2$ can be applied. This procedure is justified by the same reasoning that leads to original Bethe-Yang equations: one assumes plane waves (with imaginary momenta) except for the localized interaction, which is described by the S-matrix of the infinite volume theory. Inserting (4.4) and separating the real and imaginary parts

$$e^{im_a \cos(u) \sinh(\theta)L} e^{-m_a \sin(u) \cosh(\theta)L} S_{aa}(2iu) = 1 \quad (4.6)$$

$$e^{im_a \cos(u) \sinh(\theta)L} e^{m_a \sin(u) \cosh(\theta)L} S_{aa}(-2iu) = 1 \quad (4.7)$$

Multiplying the two equations and making use of $S(2iu) = S(-2iu)^{-1}$ one arrives at

$$e^{2im_a \cos(u) \sinh(\theta)L} = 1 \quad \text{or} \quad 2m_a \cos(u) \sinh(\theta) = \frac{2\pi I}{L} \quad (4.8)$$

which is the quantization condition for the total momentum. I is to be identified with the momentum quantum number of A_c . The quantization condition for u is found by eliminating θ from (4.6):

$$e^{-m_a L \sin(u) \sqrt{1 + \left(\frac{\pi I}{m_a L \cos(u)}\right)^2}} S_{aa}(2iu) = (-1)^I \quad (4.9)$$

The exponential factor forces u to be close to the pole of the S-matrix associated to the formation of the bound-state. For the case at hand it reads

$$S_{aa}(\theta \sim iu_{aa}^c) \sim \frac{i(\Gamma_{aa}^c)^2}{\theta - iu_{aa}^c} \quad (4.10)$$

with $u_{aa}^c = 2\bar{u}_{ac}^a$. Note the appearance of $(-1)^I$ on the rhs. of (4.9), which is a natural consequence of the quantization of the total momentum. This sign determines the direction from which the pole is approached.

The exact solution of (4.9) can be developed into a power series in $e^{-\mu_{aa}^c L}$, where the first term is found by replacing u with \bar{u}_{ac}^a in the exponent:

$$u - \bar{u}_{ac}^a = (-1)^I \frac{1}{2} (\Gamma_{aa}^c)^2 e^{-\mu_{aa}^c L} \sqrt{1 + \left(\frac{2\pi I}{m_c L}\right)^2} + O(e^{-2\mu_{aa}^c L}) \quad (4.11)$$

First order corrections to the energy are readily evaluated to give

$$E = E_0 - (-1)^I (\Gamma_{aa}^c)^2 \frac{\mu_{aa}^c m_c}{E_0} e^{-\frac{\mu_{aa}^c E_0}{m_c} L} + O(e^{-2\mu_{aa}^c L}) \quad (4.12)$$

where E_0 is the ordinary one-particle energy

$$E_0 = \sqrt{m_c^2 + \left(\frac{2\pi I}{L}\right)^2}$$

In the case of zero momentum the former result simplifies to the leading term in (1.11). For large volumes we recover

$$u \rightarrow \bar{u}_{ac}^a \quad \theta \rightarrow \operatorname{arsh} \frac{2\pi I}{m_c L}$$

Having established the quantization procedure we now turn to the question of momentum quantum numbers inside the bound state. For the phase shift we adopt the convention that was used throughout this work

$$S_{ab}(\theta) = S_{ab}(0)e^{i\delta_{ab}(\theta)}$$

Note that $\delta_{ab}(iu)$ is purely imaginary.

With this choice of the phase shift the Bethe-Yang equations in their logarithmic form

$$\begin{aligned} l \sinh(\theta + iu) + \delta_{11}(2iu) &= 2\pi I_1 \\ l \sinh(\theta - iu) + \delta_{11}(-2iu) &= 2\pi I_2 \end{aligned}$$

imply $I_1 = I_2$. Quantization of the total momentum on the other hand requires $I_1 = I_2 = I/2$. Note that different conventions for δ_{ab} would result in a less transparent rule for dividing I among the two constituents. The only disadvantage of our choice is the appearance of the unphysical half-integer quantum numbers. With this convention the bound-state quantization can be written in short-hand notation as

$$|\{I\}\rangle_{c,L} \sim |\{I/2, I/2\}\rangle_{aa,L}$$

4.1.1 Numerical analysis

It seems plausible that by exactly solving the bound state quantization condition (4.9) one obtains all higher order corrections that go as $e^{-n\mu_{aa}^c L}$ with $n \in \mathbb{N}$. In this subsection we present numerical evidence to support this claim.

We investigate the Ising model in the presence of a magnetic field. The first three particles lie below the two-particle threshold and they all show up as $A_1 A_1$ bound states. These fusions are responsible for the leading μ -term. The corresponding parameters (in units of m_1) are listed in the table below. The exponent of the next-to-leading correction (the error exponent) is denoted by μ' .

| a | m_a | μ_{11}^a | $(\Gamma_{11}^a)^2$ | μ' | |
|---|--------|--------------|---------------------|---------|-----------------|
| 1 | 1 | 0.86603 | 205.14 | 1 | (m_1) |
| 2 | 1.6180 | 0.58779 | 120.80 | 0.95106 | (μ_{12}^2) |
| 3 | 1.9890 | 0.10453 | 1.0819 | 0.20906 | $(2\mu_{11}^3)$ |

In [64] Klassen and Melzer performed the numerical analysis of mass corrections. The analytic predictions were compared to TCSA data and to transfer matrix results. They observed the expected behavior of mass corrections of A_1 and A_2 ; in the former case they were also able to verify the F-term. On the other hand, the precision of their TCSA data was not sufficient to reach volumes where the μ -term for A_3 could have been tested. This limitation is a natural consequence of the unusually small exponent μ_{11}^3 : the next-to-leading contribution is of order $e^{-2\mu_{11}^3 L}$, still very slowly decaying.

We employ the TFCSA routines that were successfully used in the previous chapter. Calculations are performed for $I = 0, 1, 2, 3$ at different values of the volume. One-particle states of A_1 , A_2 and A_3 are easily identified: they are the lowest lying levels in the spectrum, except for $I = 0$ where the lowest state is the vacuum. We use the dimensionless quantities $l = m_1 L$ and $e = E/m_1$.

The results are extrapolated from $e_{cut} = 20..30$ to $e_{cut} = \infty$. Experience from the previous results shows that this extrapolation technique reduces the numerical errors by an order of magnitude. We resign here from quantitatively monitoring the TCSA errors and constrain ourselves to a range of the volume parameter where it is safe to neglect truncation effects.

A_3

We begin our analysis with the most interesting case of A_3 . At each value of l and I the following procedure is performed.

- The energy correction is calculated according to (4.12)
- The quantization condition (4.9) is solved for u and the energy correction is calculated by

$$\Delta e = 2 \cosh(\theta) \cos(u) - e_0$$

where θ is determined by the total momentum quantization (4.8) and e_0 is the ordinary one-particle energy.

- The exact correction is calculated numerically by $\Delta e = e^{TCSA} - e_0$.

The choice for the range of the volumes is limited in two ways. On one hand, l has to be sufficiently large in order to reduce the contribution of the F terms and other higher order finite size corrections. On the other hand, numerical errors grow with the volume

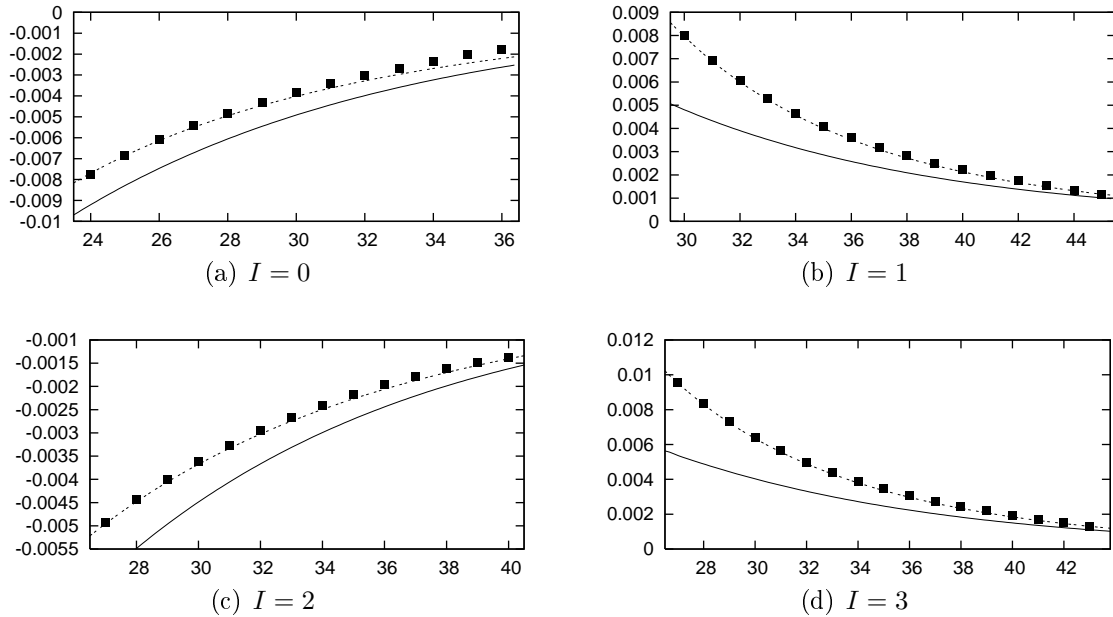


Figure 4.1: Finite size corrections to A_3 one-particle levels (in sectors $I = 0 \dots 3$) as a function of the volume. The TCSA data are plotted against theoretical predictions of the single μ -term associated to the $A_1 A_1 \rightarrow A_3$ fusion (solid curve) and the exact solution of the bound-state quantization (dotted curve).

and eventually become comparable with the finite size corrections, resulting in an upper bound on l . The window $l = 30..40$ is suitable for our purposes.

The results are shown in figure 4.1. It is clear that the μ -term yields the correct prediction in the $L \rightarrow \infty$ limit. However, higher order terms cause a significant deviation for $l < 40$, which is in turn accurately described by the bound state prediction. The sign of the correction depends on the parity of I as predicted by (4.12).

Based on the success of this first numerical test we also explored the region $l < 30$. Inspecting the behavior of u as a function of l reveals an interesting phenomenon. It is obvious from (4.11) that $u(l)$ is monotonously increasing if I is odd, with the infinite volume limit fixed to \bar{u}_{ac}^a . However, the complex conjugate pair $\theta_{1,2}$ approaches the real axis as l is decreased and they collide at a critical volume $l = l_c$. For $l < l_c$ they separate again but stay on the real line, providing a unique solution with two distinct purely real rapidities. The same behavior was also observed in [95, 109].

The interpretation of this phenomenon is evident: if the volume is comparable to the characteristic size of the bound-state, there is enough energy in the system for the constituents to become unbound. Therefore the A_3 one-particle level becomes an $A_1 A_1$ scattering state for $l < l_c$. We call this phenomenon the “dissociation of the bound state”. The same result was obtained also in the boundary sine-Gordon model by a semiclassical analysis [110].

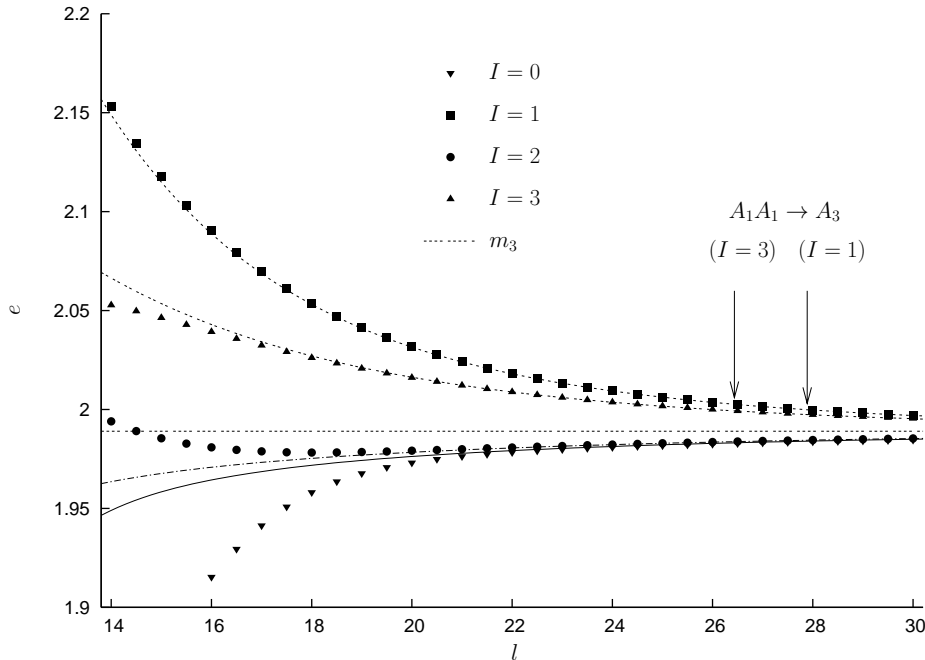


Figure 4.2: A_3 one-particle levels in sectors $I = 0 \dots 3$ as a function of the volume. Dots represent TCSA data, while the lines show the corresponding prediction of the A_1A_1 bound state quantization. In sectors $I = 1$ and $I = 3$ the bound state dissociates at l_c and for $l < l_c$ a conventional A_1A_1 scattering state replaces A_3 in the spectrum. The values of l_c are shown by the two arrows.

The value of l_c can be found by exploiting the fact that the Jacobian of the Bethe-Yang equations (viewed as a mapping from (θ_1, θ_2) to (I_1, I_2)) vanishes at the critical point. A straightforward calculation yields

$$l_c = \sqrt{4\varphi_{11}(0)^2 - I^2\pi^2}$$

where $\varphi_{11}(\theta) = \delta'_{11}(\theta)$. The numerical values for the case at hand are

$$l_c = 27.887 \quad (I = 1) \quad \text{and} \quad l_c = 26.434 \quad (I = 3)$$

We are now in the position to complete the numerical analysis. The Bethe-equations are solved at each value of l , providing two distinct real rapidities for $l < l_c$ (with I being odd), and a complex conjugate pair otherwise. The energy is calculated in either case as

$$e = \cosh(\theta_1) + \cosh(\theta_2)$$

which is compared to TCSA data. The results are exhibited in figure 4.2.

The agreement for the upper two curves ($I = 1$ and $I = 3$) is not as surprising as it may seem because what one sees here are conventional A_1A_1 scattering states. The Bethe-Yang equation determining their energy is exact up to $O(e^{-\mu'L})$ where $\mu' = \mu_{11}^1$ is

the smallest exponent that occurs in the sequence of finite volume corrections of A_1 . On the other hand, the energy levels are analytic functions of L , which leads to the conclusion that the prediction of (4.9) is correct up to $O(e^{-\mu_{11}^1 L})$ even for $L > L_c$. Comparing the numerical values one finds $\mu_{11}^1 > 8\mu_{11}^3$. We conclude that the bound state picture indeed accounts for finite volume corrections up to the first few orders in $e^{-\mu_{aa}^c L}$ (the first 8 orders in the case at hand).

A_1 and A_2

Particles A_1 and A_2 also appear as $A_1 A_1$ bound states. However, there is no point in applying the complete bound state quantization to them, because the error terms dominate over the higher order contributions from (4.9): the exponents of the sub-leading finite size corrections m_1 and μ_{12}^2 are smaller than $2\mu_{11}^1$ and $2\mu_{11}^2$. Nevertheless, the leading μ -term can be verified by choosing suitable windows in l .

In figures 4.7 and 4.8 $\log(|\Delta e|)$ is plotted against the prediction of (4.12) for $l = 6..16$ and $l = 6..22$. (the sign of Δe was found to be in accordance with (4.12) for both A_1 and A_2)

In the case of A_1 perfect agreement is observed for $l = 10..18$ in the sectors $I = 0$ and $I = 1$. For $I = 2$ and $I = 3$ the energy corrections become too small and therefore inaccessible to TCSA (note that the prediction for $I = 3$ is of order 10^{-6}).

In the case of A_2 precise agreement is found for $l = 14..22$ in all four sectors.

A_5

Here we present an interesting calculation that determines the leading mass corrections of A_5 . The standard formulas are inapplicable in this case, because m_5 lies above the two-particle threshold. However, it is instructive to consider the composition of A_5 under the bootstrap principle and to evaluate the μ -term prediction.

There are two relevant fusions

$$\begin{aligned} A_1 A_3 &\rightarrow A_5 & \text{with } \mu_{13}^5 &= 0.2079 \\ A_2 A_2 &\rightarrow A_5 & \text{with } \mu_{22}^5 &= 0.6581 \end{aligned}$$

Numerical evaluation of Lüscher's formula for the μ -term shows that the contribution of the second fusion is negligible for $l > 30$. The first fusion on the other hand yields a significant discrepancy when compared to TCSA data. This failure is connected to the two-particle threshold and it can be explained in terms of the bound state quantization. Experience with A_3 suggests that one should first take into account the energy corrections of A_3 and consider the $A_1 A_3 \rightarrow A_5$ fusion afterwards. A_3 can be split into $A_1 A_1$ leading to the "triple bound state" $A_1 A_1 A_1 \rightarrow A_5$. In infinite volume one has (see also fig. 1.1 c.)

$$|\theta\rangle_5 \sim |\theta - 2i\bar{u}_{11}^3, \theta, \theta + 2i\bar{u}_{11}^3\rangle_{111}$$

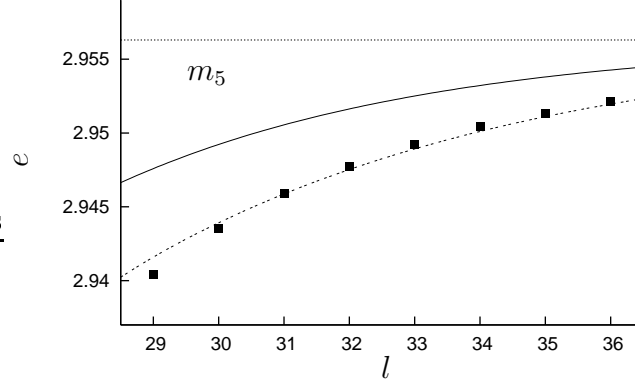


Figure 4.3: Finite size mass of A_5 as a function of the volume. The squares represent the TCSA data which is compared to the leading μ -term (solid curve) and the solution of the quantization condition for the “triple bound state“ $A_1 A_1 A_1$ (dotted curve). The straight line shows the infinite volume mass.

The finite volume realization of this identification is most easily carried out in the $I = 0$ sector with

$$|\{0\}\rangle_{5,L} \sim |\{0, 0, 0\}\rangle_{111,L}$$

Setting up the three-particle Bethe-Yang equations with rapidities $(iu, 0, -iu)$:

$$\begin{aligned} e^{-m_1 \sin(u)L} S_{11}(iu) S_{11}(2iu) &= 1 \\ S_{11}(iu) S_{11}(-iu) &= 1 \\ e^{m_1 \sin(u)L} S_{11}(-iu) S_{11}(-2iu) &= 1 \end{aligned}$$

The second equation is automatically satisfied due to unitarity and real analyticity, whereas the first and the third are equivalent and they serve as a quantization condition for u . The finite volume mass of A_5 is given in terms of the solution by

$$m_5(l) = 2 \cos(u) + 1 \quad (4.13)$$

In the large L limit the infinite volume mass is reproduced by $u \rightarrow 2\bar{u}_{11}^3$. Figure 4.3 demonstrates the agreement between TCSA and the prediction of (4.13).

The possibility of solving the quantization of the triple bound state in a moving frame looks very appealing. In the general case the rapidities are expected to take the form $(\theta_1 + iu, \theta_2, \theta_1 - iu)$ where θ_1 and θ_2 do not necessarily coincide. However, the numerical precision of our TCSA data was not sufficient to check our predictions.

4.1.2 Comparison with the TBA for excited states

As a conclusion of this section (4.11) is compared to the lowest order results of the TBA approach. The general discussion of excited states TBA equations in diagonal scattering

theories is not available. For simplicity we restrict ourselves to the Lee-Yang model which was considered in the original papers [25, 26].

The exact TBA equations for moving one-particle states read

$$E = -im(\sinh \theta_0 - \sinh \bar{\theta}_0) - \int_{-\infty}^{\infty} \frac{d\theta}{2\pi} m \cosh(\theta) L(\theta) \quad (4.14)$$

$$\varepsilon(\theta) = mR \cosh \theta + \log \frac{S(\theta - \theta_0)}{S(\theta - \bar{\theta}_0)} - (\varphi \star L)(\theta) \quad (4.15)$$

where

$$S(\theta) = \frac{\sinh(\theta) + i \sin(\pi/3)}{\sinh(\theta) - i \sin(\pi/3)} \quad \varphi(\theta) = -i \frac{\partial S(\theta)}{\partial \theta}$$

and

$$L(\theta) = \log(1 + e^{-\varepsilon(\theta)}) \quad \text{and} \quad (f \star g)(\theta) = \int_{-\infty}^{\infty} \frac{d\theta'}{2\pi} f(\theta - \theta') g(\theta')$$

Here the volume is denoted by R to avoid confusion with $L(\theta)$. The complex rapidity θ_0 satisfies the consistency equation

$$\varepsilon(\theta_0) = mR \cosh \theta_0 + i\pi - \log(S(2i\text{Im}\theta_0)) - (\varphi \star L)(\theta) = i(2n + 1)\pi \quad (4.16)$$

The convolution term in (4.16) can be neglected and one obtains $\text{Im}\theta_0 = \pi/6 + \delta$ where δ is exponentially small. To zeroth order one also has

$$mR \cosh(\text{Re}\theta_0) = (4n + (1 - \text{sign}\delta))\pi$$

which is the ordinary one-particle quantization condition with $I = 2n + \frac{1}{2}(1 - \text{sign}\delta)$. Neglecting the contribution of the integral in (4.14) and substituting $\theta_0 = \theta + iu$ one has $E = 2m \sin(u) \cosh(\theta)$. This is exactly the energy of an AA bound state with the imaginary rapidities $\theta \pm iu$. Separating the real and imaginary parts of (4.16) and still neglecting the convolution term (which is responsible for the F-term) one obtains equations (4.9) and (4.8), thus proving the consistency of the two approaches.

4.2 Multi-particle states

4.2.1 Bethe-Yang quantization in the bound state picture

Let us consider a scattering state $|\{I, I_1, \dots, I_n\}\rangle_{cb_1 \dots b_n, L}$ composed of $n + 1$ particles, the first one being A_c . The energy of this state is calculated as

$$E = \sum_{j=1}^n m_{i_j} \cosh(\bar{\theta}_j) + \dots \quad (4.17)$$

where $(\bar{\theta}, \bar{\theta}_1, \dots, \bar{\theta}_n)$ is the solution of the Bethe-Yang equations

$$Q_j(\theta_1, \dots, \theta_n) = m_{i_j} \sinh(\theta_j) L + \sum_{k \neq j} \delta_{i_j i_k}(\theta_j - \theta_k) = 2\pi I_j \quad j = 1 \dots n \quad (4.18)$$

We determine the leading part of the μ -term associated to (4.17) by considering A_c as an $A_a A_a$ bound state *inside the multi-particle state*. Therefore we write

$$|\{I, I_1, \dots, I_n\}\rangle_{cb_1 \dots b_n, L} \sim |\{I/2, I/2, I_1, \dots, I_n\}\rangle_{aab_1 \dots b_n, L} \quad (4.19)$$

The energy is then determined by analytic continuation of the $n + 2$ particle Bethe-Yang equations. They read

$$e^{-m_a \sin(u) \cosh(\theta)L} e^{im_a \cos(u) \sinh(\theta)L} S_{aa}(2iu) \prod_{j=1}^n S_{ab_j}(\theta + iu - \theta_j) = 1 \quad (4.20)$$

$$e^{m_a \sin(u) \cosh(\theta)L} e^{im_a \cos(u) \sinh(\theta)L} S_{aa}(-2iu) \prod_{j=1}^n S_{ab_j}(\theta - iu - \theta_j) = 1 \quad (4.21)$$

$$e^{im_{b_j} \sinh(\theta_j)L} S_{ab_j}(\theta_j - \theta - iu) S_{ab_j}(\theta_j - \theta + iu) \prod_{\substack{k=1 \\ k \neq j}}^n S_{b_j b_k}(\theta_j - \theta_k) = 1 \quad (4.22)$$

The ordinary $n + 1$ particle Bethe-equations are reproduced in the $L \rightarrow \infty$ limit by multiplying (4.20) and (4.21) and making use of the bootstrap equation

$$S_{cb_j}(\theta) = S_{ab_j}(\theta + i\bar{u}_{ac}^a) S_{ab_j}(\theta - i\bar{u}_{ac}^a)$$

We now proceed similar to the previous section and derive a formula for the leading correction. The shift in the imaginary part of the rapidity can be calculated by making use of (4.20) and (4.10) as

$$\Delta u = u - \bar{u}_{ac}^a = \frac{(\Gamma_{aa}^c)^2}{2} e^{-\mu \cosh(\bar{\theta})L} e^{im_c \sinh(\bar{\theta})L/2} \prod_{j=1}^n S_{ab_j}(\bar{\theta} + i\bar{u}_{ac}^a - \bar{\theta}_j) \quad (4.23)$$

Multiplying (4.20) and (4.21)

$$e^{i2m_a \cos(u) \sinh(\theta)L} \prod_{j=1}^n S_{ab_j}(\theta - iu - \theta_j) S_{ab_j}(\theta + iu - \theta_j) = 1 \quad (4.24)$$

$$e^{im_{b_j} \sinh(\theta_j)L} S_{ab_j}(\theta_j - \theta - iu) S_{ab_j}(\theta_j - \theta + iu) \prod_{\substack{k=1 \\ k \neq j}}^n S_{b_j b_k}(\theta_j - \theta_k) = 1 \quad (4.25)$$

Let us define

$$S_{ab_j}(\theta - iu - \theta_j) S_{ab_j}(\theta + iu - \theta_j) \approx S_{cb_j}(\theta - \theta_j) e^{i\Delta u \bar{\varphi}_{cb_j}(\theta - \theta_j)}$$

where

$$\bar{\varphi}_{cb_j}(\theta) = i\varphi_{cb_j}(\theta + i\bar{u}_{ac}^a) - i\varphi_{cb_j}(\theta - i\bar{u}_{ac}^a) \quad \text{with} \quad \varphi_{ab}(\theta) = \delta'_{ab}(\theta)$$

Using $2m_a \cos(u) \approx m_c - 2\mu_{aa}^c \Delta u$ the logarithm of (4.24) and (4.25) can be written as

$$\begin{aligned} Q_0(\theta, \theta_1, \dots, \theta_n) &= \left(2\mu_{aa}^c \sinh(\theta)L - \sum_{j=1}^n \bar{\varphi}_{cb_j}(\theta - \theta_j) \right) \Delta u \\ Q_j(\theta, \theta_1, \dots, \theta_n) &= \bar{\varphi}_{cb_j}(\theta - \theta_j) \Delta u \end{aligned}$$

The lhs. can be expanded around the $n+1$ particle solution $(\bar{\theta}, \bar{\theta}_1, \dots, \bar{\theta}_n)$ to arrive at

$$\begin{pmatrix} \theta - \bar{\theta} \\ \theta_1 - \bar{\theta}_1 \\ \vdots \\ \theta_n - \bar{\theta}_n \end{pmatrix} = (\mathcal{J}^{(n+1)})^{-1} \begin{pmatrix} 2\mu_{aa}^c \sinh(\bar{\theta})L - \sum_{j=1}^n \bar{\varphi}_{cb_j}(\bar{\theta} - \bar{\theta}_j) \\ \bar{\varphi}_{cb_1}(\bar{\theta} - \bar{\theta}_1) \\ \vdots \\ \bar{\varphi}_{cb_n}(\bar{\theta} - \bar{\theta}_n) \end{pmatrix} \Delta u \quad (4.26)$$

where

$$\mathcal{J}_{kl}^{(n+1)} = \frac{\partial Q_k}{\partial \theta_l}$$

The final result for the energy correction reads

$$\Delta E = -2\mu_{aa}^c \cosh(\bar{\theta}) \Delta u + \begin{pmatrix} m_c \sinh(\bar{\theta}) \\ m_{b_1} \sinh(\bar{\theta}_1) \\ \vdots \\ m_{b_n} \sinh(\bar{\theta}_n) \end{pmatrix} (\mathcal{J}^{n+1})^{-1} \begin{pmatrix} 2\mu_{aa}^c \sinh(\bar{\theta})L - \sum_{j=1}^n \bar{\varphi}_{cb_j}(\bar{\theta} - \bar{\theta}_j) \\ \bar{\varphi}_{cb_1}(\bar{\theta} - \bar{\theta}_1) \\ \vdots \\ \bar{\varphi}_{cb_n}(\bar{\theta} - \bar{\theta}_n) \end{pmatrix} \Delta u \quad (4.27)$$

with Δu given by (4.23).

Based on the previous section it is expected that there is a similar contribution for every fusion leading to each one of the constituents of the multi-particle state.

We wish to remark that in the case of the Lee-Yang model it is possible to derive (4.27) from the excited state TBA, along the lines of subsection 4.1.2. This carries over to other models with diagonal scattering, provided that the excited state TBA equations are available. The point of our calculation is, that the μ -term can be obtained without any reference to the TBA equations. Moreover, our arguments can be applied directly to form factors as well (see section 4.3).

4.2.2 Multi-particle states – Numerical analysis

We first consider finite size corrections to $A_1 A_3$ states. They are not the lowest lying two-particle states in the spectrum, but they possess the largest μ -term which is connected to the $A_1 A_1 \rightarrow A_3$ fusion. Given a particular state $|\{I_1, I_3\}\rangle_{13,L}$ the following procedure is performed at each value of the volume:

- The two-particle Bethe-Yang equation for $|\{I_1, I_3\}\rangle_{13,L}$ is solved and the μ -term is calculated according to (4.27).

- The exact three-particle Bethe-Yang equation is solved for $|\{I_1, I_3/2, I_3/2\}\rangle_{111,L}$

The results for different A_1A_3 levels are shown in figure 4.9. The situation is similar to the case of the A_3 one-particle levels: the bound state quantization yields a remarkably accurate prediction, whereas the single μ -term prediction only becomes correct in the $L \rightarrow \infty$ limit.

In table 4.1 we present a numerical example for the dissociation of the bound state inside the two-particle state. In this case an A_1A_3 state turns into a conventional $A_1A_1A_1$ three-particle state at $l_c \approx 30$.

Finite size corrections to A_1A_1 and A_1A_2 states are also investigated, the leading μ -term given by the fusions $A_1A_1 \rightarrow A_1$ and $A_1A_1 \rightarrow A_2$, respectively. In the former case we calculate separately the contribution associated to both A_1 particles and add them to get the total correction. Results are exhibited in figures 4.10 and 4.11 and formula (4.27) is verified in both cases.

4.3 Finite volume form factors

The connection between finite volume and infinite volume form factors was derived in section 2.2 as

$$\frac{j_1 \dots j_m, L \langle \{I'_1, \dots, I'_m\} | \mathcal{O}(0, 0) | \{I_1, \dots, I_n\} \rangle_{i_1 \dots i_n, L} = F^{\mathcal{O}}(\bar{\theta}'_m + i\pi, \dots, \bar{\theta}'_1 + i\pi, \bar{\theta}_1, \dots, \bar{\theta}_n)_{j_m \dots j_1 i_1 \dots i_n} + O(e^{-\mu' L})}{\sqrt{\rho_{i_1 \dots i_n}(\theta_1, \dots, \theta_n) \rho_{j_1 \dots j_m}(\theta'_1, \dots, \theta'_m)}} \quad (4.28)$$

where the rapidities $\bar{\theta}$ are solutions of the corresponding Bethe-Yang equations. Here we assume for simplicity, that there are no disconnected terms present, ie. it is supposed that $\bar{\theta}_j \neq \bar{\theta}'_k$ whenever $i_j = i_k$.

Based on general arguments it was shown in subsection 2.2.3 that $\mu' \geq \mu$ where μ is determined by the pole of the S-matrix closest to the physical line. A systematic finite volume perturbation theory (Lüscher's method applied to form factors) is not available. However, it is expected that the actual value of μ' depends on what diagrams contribute to the form factor in question. Apart from the insertion of the local operator they coincide with the diagrams determining the finite size corrections of the multi-particle state. Therefore μ' is associated to the bound state structure of the constituents of the multi-particle state.

In this section we show that the leading correction term can be obtained by the bound state quantization.

4.3.1 Elementary one-particle form factors

(4.28) yields a simple prediction for the elementary one-particle form factor:

$$F_c^\mathcal{O}(I, L) \equiv \langle 0 | \mathcal{O}(0, 0) | \{I\} \rangle_{c, L} = \frac{F_c^\mathcal{O}}{\sqrt{EL}} + O(e^{-\mu' L}) \quad (4.29)$$

where E is the one-particle energy, and $F_c^\mathcal{O} = F_c^\mathcal{O}(\theta)$ is the infinite volume one-particle form factor, which is constant by Lorentz symmetry.

The μ -term associated to (4.29) is derived by employing the bound state quantization. We gain some intuition from the section 4.1 where it was found that the bound state $A_a A_a$ may dissociate at a critical volume L_c . For $L < L_c$ there is no one-particle level of type A_c in the given sector of the spectrum, however an $A_a A_a$ scattering state appears instead. Finite volume form factors of this state are calculated using (4.28) as

$$F_c^\mathcal{O}(I, L) = \frac{F^\mathcal{O}(\theta_1, \theta_2)_{aa}}{\sqrt{\rho_{aa}(\theta_1, \theta_2)}} \quad \text{for } L < L_c \quad (4.30)$$

The generalization to $L > L_c$ seems to be straightforward: one has to continue analytically (4.30) to the solutions of the Bethe-Yang equation with imaginary rapidities $\theta_{1,2} = \theta \pm iu$. However, note that equations (4.29) and (4.30) are valid up to a phase factor. In order to continue analytically to imaginary rapidities we also need to fix this phase¹.

The two-particle form factor satisfies

$$F^\mathcal{O}(\theta_1, \theta_2)_{aa} = S_{aa}(\theta_1 - \theta_2) F^\mathcal{O}(\theta_2, \theta_1)_{aa}$$

The simplest choice for the phase is therefore

$$F^\mathcal{O}(\theta_1, \theta_2)_{aa} = \sqrt{S_{aa}(\theta_1 - \theta_2)} |F^\mathcal{O}(\theta_1, \theta_2)_{aa}| \quad (4.31)$$

This choice is dictated by CPT symmetry [111, 52, 112], and it is respected by all known solutions of the form factor bootstrap axioms. There is a sign ambiguity caused by the square root, but it can be fixed by demanding $(S_{aa}(0))^{1/2} = i$ and continuity. Using (4.31)

$$F_c^\mathcal{O}(I, L) = \frac{\sqrt{S_{aa}(\theta_2 - \theta_1)} F^\mathcal{O}(\theta_1, \theta_2)_{aa}}{\sqrt{\rho_{aa}(\theta_1, \theta_2)}}$$

and upon analytic continuation

$$F_c^\mathcal{O}(I, L) = \frac{\sqrt{S_{aa}(-2iu)} F^\mathcal{O}(\theta + iu, \theta - iu)_{aa}}{\sqrt{\rho_{aa}(\theta + iu, \theta - iu)}} \quad \text{for } L > L_c \quad (4.32)$$

¹As we noted in earlier the phase of a (non-diagonal) infinite volume form factor is unphysical in the sense that it may be redefined by a complex rotation of the state vectors and physical quantities, e.g. correlation functions, do not depend on such redefinitions. However, the bootstrap program uniquely assigns a phase to each form factor.

It is easy to see that the result (4.29) is reproduced in the $L \rightarrow \infty$ limit. First observe that

$$F^\mathcal{O}(\theta + iu, \theta - iu)_{aa} \sim \frac{\Gamma_{aa}^c}{2(u - \bar{u}_{aa}^c)} F_c^\mathcal{O}(\theta)$$

The residue of ρ_{aa} is determined by $\varphi_{aa}(2iu)$ and it reads

$$\rho(\theta + iu, \theta - iu)_{aa} \sim 2m_a L \cos(u) \cosh(\theta) (-i) \frac{S'_{aa}(2iu)}{S_{aa}(2iu)} = m_c L \cosh(\theta) \frac{1}{2(u - \bar{u}_{aa}^a)}$$

The singularities in the numerator and denominator of (4.32) cancel and indeed

$$F_c^\mathcal{O}(I, L) \sim \frac{F_c^\mathcal{O}}{\sqrt{m_c L \cosh(\theta)}}$$

We emphasize that it is crucial to include the extra normalization factor $\sqrt{S_{aa}(-2iu)}$ to obtain a meaningful result.

Expression (4.32) can be developed into a Taylor-series in $u - \bar{u}_{aa}^a$. First we use the exchange axiom to arrive at

$$F_c^\mathcal{O}(I, L) = \frac{F^\mathcal{O}(\theta - iu, \theta + iu)_{aa}}{\sqrt{S_{aa}(-2iu) \rho_{aa}(\theta + iu, \theta - iu)}} \quad (4.33)$$

The form factor axioms imply that

$$\lim_{u \rightarrow \bar{u}_{aa}^a} F^\mathcal{O}(\theta - iu, \theta + iu)_{aa} = \frac{1}{\Gamma_{aa}^c} F_c^\mathcal{O}$$

The simple pole of $\varphi_{aa}(2iu)$ in ρ_{aa} is canceled by $S_{aa}(-2iu)$, therefore both the numerator and the denominator of (4.33) have continuous limits as $u \rightarrow \bar{u}_{aa}^a$.

The form factor $F^\mathcal{O}(\theta - iu, \theta + iu)_{aa}$ only depends on u by Lorentz-symmetry. Therefore

$$F^\mathcal{O}(\theta - iu, \theta + iu)_{aa} = \frac{1}{\Gamma_{aa}^c} F_c^\mathcal{O} - 2i (F_{aa}^\mathcal{O})' (u - \bar{u}_{aa}^a) + \dots$$

where

$$(F_{aa}^\mathcal{O})' = \frac{d}{d\theta} F^\mathcal{O}(\theta, \theta')_{aa} \Big|_{\theta - \theta' = -2i\bar{u}_{aa}^a}$$

Expanding the S-matrix element into a Laurent-series in the vicinity of the pole

$$\begin{aligned} S_{aa}(2iu) &= \frac{(\Gamma_{aa}^c)^2}{2(u - \bar{u}_{aa}^a)} + S_{aa}^{c,0} + \dots \\ S_{aa}(-2iu) &= \frac{2(u - \bar{u}_{aa}^a)}{(\Gamma_{aa}^c)^2} - \left(\frac{2(u - \bar{u}_{aa}^a)}{(\Gamma_{aa}^c)^2} \right)^2 S_{aa}^{c,0} + \dots \end{aligned}$$

Expanding the denominator:

$$\begin{aligned} S(-2iu) \rho_{aa}(\theta + iu, \theta - iu) &= \\ S(-2iu) E_1 E_2 L^2 - i(E_1 + E_2) L S'(2iu) \left(S(-2iu) \right)^2 &= \\ \frac{E_c L}{(\Gamma_{aa}^c)^2} + \left(\frac{2E_1 E_2 L^2}{(\Gamma_{aa}^c)^2} - \frac{4E_c L}{(\Gamma_{aa}^c)^4} S_{aa}^{c,0} \right) (u - \bar{u}_{aa}^a) + \dots \end{aligned}$$

where

$$E_c = E_1 + E_2 = 2m_a \cos(u) \cosh(\theta)$$

Putting all this together

$$\begin{aligned} F_c^{\mathcal{O}}(I, L) &= \frac{F_c^{\mathcal{O}}}{\sqrt{E_c L}} + \\ &+ \left[\frac{-2i\Gamma_{aa}^c (F_{aa}^{\mathcal{O}})'}{\sqrt{E_c L}} + \frac{F_c^{\mathcal{O}}}{\sqrt{E_c L}^3} \left(-E_1 E_2 L^2 + \frac{2E_c L}{(\Gamma_{aa}^c)^2} S_{aa}^{c,0} \right) \right] (u - \bar{u}_{ac}^a) + \dots \end{aligned}$$

Note that in the preceding formulas E_c does include the leading order correction to the usual one-particle energy $E_c^0 = \sqrt{m_c^2 + (2\pi I)^2/L^2}$. Using

$$E_c = E_c^0 - 2\frac{m_c \mu}{E_c^0} (u - \bar{u}_{ac}^a) + O(e^{-2\mu L}) \quad \text{and} \quad E_1 E_2 = \frac{m_a^2}{m_c^2} E_c^2 - \mu^2$$

the final result is given by

$$\begin{aligned} F_c^{\mathcal{O}}(I, L) &= \frac{F_c^{\mathcal{O}}}{\sqrt{E_c^0 L}} - \frac{2i\Gamma_{aa}^c (F_{aa}^{\mathcal{O}})'}{\sqrt{E_c^0 L}} (u - \bar{u}_{ac}^a) + \\ &+ \frac{F_c^{\mathcal{O}}}{\sqrt{E_c^0 L}} \left[\frac{2S_{aa}^{c,0}}{(\Gamma_{aa}^c)^2} + \frac{m_c \mu}{(E_c^0)^2} - \left(\frac{m_a^2}{m_c^2} E_c^0 - \frac{\mu^2}{E_c^0} \right) L \right] (u - \bar{u}_{ac}^a) + O(e^{-2\mu L}) \end{aligned} \quad (4.34)$$

with

$$u - \bar{u}_{ac}^a = \pm \frac{1}{2} (\Gamma_{aa}^c)^2 e^{-\mu_{aa}^c L} \sqrt{1 + \left(\frac{\pi I}{m_a L \cos(\bar{u}_{ac}^a)} \right)^2}$$

4.3.2 One-particle form factors – Numerical analysis

Let us introduce the dimensionless form factors as

$$f_i(I, l) = \frac{\langle 0 | \varepsilon(0, 0) | \{I\} \rangle_{i,L}}{m_1}$$

We use the methods described in section 3.1 to determine $f_i(I, l)$ for $i = 1, 2, 3$ and $I = 0, 1, 2, 3$. The numerical results are compared to the exact infinite volume form factors.

We start our investigation with $f_3(I, l)$, for which relatively large exponential corrections were found in subsection 3.2.2. It is convenient to consider

$$\bar{f}_3(I, l) = (e_0 l)^{1/2} f_3(I, L) \quad \text{with} \quad \lim_{l \rightarrow \infty} \bar{f}_3(I, l) = F_3 \quad (4.35)$$

The numerical results are demonstrated in fig. 4.4. Note, that this is the same figure as fig. 3.7, but here the interpretation of the huge deviations from F_3 is also provided.

We also tried to verify the predictions for f_1 and f_2 . In the latter case reasonably good agreement was found with TCSA, the results are demonstrated in fig. 4.12. In the case of

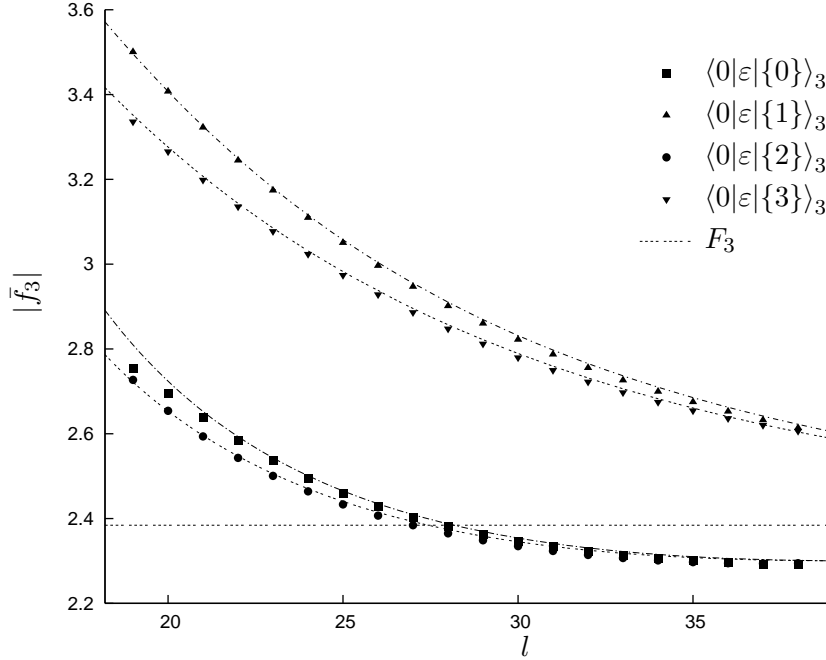


Figure 4.4: Elementary finite volume form factors of A_3 one-particle levels. Here the normalization (4.35) is applied to obtain a finite $l \rightarrow \infty$ limit, which is given by the infinite volume form factor $F_3 = \langle 0|\varepsilon|A_3(\theta)\rangle$. The TCSA data are plotted against the bound state prediction. The ordinary evaluation of \bar{f}_3 is simply the constant F_3 .

f_1 we encountered the unpleasant situation that the F-term decays slower than the TCSA errors grow, thus making the observation of the μ -term impossible.

It is straightforward to generalize (4.32) to matrix elements between two different one-particle states. For $b \neq c$ one has for example

$${}_b\langle\{I_b\}|\varepsilon|\{I_c\}\rangle_{c,L} = \frac{F^\varepsilon(\theta_b + i\pi, \theta + iu, \theta - iu)_{baa}}{\sqrt{\rho_b(\theta_b)\rho_{aa}(\theta + iu, \theta - iu)}}$$

Numerical examples are presented in figures 4.5 (a)-(c) for $c = 3$ and $b = 1, 2$.

The most interesting case is the one shown in fig. 4.5 (d) where the matrix element between two different A_3 one-particle states are investigated. This can be done by considering both A_3 particles as the appropriate A_1A_1 bound states and then calculating the finite volume form factor ${}_3\langle\{I\}|\varepsilon|\{I'\}\rangle_{3,L}$ as

$${}_{11}\langle\{I/2, I/2\}|\varepsilon|\{I'/2, I'/2\}\rangle_{11,L} = \frac{F^\varepsilon(\theta + iu + i\pi, \theta - iu + i\pi, \theta' + iu', \theta' - iu')_{1111}}{\sqrt{\rho_{11}(\theta' + iu', \theta' - iu')\rho_{11}(\theta + iu, \theta - iu)}}$$

Once again we find complete agreement with the TCSA data.

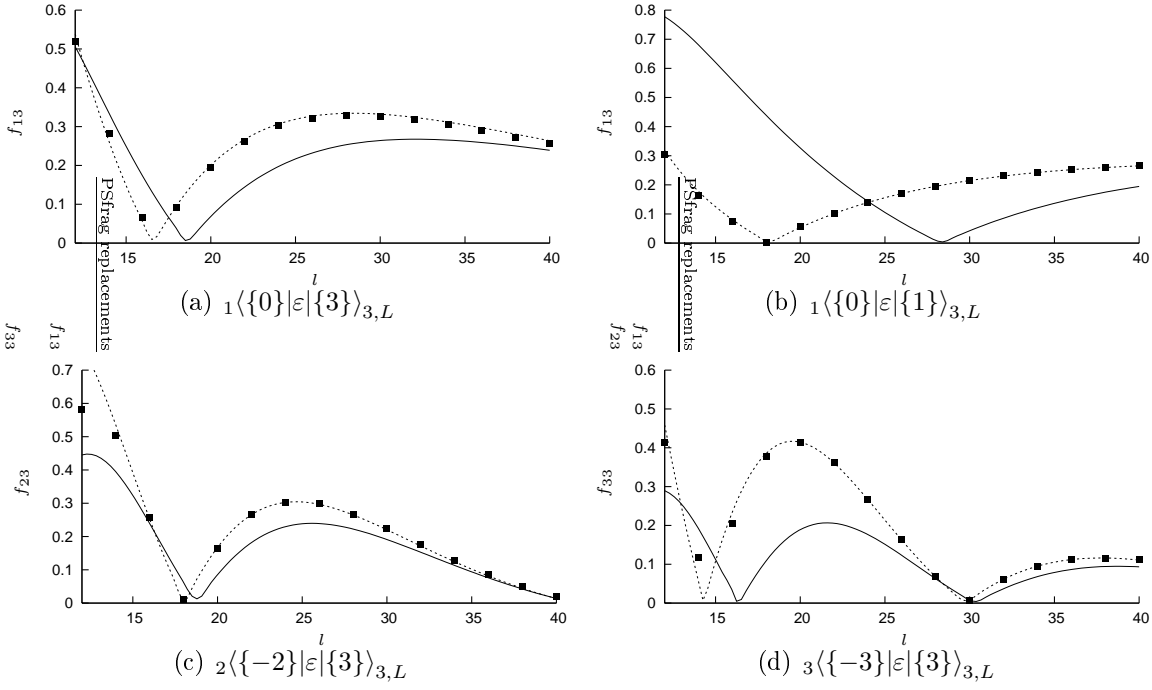


Figure 4.5: One-particle–one-particle form factors, dots correspond to TCSA data. The solid lines represent the ordinary evaluation of the finite volume form factors, while the dotted lines show the bound state prediction.

4.3.3 Elementary multi-particle form factors

The generalization of (4.32) to multi-particle states is straightforward, the only task is to find the appropriate phase factor. Similar to the one-particle case one has

$$F^{\mathcal{O}}(\theta_1, \dots, \theta_m)_{b_1 \dots b_m} = \sqrt{\prod_{i < j} S_{b_i b_j}(\theta_i - \theta_j)} |F^{\mathcal{O}}(\theta_1, \dots, \theta_m)_{b_1 \dots b_m}|$$

A general n particle finite volume form factor with real rapidities can thus be written as

$$\sqrt{\frac{\prod_{i < j} S_{b_i b_j}(\theta_j - \theta_i)}{\rho^n(\theta_1, \dots, \theta_n)_{b_1 \dots b_n}}} F^{\mathcal{O}}(\theta_1, \dots, \theta_n)_{b_1 \dots b_n}$$

Substituting the solution of the Bethe-equation for the state $|\{I/2, I/2, I_1, \dots, I_n\}\rangle_{aab_1 \dots b_n, L}$ and making use of the real analyticity condition

$$|S_{ab_j}(\theta_j - \theta - iu)S_{ab_j}(\theta_j - \theta + iu)| = 1$$

one gets

$$\langle 0 | \mathcal{O} | \{I/2, I/2, I_1, \dots, I_n\} \rangle_{aab_1 \dots b_n, L} = \frac{\sqrt{S_{aa}(-2iu)} |F^{\mathcal{O}}(\theta + iu, \theta - iu, \theta_1, \dots, \theta_n)_{aab_1 \dots b_n}|}{\sqrt{\rho^{(n+2)}(\theta + iu, \theta - iu, \theta_1, \dots, \theta_n)_{aab_1 \dots b_n}}} \quad (4.36)$$

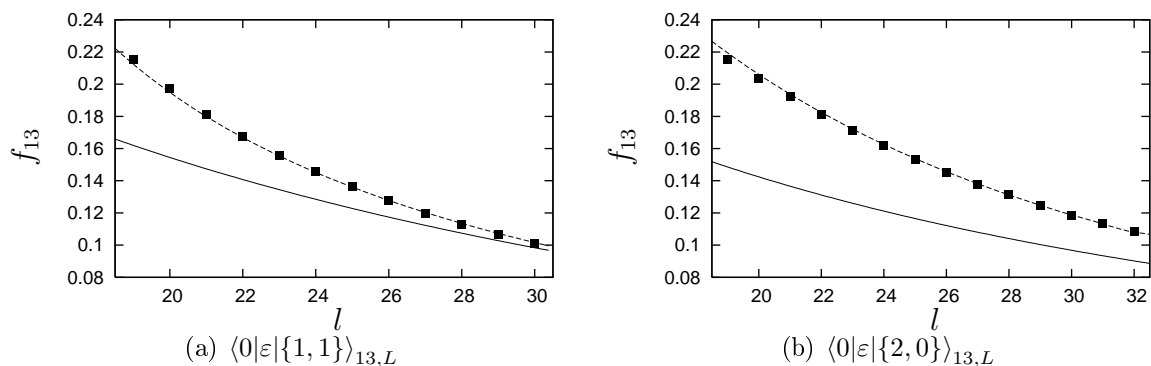


Figure 4.6: Elementary form factors of A_1A_3 scattering states, dots correspond to TCSA data. The solid lines are obtained by a “naive“ evaluation of the finite volume form factors, while the dotted line represents the bound state prediction. (in this case $A_1A_1A_1$ form factors at the appropriate rapidities)

up to a physically irrelevant phase.

It is easy to show once again that the “naive” result is reproduced in the $L \rightarrow \infty$ limit. To do so, we first quote the dynamical pole equation of the infinite volume form factor:

$$F^{\mathcal{O}}(\theta + iu, \theta - iu, \theta_1, \dots, \theta_n)_{aab_1\dots b_n} = \frac{\Gamma_{aa}^c}{2(u - \bar{u}_{ac}^a)} F^{\mathcal{O}}(\theta, \theta_1, \dots, \theta_n)_{cb_1\dots b_n} + O(1)$$

The singularity of $\rho^{(n+2)}$ is given by

$$\text{Res}_{u \rightarrow \bar{u}_{ac}^a} \rho^{(n+2)}(\theta + iu, \theta - iu, \theta_1, \dots, \theta_n)_{aab_1\dots b_n} = \frac{1}{2} \rho^{(n+1)}(\theta, \theta_1, \dots, \theta_n)_{cb_1\dots b_n}$$

The “naive” formula is now recovered by inserting the last two equations into (4.36).

The leading exponential corrections can be obtained by plugging (4.23) and (4.26) into (4.36) and expanding to first order in $u - \bar{u}_{ac}^a$. This procedure is straightforward but quite lengthy, therefore we refrain from giving the details of the calculations.

In fig. 4.6 two examples are presented for the evaluation of (4.36) applied to A_1A_3 two-particle states.

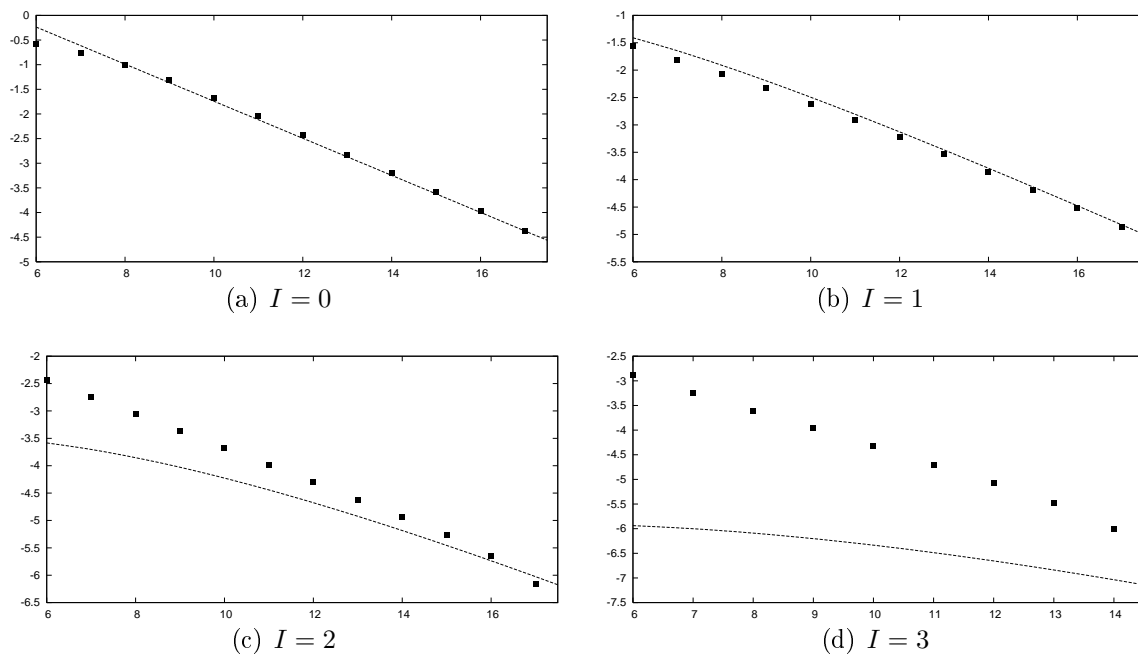


Figure 4.7: Finite size corrections to A_1 one-particle levels in sectors $I = 0 \dots 3$, $\log_{10}\Delta e$ is plotted as a function of the volume. Dots represent TCSA data, while the lines show the μ -term corresponding to the $A_1A_1 \rightarrow A_1$ fusion.

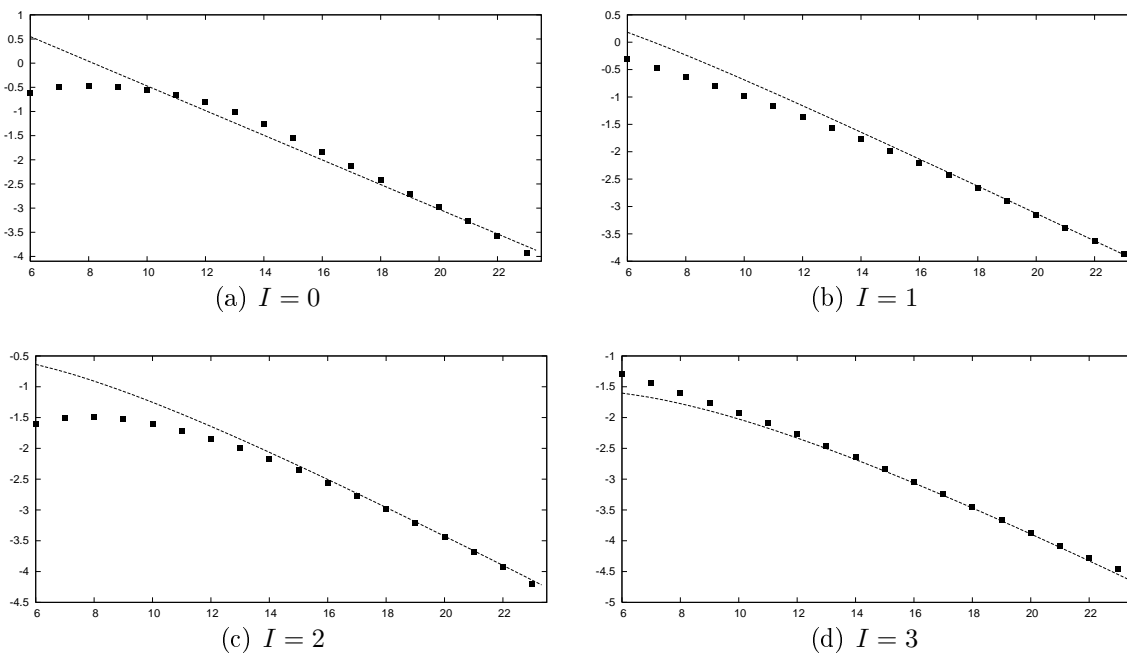


Figure 4.8: Finite size corrections to A_2 one-particle levels in sectors $I = 0 \dots 3$, $\log_{10}\Delta e$ is plotted as a function of the volume. Dots represent TCSA data, while the lines show the μ -term corresponding to the $A_1A_1 \rightarrow A_2$ fusion.

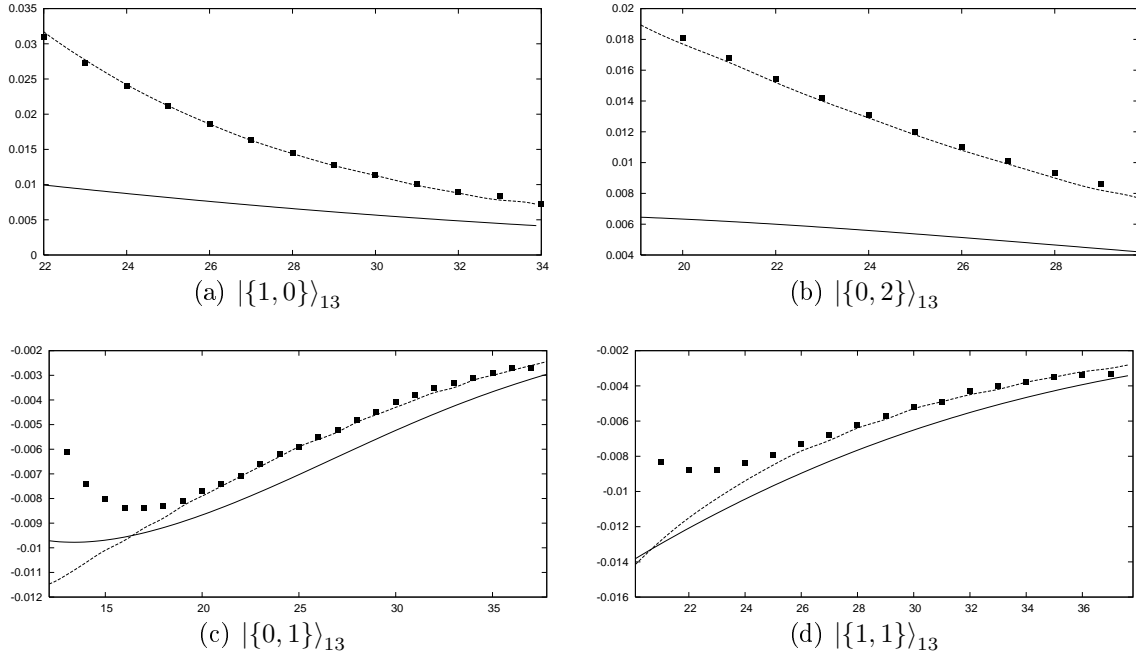


Figure 4.9: Finite size corrections to A_1A_3 scattering states as a function of the volume. Dots represent TCSA data, the solid line shows the μ -term corresponding to the $A_1A_1 \rightarrow A_3$ fusion. The dotted lines are obtained by the exact solution of the quantization condition for the $A_1A_1A_1$ three-particle system.

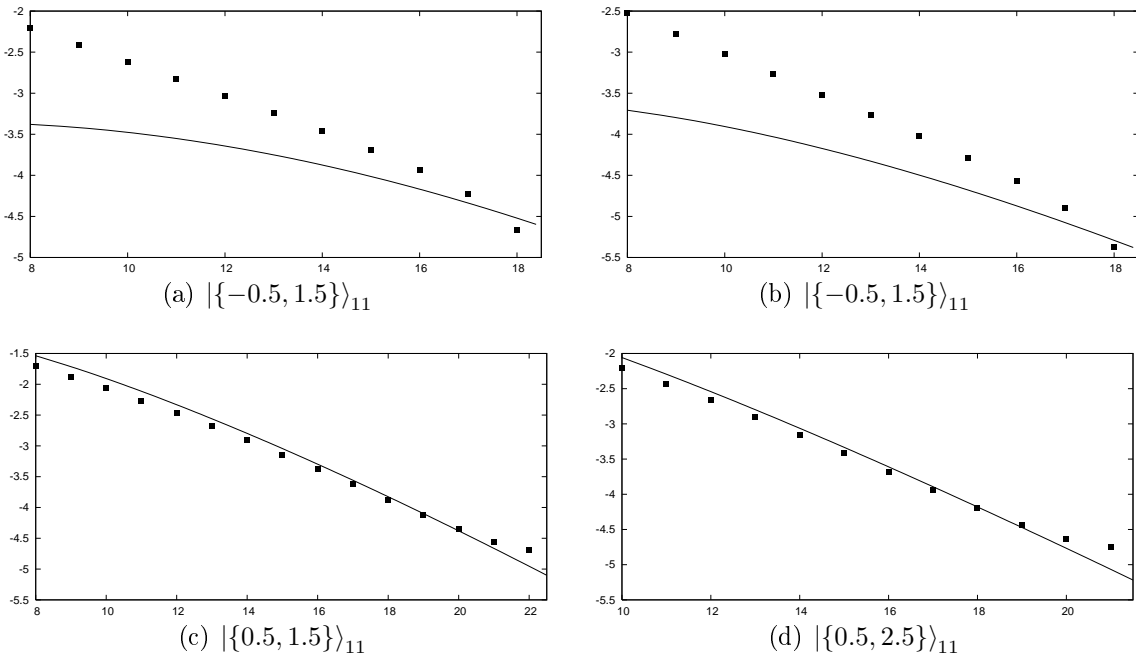


Figure 4.10: Finite size corrections to A_1A_1 scattering states, $\log_{10}\Delta e$ is plotted as a function of the volume. Dots represent TCSA data, while the solid line show the sum of the two μ -terms corresponding to the $A_1A_1 \rightarrow A_1$ fusions.

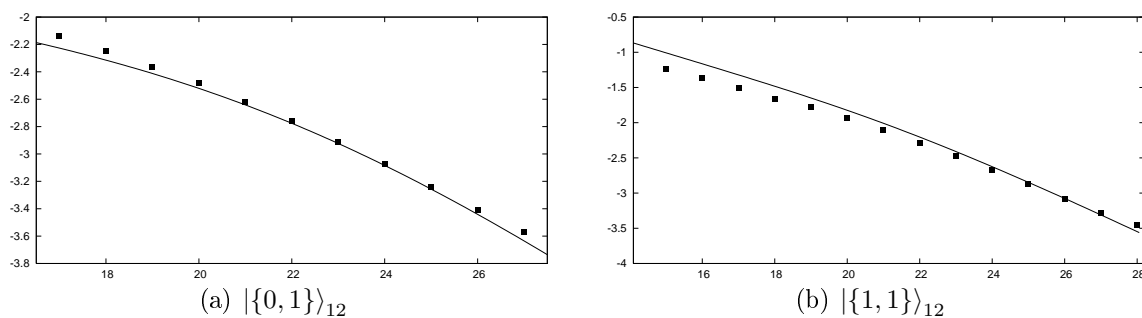


Figure 4.11: Finite size corrections to A_1A_2 scattering states, $\log_{10}\Delta e$ is plotted as a function of the volume. Dots represent TCSA data, while the solid line show the μ -term corresponding to the $A_1A_1 \rightarrow A_2$ fusion.

| l | θ_1 | θ_2 | θ_3 | $e(l)$ (predicted) | $e(l)$ (TCSA) |
|-----|-----------------------|-----------------------|------------|--------------------|---------------|
| 22 | 0.44191 | 0.68235 | -0.58742 | 3.51877 | 3.51900 |
| 23 | 0.42574 | 0.64280 | -0.55190 | 3.46201 | 3.46219 |
| 24 | 0.60523 | 0.41155 | -0.51892 | 3.41239 | 3.41255 |
| 25 | 0.56934 | 0.39931 | -0.48831 | 3.36890 | 3.36907 |
| 26 | 0.38910 | 0.53475 | -0.45989 | 3.33071 | 3.33089 |
| 27 | 0.50092 | 0.38119 | -0.43350 | 3.29709 | 3.29729 |
| 28 | 0.46686 | 0.37634 | -0.40899 | 3.26743 | 3.26767 |
| 29 | 0.42947 | 0.37739 | -0.38622 | 3.24122 | 3.24164 |
| 30 | $0.38646 + 0.02332 i$ | $0.38646 - 0.02332 i$ | -0.36505 | 3.21801 | 3.21832 |
| 31 | $0.37059 + 0.04042 i$ | $0.37059 - 0.04042 i$ | -0.34537 | 3.19741 | 3.19775 |
| 32 | $0.35572 + 0.05104 i$ | $0.35575 - 0.05104 i$ | -0.32706 | 3.17908 | 3.17945 |
| 33 | $0.34182 + 0.05891 i$ | $0.34182 - 0.05891 i$ | -0.31002 | 3.16275 | 3.16313 |
| 34 | $0.32876 + 0.06513 i$ | $0.32876 - 0.06513 i$ | -0.29415 | 3.14816 | 3.14856 |
| 35 | $0.31650 + 0.07022 i$ | $0.31650 - 0.07022 i$ | -0.27936 | 3.13511 | 3.13547 |
| 36 | $0.30498 + 0.07446 i$ | $0.30498 - 0.07446 i$ | -0.26556 | 3.12341 | 3.12235 |

Table 4.1: An example for the dissociation of the A_1A_1 bound state inside a scattering state. $|\{2,0\}\rangle_{31,L}$ is identified with $|\{1,1,0\}\rangle_{111,L}$ and the corresponding Bethe-Yang equations is solved. For $l < 30$ there is a real $A_1A_1A_1$ three-particle state in the spectrum, whereas at $l \approx 30$ two of the rapidities become complex and the two-particle state A_1A_3 emerges.

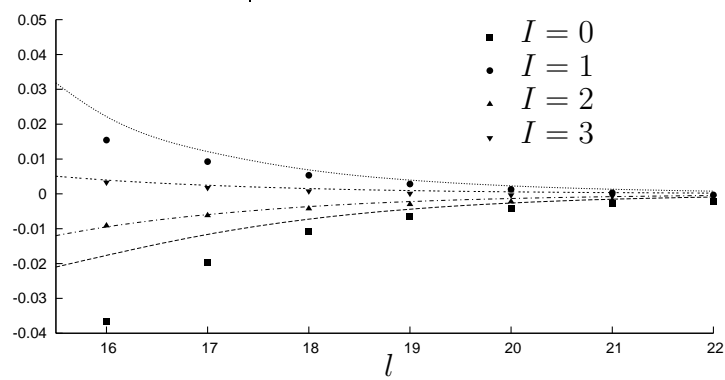


Figure 4.12: Finite size corrections to the elementary form factors of A_2 . Dots represent TCSA data, while the lines show the μ -term prediction corresponding to the $A_1 A_1 \rightarrow A_2$ fusion.

Chapter 5

Correlation functions at finite temperature

5.1 The form factor expansion for correlation functions

The finite temperature correlation function of local operators \mathcal{O}_1 and \mathcal{O}_2 is defined by

$$\langle \mathcal{O}_1(x_1, t_1) \mathcal{O}_2(x_2, t_2) \rangle^R = \frac{\text{Tr} (e^{-RH} \mathcal{O}_1(x_1, t_1) \mathcal{O}_2(x_2, t_2))}{\text{Tr} (e^{-RH})} \quad (5.1)$$

where $R = 1/T$ is the temperature dependent extension of the Euclidean time direction used in thermal quantum field theory and H is the Hamiltonian.

In the following we briefly discuss the evaluation of the correlation function at zero temperature using the form factor expansion and show that there is no straightforward generalization of this method to the finite temperature case. To keep the exposition simple we assume that the spectrum contains a single massive particle of mass m .

At zero temperature the two-point function of operators \mathcal{O}_1 and \mathcal{O}_2 is given by the vacuum expectation value

$$\langle 0 | \mathcal{O}_1(x_1, \tau_1) \mathcal{O}_2(x_2, \tau_2) | 0 \rangle$$

Inserting a complete set of asymptotic states and using Euclidean invariance one obtains

$$\langle 0 | \mathcal{O}_1(x_1, t_1) \mathcal{O}_2(x_2, t_2) | 0 \rangle = \sum_{n=0}^{\infty} \frac{1}{n!} \int d\theta_1 \dots d\theta_n F_n^{\mathcal{O}_1}(\theta_1 \dots \theta_n) F_n^{\mathcal{O}_2}(\theta_1 \dots \theta_n)^* e^{-mr \sum_{i=1}^n \cosh(\theta_i)} \quad (5.2)$$

where $r = \sqrt{(x_1 - x_2)^2 + (\tau_1 - \tau_2)^2}$. The essence of the form factor approach [88, 18, 113, 114, 19] is to determine the form factors appearing in (5.2) as solutions of the form factor bootstrap program, and then numerically integrate the resulting expressions to obtain the contributions to the correlator. Due to the exponential damping factor and the vanishing

property of the form factor functions at $\theta_i = 0$ the series (5.2) is rapidly converging even for relatively small values of mr , therefore in most cases it is sufficient to consider only the first few terms in (5.2).

Switching on a non-zero temperature one faces severe problems. A straightforward application of the form factor expansion results in

$$\langle \mathcal{O}_1(0, 0) \mathcal{O}_2(0, \tau) \rangle^R = \frac{1}{Z} \sum_{m,n} \langle m | \mathcal{O}_1 | n \rangle \langle n | \mathcal{O}_2 | m \rangle e^{-(R-\tau)E_\Psi} e^{-\tau E_{\Psi'}} \quad (5.3)$$

where for simplicity we have chosen the displacement between the two operators to lie in the imaginary time direction and the summation over m and n runs over the complete set of asymptotic states of the theory. Expression (5.3) is ill-defined in two ways:

- The partition function Z is infinite if one considers the infinite volume theory.
- One has to integrate over the poles of the form factors associated to the disconnected contributions, whenever the rapidities of two particles entering m and n approach each other.

One encounters similar problems already by the evaluation of the thermal expectation value of local operators. The formal form factor expansion for the one-point function reads

$$\langle \mathcal{O} \rangle^R = \frac{\text{Tr}(e^{-RH} \mathcal{O})}{\text{Tr}(e^{-RH})} = \frac{1}{Z} \sum_m \langle m | \mathcal{O} | m \rangle e^{-RE_\Psi} \quad (5.4)$$

The diagonal form factors entering the expression above are ill-defined in the infinite volume theory due to disconnected terms.

In order to obtain well-defined expressions for the correlation functions it is necessary to introduce a regularization scheme.

A. LeClair and G. Mussardo proposed an evaluation scheme [30] based on the Thermodynamic Bethe Ansatz. It was proven by Saleur [31] that it yields the correct results for expectation values of local conserved charges. However it was also argued in [31] that the LeClair-Mussardo formalism fails in the case of the two-point function. The same conclusion was reached in [35] studying massless limits of correlation functions. G. Delfino proposed a second, independent regularization scheme [33] for the one-point function; these two approaches are presented and compared in subsection 5.1.1. Mussardo showed using a toy model, that the two methods yield different results [34]; the same conclusion is reached by comparing the systematic low-temperature expansion of the two proposals (see 5.1.1).

A third approach is to consider a theory in finite volume L , to evaluate the form factor expansion using the well-defined finite volume form factors, and to take the limit $L \rightarrow \infty$. This method is built on first principles and it does not rely on any additional assumptions; moreover it is expected to work for any n-point function.

In this work we develop a systematic low-temperature expansion for the one-point function with a well-defined $L \rightarrow \infty$ limit; this calculation is presented in section 5.2. We find complete agreement with the LeClair-Mussardo proposal up to the third non-trivial order. In section 5.3 we apply our method to the two-point function. However, we only calculate the simplest terms; the systematic evaluation of the form factor expansion is out of the scope of the present work.

Finally we note, that it is also possible to numerically evaluate the form-factor expansion [38, 39, 40] or to develop a term by term regularization scheme based on the infinite volume connected form factors [115]. Eventually, after the completion of this thesis there appeared an independent work by Konik and Essler [116] which uses (in addition to a novel infinite volume regularization procedure) finite volume techniques similar to the ones presented in this work.

5.1.1 Comparison of the LeClair-Mussardo and the Delfino approaches

LeClair and Mussardo proposed the following expression for the low temperature ($T \ll m$, or equivalently $mR \gg 1$) expansion for the one-point function (5.4):

$$\langle \mathcal{O} \rangle^R = \sum_{n=0}^{\infty} \frac{1}{n!} \frac{1}{(2\pi)^n} \int \left[\prod_{i=1}^n d\theta_i \frac{e^{-\epsilon(\theta_i)}}{1 + e^{-\epsilon(\theta_i)}} \right] F_{2n}^c(\theta_1, \dots, \theta_n) \quad (5.5)$$

where F_{2n}^c is the connected diagonal form factor defined in eqn. (2.38) and $\epsilon(\theta)$ is the pseudo-energy function, which is the solution of the thermodynamic Bethe Ansatz equation

$$\epsilon(\theta) = mR \cosh(\theta) - \int \frac{d\theta'}{2\pi} \varphi(\theta - \theta') \log(1 + e^{-\epsilon(\theta')}) \quad (5.6)$$

The solution of this equation can be found by successive iteration, which results in

$$\begin{aligned} \epsilon(\theta) &= mR \cosh(\theta) - \int \frac{d\theta'}{2\pi} \varphi(\theta - \theta') e^{-mR \cosh \theta'} + \frac{1}{2} \int \frac{d\theta'}{2\pi} \varphi(\theta - \theta') e^{-2mR \cosh \theta'} + \\ &+ \int \frac{d\theta'}{2\pi} \frac{d\theta''}{2\pi} \varphi(\theta - \theta') \varphi(\theta' - \theta'') e^{-mR \cosh \theta'} e^{-mR \cosh \theta''} + O(e^{-3mR}) \end{aligned} \quad (5.7)$$

Using this expression, it is easy to derive the following expansion from (5.5)

$$\begin{aligned} \langle \mathcal{O} \rangle^R &= \langle \mathcal{O} \rangle + \int \frac{d\theta}{2\pi} F_2^c(e^{-mR \cosh \theta} - e^{-2mR \cosh \theta}) \\ &+ \frac{1}{2} \int \frac{d\theta_1}{2\pi} \frac{d\theta_2}{2\pi} (F_4^c(\theta_1, \theta_2) + 2\Phi(\theta_1 - \theta_2) F_2^c) e^{-mR \cosh \theta_1} e^{-mR \cosh \theta_2} \\ &+ O(e^{-3mR}) \end{aligned} \quad (5.8)$$

where $\langle \mathcal{O} \rangle$ denotes the zero-temperature vacuum expectation value. The above result can also be written in terms of the symmetric evaluation (2.35) as

$$\begin{aligned}
\langle \mathcal{O} \rangle^R &= \langle \mathcal{O} \rangle + \int \frac{d\theta}{2\pi} F_2^s (e^{-mR \cosh \theta} - e^{-2mR \cosh \theta}) + \\
&\quad \frac{1}{2} \int \frac{d\theta_1}{2\pi} \frac{d\theta_2}{2\pi} F_4^s(\theta_1, \theta_2) e^{-mR(\cosh \theta_1 + \cosh \theta_2)} + O(e^{-3mR})
\end{aligned} \tag{5.9}$$

where we used relations (2.39) and (2.41). Obtaining the third order correction from the LeClair-Mussardo expansion is a somewhat lengthy, but elementary computation, which results in

$$\begin{aligned}
&\frac{1}{6} \int \frac{d\theta_1}{2\pi} \frac{d\theta_2}{2\pi} \frac{d\theta_3}{2\pi} F_6^s(\theta_1, \theta_2, \theta_3) e^{-mR(\cosh \theta_1 + \cosh \theta_2 + \cosh \theta_3)} \\
&- \int \frac{d\theta_1}{2\pi} \frac{d\theta_2}{2\pi} F_4^s(\theta_1, \theta_2) e^{-mR(\cosh \theta_1 + 2 \cosh \theta_2)} + \int \frac{d\theta_1}{2\pi} F_2^s e^{-3mR \cosh \theta_1} \\
&- \frac{1}{2} \int \frac{d\theta_1}{2\pi} \frac{d\theta_2}{2\pi} F_2^s \varphi(\theta_1 - \theta_2) e^{-mR(\cosh \theta_1 + 2 \cosh \theta_2)}
\end{aligned} \tag{5.10}$$

where we used eqns. (2.39, 2.41, 2.42) to express the result in terms of the symmetric evaluation.

Delfino's proposal for the one-point function reads:

$$\langle \mathcal{O} \rangle_D^R = \sum_{n=0}^{\infty} \frac{1}{n!} \frac{1}{(2\pi)^n} \int \left[\prod_{i=1}^n d\theta_i \frac{e^{-mR \cosh \theta_i}}{1 + e^{-mR \cosh \theta_i}} \right] F_{2n}^s(\theta_1, \dots, \theta_n) \tag{5.11}$$

which gives the following result when expanded to second order:

$$\begin{aligned}
\langle \mathcal{O} \rangle_D^R &= \langle \mathcal{O} \rangle + \int \frac{d\theta}{2\pi} F_2^s (e^{-mR \cosh \theta} - e^{-2mR \cosh \theta}) + \\
&\quad \frac{1}{2} \int \frac{d\theta_1}{2\pi} \frac{d\theta_2}{2\pi} F_4^s(\theta_1, \theta_2) e^{-mR(\cosh \theta_1 + \cosh \theta_2)} + O(e^{-3mR})
\end{aligned} \tag{5.12}$$

Note that the two proposals coincide with each other to this order, which was already noted in [33]. However, this is not the case in the next order. Expanding (5.11) results in

$$\begin{aligned}
&\frac{1}{6} \int \frac{d\theta_1}{2\pi} \frac{d\theta_2}{2\pi} \frac{d\theta_3}{2\pi} F_6^s(\theta_1, \theta_2, \theta_3) e^{-mR(\cosh \theta_1 + \cosh \theta_2 + \cosh \theta_3)} \\
&- \int \frac{d\theta_1}{2\pi} \frac{d\theta_2}{2\pi} F_4^s(\theta_1, \theta_2) e^{-mR(\cosh \theta_1 + 2 \cosh \theta_2)} + \int \frac{d\theta_1}{2\pi} F_2^s e^{-3mR \cosh \theta_1}
\end{aligned} \tag{5.13}$$

It can be seen that the two proposals differ at this order (the last term of (5.10) is missing from (5.13)), which was already noted by Mussardo using a toy model in [34], but the computation presented above is model independent and shows the general form of the discrepancy.

5.2 Low-temperature expansion for the one-point function

We now evaluate the finite temperature expectations value in a finite, but large volume L :

$$\langle \mathcal{O} \rangle_L^R = \frac{\text{Tr}_L (e^{-RH_L} \mathcal{O})}{\text{Tr}_L (e^{-RH_L})} \quad (5.14)$$

where H_L is the finite volume Hamiltonian, and Tr_L means that the trace is now taken over the finite volume Hilbert space. For later convenience we introduce a new notation:

$$|\theta_1, \dots, \theta_n\rangle_L = |\{I_1, \dots, I_n\}\rangle_L$$

where $\theta_1, \dots, \theta_n$ solve the Bethe-Yang equations for n particles with quantum numbers I_1, \dots, I_n at the given volume L . We can develop the low temperature expansion of (5.14) in powers of e^{-mR} using

$$\begin{aligned} \text{Tr}_L (e^{-RH_L} \mathcal{O}) &= \langle \mathcal{O} \rangle_L + \sum_{\theta^{(1)}} e^{-mR \cosh \theta^{(1)}} \langle \theta^{(1)} | \mathcal{O} | \theta^{(1)} \rangle_L \\ &+ \frac{1}{2} \sum_{\theta_1^{(2)}, \theta_2^{(2)}} ' e^{-mR(\cosh \theta_1^{(2)} + \cosh \theta_2^{(2)})} \langle \theta_1^{(2)}, \theta_2^{(2)} | \mathcal{O} | \theta_1^{(2)}, \theta_2^{(2)} \rangle_L + \\ &+ \frac{1}{6} \sum_{\theta_1^{(3)}, \theta_2^{(3)}, \theta_3^{(3)}} ' e^{-mR(\cosh \theta_1^{(3)} + \cosh \theta_2^{(3)} + \cosh \theta_3^{(3)})} \langle \theta_1^{(3)}, \theta_2^{(3)}, \theta_3^{(3)} | \mathcal{O} | \theta_1^{(3)}, \theta_2^{(3)}, \theta_3^{(3)} \rangle_L \\ &+ O(e^{-4mR}) \end{aligned} \quad (5.15)$$

and

$$\begin{aligned} \text{Tr}_L (e^{-RH_L}) &= 1 + \sum_{\theta^{(1)}} e^{-mR \cosh(\theta^{(1)})} + \frac{1}{2} \sum_{\theta_1^{(2)}, \theta_2^{(2)}} ' e^{-mR(\cosh(\theta_1^{(2)}) + \cosh(\theta_2^{(2)}))} \\ &+ \frac{1}{6} \sum_{\theta_1^{(3)}, \theta_2^{(3)}, \theta_3^{(3)}} ' e^{-mR(\cosh \theta_1^{(3)} + \cosh \theta_2^{(3)} + \cosh \theta_3^{(3)})} + O(e^{-4mR}) \end{aligned} \quad (5.16)$$

The denominator of (5.14) can then be easily expanded:

$$\begin{aligned} \frac{1}{\text{Tr}_L (e^{-RH_L})} &= 1 - \sum_{\theta^{(1)}} e^{-mR \cosh \theta^{(1)}} + \left(\sum_{\theta^{(1)}} e^{-mR \cosh \theta^{(1)}} \right)^2 - \frac{1}{2} \sum_{\theta_1^{(2)}, \theta_2^{(2)}} ' e^{-mR(\cosh \theta_1^{(2)} + \cosh \theta_2^{(2)})} \\ &- \left(\sum_{\theta^{(1)}} e^{-mR \cosh \theta^{(1)}} \right)^3 + \left(\sum_{\theta^{(1)}} e^{-mR \cosh \theta^{(1)}} \right) \sum_{\theta_1^{(2)}, \theta_2^{(2)}} ' e^{-mR(\cosh \theta_1^{(2)} + \cosh \theta_2^{(2)})} \\ &- \frac{1}{6} \sum_{\theta_1^{(3)}, \theta_2^{(3)}, \theta_3^{(3)}} ' e^{-mR(\cosh \theta_1^{(3)} + \cosh \theta_2^{(3)} + \cosh \theta_3^{(3)})} + O(e^{-4mR}) \end{aligned} \quad (5.17)$$

The primes in the multi-particle sums serve as a reminder that there exist only states for which all quantum numbers are distinct. Since we assumed that there is a single particle species, this means that terms in which any two of the rapidities coincide are excluded. All n -particle terms in (5.15) and (5.16) have a $1/n!$ pre-factor which takes into account that different ordering of the same rapidities give the same state; as the expansion contains only diagonal matrix elements, phases resulting from reordering the particles cancel. The upper indices of the rapidity variables indicate the number of particles in the original finite volume states; this is going to be handy when replacing the discrete sums with integrals since it keeps track of which multi-particle state density is relevant.

We also need an extension of the finite volume matrix elements to rapidities that are not necessarily solutions of the appropriate Bethe-Yang equations. The required analytic continuation is simply given by eqn. (2.36)

$$\langle \theta_1, \dots, \theta_n | \mathcal{O} | \theta_1, \dots, \theta_n \rangle_L = \frac{1}{\rho_n(\theta_1, \dots, \theta_n)_L} \sum_{A \subset \{1, 2, \dots, n\}} F_{2|A|}^s(\{\theta_i\}_{i \in A}) \rho_{n-|A|}(\{\theta_i\}_{i \notin A})_L + O(e^{-\mu L}) \quad (5.18)$$

where we made explicit the volume dependence of the n -particle density factors. The last term serves as a reminder that this prescription only defines the form factor to all orders in $1/L$ (i.e. up to residual finite size corrections), but this is sufficient to perform the computations in the sequel.

Using the leading behavior of the n -particle state density, contributions from the n -particle sector scale as L^n , and for the series expansions (5.15), (5.16) and (5.17) it is necessary that $mL \ll e^{mR}$. However if mR is big enough there remains a large interval

$$1 \ll mL \ll e^{mR}$$

where the expansions are expected to be valid. After substituting these expansions into (5.14) we will find order by order that the leading term of the net result is $O(L^0)$, and the corrections scale as negative powers of L . Therefore in (5.14) we can continue analytically to large L and take the $L \rightarrow \infty$ limit.

It is an interesting question why this limit exists, or to be more precise, why do form factors with low number of particles determine the leading terms of the low-temperature expansion. As a matter of fact, the particle density N/L has a non-vanishing $L \rightarrow \infty$ limit, the thermal average is therefore dominated by thermodynamic configurations where the particle number grows proportional with the volume. However, the leading contributions come from disconnected terms and they still involve form factors with a low number of particles, as it was pointed out in [115].

5.2.1 Corrections of order e^{-mR}

Substituting the appropriate terms from (5.17) and (5.15) into (5.14) gives the result

$$\langle \mathcal{O} \rangle_L^R = \langle \mathcal{O} \rangle_L + \sum_{\theta^{(1)}} e^{-mR \cosh \theta^{(1)}} (\langle \theta^{(1)} | \mathcal{O} | \theta^{(1)} \rangle_L - \langle \mathcal{O} \rangle_L) + O(e^{-2mR})$$

Taking the $L \rightarrow \infty$ limit one can replace the summation with an integral over the states in the rapidity space:

$$\sum_i \rightarrow \int \frac{d\theta}{2\pi} \rho_1(\theta)$$

and using (2.32) we can write

$$\rho_1(\theta) (\langle \theta | \mathcal{O} | \theta \rangle_L - \langle \mathcal{O} \rangle_L) = F_2^s + O(e^{-\mu L}) \quad (5.19)$$

so we obtain

$$\langle \mathcal{O} \rangle_L^R = \langle \mathcal{O} \rangle + \int \frac{d\theta}{2\pi} F_2^s e^{-mR \cosh \theta} + O(e^{-2mR})$$

which coincides with eqn. (5.9) to this order.

5.2.2 Corrections of order e^{-2mR}

Substituting again the appropriate terms from (5.17) and (5.15) into (5.14) gives the result

$$\begin{aligned} \langle \mathcal{O} \rangle_L^R &= \langle \mathcal{O} \rangle_L + \sum_{\theta^{(1)}} e^{-mR \cosh \theta^{(1)}} (\langle \theta^{(1)} | \mathcal{O} | \theta^{(1)} \rangle_L - \langle \mathcal{O} \rangle_L) \\ &\quad - \left(\sum_{\theta_1^{(1)}} e^{-mR \cosh \theta_1^{(1)}} \right) \left(\sum_{\theta_2^{(1)}} e^{-mR \cosh \theta_2^{(1)}} (\langle \theta_2^{(1)} | \mathcal{O} | \theta_2^{(1)} \rangle_L - \langle \mathcal{O} \rangle_L) \right) \\ &\quad + \frac{1}{2} \sum_{\theta_1^{(2)}, \theta_2^{(2)}} e^{-mR(\cosh \theta_1^{(2)} + \cosh \theta_2^{(2)})} (\langle \theta_1^{(2)}, \theta_2^{(2)} | \mathcal{O} | \theta_1^{(2)}, \theta_2^{(2)} \rangle_L - \langle \mathcal{O} \rangle_L) + O(e^{-3mR}) \end{aligned}$$

The $O(e^{-2mR})$ terms can be rearranged as follows. We add and subtract a term to remove the constraint from the two-particle sum:

$$\begin{aligned} &+ \frac{1}{2} \sum_{\theta_1^{(2)}, \theta_2^{(2)}} e^{-mR(\cosh \theta_1^{(2)} + \cosh \theta_2^{(2)})} (\langle \theta_1^{(2)}, \theta_2^{(2)} | \mathcal{O} | \theta_1^{(2)}, \theta_2^{(2)} \rangle_L - \langle \mathcal{O} \rangle_L) \\ &- \frac{1}{2} \sum_{\theta_1^{(2)} = \theta_2^{(2)}} e^{-2mR \cosh \theta_1^{(2)}} (\langle \theta_1^{(2)}, \theta_1^{(2)} | \mathcal{O} | \theta_1^{(2)}, \theta_1^{(2)} \rangle_L - \langle \mathcal{O} \rangle_L) \\ &- \frac{1}{2} \sum_{\theta_1^{(1)}} \sum_{\theta_2^{(1)}} e^{-mR(\cosh \theta_1^{(1)} + \cosh \theta_2^{(1)})} (\langle \theta_1^{(1)} | \mathcal{O} | \theta_1^{(1)} \rangle_L + \langle \theta_2^{(1)} | \mathcal{O} | \theta_2^{(1)} \rangle_L - 2\langle \mathcal{O} \rangle_L) \end{aligned}$$

The $\theta_1^{(2)} = \theta_2^{(2)}$ terms correspond to insertion of some spurious two-particle states with equal Bethe quantum numbers for the two particles ($I_1 = I_2$). The two-particle Bethe-Yang equations in this case degenerates to the one-particle case (as discussed before, the matrix elements can be defined for these “states” without any problems since we have the analytic formula (5.18) valid to any order in $1/L$). This also means that the density relevant to the diagonal two-particle sum is ρ_1 and so for large L we can substitute the sums with the following integrals

$$\sum_{\theta_{1,2}^{(1)}} \rightarrow \int \frac{d\theta_{1,2}}{2\pi} \rho_1(\theta_{1,2}) \quad , \quad \sum_{\theta_1^{(2)}=\theta_2^{(2)}} \rightarrow \int \frac{d\theta}{2\pi} \rho_1(\theta) \quad , \quad \sum_{\theta_1^{(2)}, \theta_2^{(2)}} \rightarrow \int \frac{d\theta_1}{2\pi} \frac{d\theta_2}{2\pi} \rho_2(\theta_1, \theta_2)$$

Let us express the finite volume matrix elements in terms of form factors using (2.32) and (2.33):

$$\begin{aligned} & \rho_2(\theta_1, \theta_2) \left(\langle \theta_1^{(2)}, \theta_2^{(2)} | \mathcal{O} | \theta_1^{(2)}, \theta_2^{(2)} \rangle_L - \langle \mathcal{O} \rangle_L \right) \\ & - \rho_1(\theta_1) \rho_1(\theta_2) (\langle \theta_1 | \mathcal{O} | \theta_1 \rangle_L + \langle \theta_2 | \mathcal{O} | \theta_2 \rangle_L - 2\langle \mathcal{O} \rangle_L) = F_4^s(\theta_1, \theta_2) + O(e^{-\mu L}) \end{aligned}$$

Combining the above relation with (5.19), we also have

$$\langle \theta, \theta | \mathcal{O} | \theta, \theta \rangle_L - \langle \mathcal{O} \rangle_L = \frac{2\rho_1(\theta)}{\rho_2(\theta, \theta)} F_2^s + O(e^{-\mu L})$$

where we used that $F_4^s(\theta, \theta) = 0$, which is just the exclusion property mention after eqn. (2.35). Note that

$$\frac{\rho_1(\theta)^2}{\rho_2(\theta, \theta)} = 1 + O(L^{-1})$$

and therefore in the limit $L \rightarrow \infty$ we obtain

$$- \int \frac{d\theta}{2\pi} e^{-2mR \cosh \theta} F_2^s + \frac{1}{2} \int \frac{d\theta_1}{2\pi} \frac{d\theta_2}{2\pi} F_4^s(\theta_1, \theta_2) e^{-mR(\cosh \theta_1 + \cosh \theta_2)}$$

which is equal to the relevant contributions in the LeClair-Mussardo expansion (5.9).

5.2.3 Corrections of order e^{-3mR}

In order to shorten the presentation, we introduce some further convenient notations:

$$\begin{aligned} E_i &= m \cosh \theta_i \\ \langle \theta_1, \dots, \theta_n | \mathcal{O} | \theta_1, \dots, \theta_n \rangle_L &= \langle 1 \dots n | \mathcal{O} | 1 \dots n \rangle_L \\ \rho_n(\theta_1, \dots, \theta_n) &= \rho(1 \dots n) \end{aligned}$$

Summations will be shortened to

$$\begin{aligned} \sum_{\theta_1 \dots \theta_n} &\rightarrow \sum_{1 \dots n} \\ \sum'_{\theta_1 \dots \theta_n} &\rightarrow \sum'_{1 \dots n} \end{aligned}$$

Given these notations, we now multiply (5.15) with (5.17) and collect the third order correction terms:

$$\begin{aligned}
 & \frac{1}{6} \sum'_{123} e^{-R(E_1+E_2+E_3)} (\langle 123|\mathcal{O}|123\rangle_L - \langle \mathcal{O}\rangle_L) \\
 & - \left(\sum_1 e^{-RE_1} \right) \frac{1}{2} \sum'_{23} e^{-R(E_2+E_3)} (\langle 23|\mathcal{O}|23\rangle_L - \langle \mathcal{O}\rangle_L) \\
 & + \left\{ \left(\sum_1 e^{-RE_1} \right) \left(\sum_2 e^{-RE_2} \right) - \frac{1}{2} \sum'_{12} e^{-R(E_1+E_2)} \right\} \left(\sum_3 e^{-RE_3} \right) (\langle 3|\mathcal{O}|3\rangle_L - \langle \mathcal{O}\rangle_L)
 \end{aligned}$$

To keep trace of the state densities, we avoid combining rapidity sums. Now we replace the constrained summations by free sums with the diagonal contributions subtracted:

$$\begin{aligned}
 \sum'_{12} &= \sum_{12} - \sum_{1=2} \\
 \sum'_{123} &= \sum_{123} - \left(\sum_{1=2,3} + \sum_{2=3,1} + \sum_{1=3,2} \right) + 2 \sum_{1=2=3}
 \end{aligned}$$

where the diagonal contributions are labeled to show which diagonal it sums over, but otherwise the given sum is free, e.g.

$$\sum_{1=2,3}$$

shows a summation over all triplets $\theta_1^{(3)}, \theta_2^{(3)}, \theta_3^{(3)}$ where $\theta_1^{(3)} = \theta_2^{(3)}$ and $\theta_3^{(3)}$ runs free (it can also be equal with the other two). We also make use of the notation

$$F(12\dots n) = F_{2n}^s(\theta_1, \dots, \theta_n)$$

so the necessary matrix elements can be written in the form

$$\begin{aligned}
 \rho(123) (\langle 123|\mathcal{O}|123\rangle_L - \langle \mathcal{O}\rangle_L) &= F(123) + \rho(1)F(23) + \dots + \rho(12)F(3) + \dots \\
 \rho(122) (\langle 122|\mathcal{O}|122\rangle_L - \langle \mathcal{O}\rangle_L) &= 2\rho(2)F(12) + 2\rho(12)F(3) + \rho(22)F(1) \\
 \rho(111) (\langle 111|\mathcal{O}|111\rangle_L - \langle \mathcal{O}\rangle_L) &= 3\rho(111)F(1) \\
 \rho(12) (\langle 12|\mathcal{O}|12\rangle_L - \langle \mathcal{O}\rangle_L) &= F(12) + \rho(1)F(2) + \rho(2)F(1) \\
 \rho(11) (\langle 11|\mathcal{O}|11\rangle_L - \langle \mathcal{O}\rangle_L) &= 2\rho(1)F(1) \\
 \rho(1) (\langle 1|\mathcal{O}|1\rangle_L - \langle \mathcal{O}\rangle_L) &= F(1)
 \end{aligned} \tag{5.20}$$

where we used that F and ρ are entirely symmetric in all their arguments, and the ellipsis in the the first line denote two plus two terms of the same form, but with different partitioning of the rapidities, which can be obtained by cyclic permutation from those displayed. We also used the exclusion property mentioned after eqn. (2.35).

We can now proceed by collecting terms according to the number of free rapidity variables. The terms containing threefold summation are

$$\begin{aligned} & \frac{1}{6} \sum_{123} e^{-R(E_1+E_2+E_3)} (\langle 123|\mathcal{O}|123\rangle_L - \langle \mathcal{O}\rangle_L) - \frac{1}{2} \sum_1 \sum_{2,3} (\langle 23|\mathcal{O}|23\rangle_L - \langle \mathcal{O}\rangle_L) \\ & + \left(\sum_1 \sum_2 \sum_3 - \frac{1}{2} \sum_{1,2} \sum_3 \right) (\langle 3|\mathcal{O}|3\rangle_L - \langle \mathcal{O}\rangle_L) \end{aligned}$$

Replacing the sums with integrals

$$\begin{aligned} \sum_1 & \rightarrow \int \frac{d\theta_1}{2\pi} \rho(1) \\ \sum_{1,2} & \rightarrow \int \frac{d\theta_1}{2\pi} \frac{d\theta_2}{2\pi} \rho(12) \\ \sum_{1,2,3} & \rightarrow \int \frac{d\theta_1}{2\pi} \frac{d\theta_2}{2\pi} \frac{d\theta_3}{2\pi} \rho(123) \end{aligned}$$

and using (5.20) we get

$$\begin{aligned} & \frac{1}{6} \int \frac{d\theta_1}{2\pi} \frac{d\theta_2}{2\pi} \frac{d\theta_3}{2\pi} e^{-R(E_1+E_2+E_3)} (F(123) + 3\rho(1)F(23) + 3\rho(12)F(3)) \\ & - \frac{1}{2} \int \frac{d\theta_1}{2\pi} \frac{d\theta_2}{2\pi} \frac{d\theta_3}{2\pi} e^{-R(E_1+E_2+E_3)} (\rho(1)F(23) + 2\rho(1)\rho(2)F(3)) \\ & + \int \frac{d\theta_1}{2\pi} \frac{d\theta_2}{2\pi} \frac{d\theta_3}{2\pi} e^{-R(E_1+E_2+E_3)} \left(\rho(1)\rho(2)F(3) - \frac{1}{2}\rho(12)F(3) \right) \end{aligned}$$

where we reshuffled some of the integration variables. Note that all terms cancel except the one containing $F(123)$ and writing it back to its usual form we obtain

$$\frac{1}{6} \int \frac{d\theta_1}{2\pi} \frac{d\theta_2}{2\pi} \frac{d\theta_3}{2\pi} F_6^s(\theta_1, \theta_2, \theta_3) e^{-mR(\cosh \theta_1 + \cosh \theta_2 + \cosh \theta_3)} \quad (5.21)$$

It is also easy to deal with terms containing a single integral. The only term of this form is

$$\frac{1}{3} \sum_{1=2=3} e^{-R(E_1+E_2+E_3)} (\langle 123|\mathcal{O}|123\rangle_L - \langle \mathcal{O}\rangle_L)$$

When all rapidities $\theta_1^{(3)}, \theta_2^{(3)}, \theta_3^{(3)}$ are equal, the three-particle Bethe-Yang equations reduce to the one-particle case

$$mL \sinh \theta_1^{(3)} = 2\pi I_1$$

Therefore the relevant state density is that of the one-particle state:

$$\begin{aligned} \frac{1}{3} \int \frac{d\theta_1}{2\pi} e^{-3RE_1} \rho(1) (\langle 111|\mathcal{O}|111\rangle_L - \langle \mathcal{O}\rangle_L) & = \int \frac{d\theta_1}{2\pi} e^{-3RE_1} \rho(1) \frac{\rho(11)}{\rho(111)} F(1) \\ & \rightarrow \int \frac{d\theta_1}{2\pi} e^{-3mR \cosh \theta_1} F_2^s \end{aligned} \quad (5.22)$$

where we used that

$$\rho(1) \frac{\rho(11)}{\rho(111)} \rightarrow 1$$

when $L \rightarrow \infty$.

The calculation of double integral terms is much more involved. We need to consider

$$\begin{aligned} & -\frac{1}{6} \left(\sum_{1=2,3} + \sum_{1=3,2} + \sum_{2=3,1} \right) e^{-R(E_1+E_2+E_3)} (\langle 123|\mathcal{O}|123\rangle_L - \langle \mathcal{O}\rangle_L) \\ & + \frac{1}{2} \sum_1 \sum_{2=3} e^{-R(E_1+E_2+E_3)} (\langle 23|\mathcal{O}|23\rangle_L - \langle \mathcal{O}\rangle_L) \\ & + \frac{1}{2} \sum_{1=2} \sum_3 e^{-R(E_1+E_2+E_3)} (\langle 3|\mathcal{O}|3\rangle_L - \langle \mathcal{O}\rangle_L) \end{aligned} \quad (5.23)$$

We need the density of partially degenerate three-particle states. The relevant Bethe-Yang equations are

$$\begin{aligned} mL \sinh \theta_1 + \delta(\theta_1 - \theta_2) &= 2\pi I_1 \\ mL \sinh \theta_2 + 2\delta(\theta_2 - \theta_1) &= 2\pi I_2 \end{aligned}$$

where we supposed that the first and the third particles are degenerate (i.e. $I_3 = I_1$), and used a convention for the phase-shift and the quantum numbers where $\delta(0) = 0$. The density of these degenerate states is then given by

$$\bar{\rho}(13, 2) = \det \begin{pmatrix} LE_1 + \varphi(\theta_1 - \theta_2) & -\varphi(\theta_1 - \theta_2) \\ -2\varphi(\theta_1 - \theta_2) & LE_2 + 2\varphi(\theta_1 - \theta_2) \end{pmatrix}$$

where we used that $\varphi(\theta) = \varphi(-\theta)$. Using the above result and substituting integrals for the sums, we can rewrite eqn. (5.23) in the form

$$\begin{aligned} & -\frac{1}{6} \int \frac{d\theta_1}{2\pi} \frac{d\theta_2}{2\pi} e^{-R(2E_1+E_2)} \frac{\bar{\rho}(13, 2)}{\rho(112)} (2\rho(1)F(12) + 2\rho(12)F(1) + \rho(11)F(2)) + \dots \\ & + \frac{1}{2} \int \frac{d\theta_1}{2\pi} \frac{d\theta_2}{2\pi} e^{-R(E_1+2E_2)} \rho(1)\rho(2) \frac{2\rho(2)}{\rho(22)} F(2) \\ & + \frac{1}{2} \int \frac{d\theta_1}{2\pi} \frac{d\theta_3}{2\pi} e^{-R(2E_1+E_3)} \rho(1)\rho(3) \frac{1}{\rho(3)} F(3) \end{aligned}$$

where the ellipsis denote two terms that can be obtained by cyclical permutation of the indices 1, 2, 3 from the one that is explicitly displayed, and these three contributions can be shown to be equal to each other by relabeling the integration variables:

$$\begin{aligned} & -\frac{1}{2} \int \frac{d\theta_1}{2\pi} \frac{d\theta_2}{2\pi} e^{-R(2E_1+E_2)} \frac{\bar{\rho}(13, 2)}{\rho(112)} (2\rho(1)F(12) + 2\rho(12)F(1) + \rho(11)F(2)) \\ & + \frac{1}{2} \int \frac{d\theta_1}{2\pi} \frac{d\theta_2}{2\pi} e^{-R(E_1+2E_2)} \rho(1)\rho(2) \frac{2\rho(2)}{\rho(22)} F(2) \\ & + \frac{1}{2} \int \frac{d\theta_1}{2\pi} \frac{d\theta_3}{2\pi} e^{-R(2E_1+E_3)} \rho(1)\rho(3) \frac{1}{\rho(3)} F(3) \end{aligned} \quad (5.24)$$

We first evaluate the terms containing $F(23)$ which results in

$$- \int \frac{d\theta_1}{2\pi} \frac{d\theta_2}{2\pi} F_4^s(\theta_1, \theta_2) e^{-mR(\cosh \theta_1 + 2 \cosh \theta_2)} \quad (5.25)$$

using that

$$\frac{\bar{\rho}(13, 2)}{\rho(112)} \rho(1) = 1 + O(L^{-1})$$

We can now treat the terms containing the amplitude $F(1) = F(2) = F(3) = F_2^s$. Exchanging the variables $\theta_1 \leftrightarrow \theta_2$ in the second line and redefining $\theta_3 \rightarrow \theta_2$ in the third line of eqn. (5.24) results in

$$\frac{F_2^s}{2} \int \frac{d\theta_1}{2\pi} \frac{d\theta_2}{2\pi} e^{-R(2E_1 + E_2)} \left\{ -\frac{\bar{\rho}(13, 2)}{\rho(112)} (2\rho(12) + \rho(11)) + \frac{2\rho(1)^2 \rho(2)}{\rho(11)} + \rho(1) \right\}$$

The combination of the various densities in this expression requires special care. From the large L asymptotics

$$\rho(i) \sim E_i L \quad , \quad \rho(ij) \sim E_i E_j L^2 \quad , \quad \rho(ijk) \sim E_i E_j E_k L^3 \quad , \quad \bar{\rho}(13, 2) \sim E_1 E_2 L^2$$

it naively scales with L . However, it can be easily verified that the coefficient of the leading term, which is linear in L , is exactly zero. Without this, the large L limit would not make sense, so this is rather reassuring. We can then calculate the sub-leading term, which requires tedious but elementary manipulations. The end result turns out to be extremely simple

$$- \frac{\bar{\rho}(13, 2)}{\rho(112)} (2\rho(12) + \rho(11)) + \frac{2\rho(1)^2 \rho(2)}{\rho(11)} + \rho(1) = -\varphi(\theta_1 - \theta_2) + O(L^{-1}) \quad (5.26)$$

so the contribution in the $L \rightarrow \infty$ limit turns out to be just

$$- \frac{1}{2} \int \frac{d\theta_1}{2\pi} \frac{d\theta_2}{2\pi} F_2^s \varphi(\theta_1 - \theta_2) e^{-mR(2 \cosh \theta_1 + \cosh \theta_2)} \quad (5.27)$$

Summing up the contributions (5.21), (5.22), (5.25) and (5.27) we obtain

$$\begin{aligned} & \frac{1}{6} \int \frac{d\theta_1}{2\pi} \frac{d\theta_2}{2\pi} \frac{d\theta_3}{2\pi} F_6^s(\theta_1, \theta_2, \theta_3) e^{-mR(\cosh \theta_1 + \cosh \theta_2 + \cosh \theta_3)} \\ & - \int \frac{d\theta_1}{2\pi} \frac{d\theta_2}{2\pi} F_4^s(\theta_1, \theta_2) e^{-mR(\cosh \theta_1 + 2 \cosh \theta_2)} + \int \frac{d\theta_1}{2\pi} F_2^s e^{-3mR \cosh \theta_1} \\ & - \frac{1}{2} \int \frac{d\theta_1}{2\pi} \frac{d\theta_2}{2\pi} F_2^s \varphi(\theta_1 - \theta_2) e^{-mR(\cosh \theta_1 + 2 \cosh \theta_2)} \end{aligned} \quad (5.28)$$

which agrees exactly with eqn. (5.10).

This result gives an independent support for the LeClair-Mussardo expansion. The calculation is model independent, and although we only worked it out to order e^{-3mR} , it is expected that it coincides with the LeClair-Mussardo expansion to all orders. For a complete proof we need a better understanding of its structure, which is out of the scope of the present work.

5.3 Low-temperature expansion for the two-point function

The method presented in the previous section has a straightforward extension to higher point correlation functions. For example, a two-point correlation function

$$\langle \mathcal{O}_1(x, t) \mathcal{O}_2(0) \rangle_L^R = \frac{\text{Tr}_L (e^{-RH_L} \mathcal{O}_1(x, t) \mathcal{O}_2(0))}{\text{Tr}_L (e^{-RH_L})}$$

can be expanded inserting two complete sets of states

$$\text{Tr}_L (e^{-RH_L} \mathcal{O}_1(x, t) \mathcal{O}_2(0)) = \sum_{m, n} e^{-RE_n(L)} \langle n | \mathcal{O}(x, t)_1 | m \rangle_L \langle m | \mathcal{O}_2(0) | n \rangle_L \quad (5.29)$$

The above expression can be evaluated along the lines presented in the previous section, provided that the intermediate state sums are properly truncated. The explicit evaluation of expansion (5.29) has not yet been carried out. As a first step, here we investigate the simplest terms and calculate the first nontrivial contribution; the systematic evaluation of higher order terms is left for further work. We wish to remark, that the material presented in this section is unpublished.

We define

$$\langle \mathcal{O}_1(x, t) \mathcal{O}_2(0) \rangle_L^R = \frac{1}{Z} \sum_{N, M} I_{NM} \quad (5.30)$$

where

$$I_{NM} = \sum_{I_1 \dots I_N} \sum_{J_1 \dots J_M} \langle \{I_1 \dots I_N\} | \mathcal{O}_1(0) | \{J_1 \dots J_M\} \rangle_L \times \langle \{J_1 \dots J_M\} | \mathcal{O}_2(0) | \{I_1 \dots I_N\} \rangle_L e^{i(P_1 - P_2)x} e^{-E_1(R-t)} e^{-E_2t} \quad (5.31)$$

and $E_{1,2}$ and $P_{1,2}$ are the total energies and momenta of the multi-particle states.

It is easy to see, that the terms $N = 0, M = 0 \dots \infty$ and $N = 0 \dots \infty, M = 0$ add up to zero-temperature correlation functions

$$\sum_{M=0}^{\infty} I_{0M} = \langle \mathcal{O}_1(x, t) \mathcal{O}_2(0) \rangle_L \quad \sum_{N=0}^{\infty} I_{N0} = \langle \mathcal{O}_1(x, R-t) \mathcal{O}_2(0) \rangle_L$$

The first nontrivial term is therefore I_{11} , which is given by

$$I_{11} = \sum_{I, J} \langle \{I\} | \mathcal{O}_1(0) | \{J\} \rangle_L \langle \{J\} | \mathcal{O}_2(0) | \{I\} \rangle_L e^{i(p_1 - p_2)x} e^{-E_1(R-t)} e^{-E_2t} \quad (5.32)$$

where now $E_{1,2} = m \cosh(\theta_{1,2})$ and $p_{1,2} = m \sinh(\theta_{1,2})$ are finite size one-particle energies and momenta. Upon (2.18) and (2.32) the two-particle matrix elements are given by

$$\begin{aligned} \langle \{I\} | \mathcal{O}_1(0) | \{J\} \rangle_L &= \frac{F_2^{\mathcal{O}_1}(\theta_1 + i\pi, \theta_2)}{\sqrt{\rho_1(\theta_1)\rho_1(\theta_2)}} + \delta_{IJ} \langle \mathcal{O}_1 \rangle \\ \langle \{J\} | \mathcal{O}_2(0) | \{I\} \rangle_L &= \frac{F_2^{\mathcal{O}_2}(\theta_2 + i\pi, \theta_1)}{\sqrt{\rho_1(\theta_1)\rho_1(\theta_2)}} + \delta_{IJ} \langle \mathcal{O}_2 \rangle \end{aligned}$$

Substituting the above formulas into (5.32) one obtains

$$\begin{aligned}
I_{11} = & \sum_{I,J} \frac{F_2^{\mathcal{O}_1}(\theta_1 + i\pi, \theta_2) F_2^{\mathcal{O}_2}(\theta_2 + i\pi, \theta_1)}{\rho_1(\theta_1) \rho_1(\theta_2)} e^{i(p_1 - p_2)x} e^{-E_1(R-t)} e^{-E_2 t} \\
& + \langle \mathcal{O}_1 \rangle \sum_J \frac{F_2^{\mathcal{O}_2}(\theta_2 + i\pi, \theta_2)}{\rho_1(\theta_2)} e^{-E_2 R} + \langle \mathcal{O}_2 \rangle \sum_J \frac{F_2^{\mathcal{O}_1}(\theta_1 + i\pi, \theta_1)}{\rho_1(\theta_1)} e^{-E_1 R} \\
& \qquad \qquad \qquad + \sum_I \langle \mathcal{O}_1 \rangle \langle \mathcal{O}_2 \rangle e^{-E_1 R} \tag{5.33}
\end{aligned}$$

The first term in (5.33) can be transformed in the $L \rightarrow \infty$ limit into the well-defined (singularity free) double integral

$$\int \frac{d\theta_1}{2\pi} \frac{d\theta_2}{2\pi} F_2^{\mathcal{O}_1}(\theta_1 + i\pi, \theta_2) F_2^{\mathcal{O}_2}(\theta_2 + i\pi, \theta_1) e^{i(\sinh(\theta_1) - \sinh(\theta_2))mx} e^{-m(R-t) \cosh(\theta_1) - mt \cosh(\theta_2)} \tag{5.34}$$

In the second and third terms of (5.33) one can recognize the first thermal corrections to the expectation values of \mathcal{O}_2 and \mathcal{O}_1 , as given by (5.19). The last term is of $\mathcal{O}(L)$ and thus divergent; however, it gets canceled by the $\mathcal{O}(L)$ term coming from the expansion

$$1/Z = 1 - \sum_I e^{-E_1 R} + \mathcal{O}(e^{-2mR})$$

Putting everything together

$$\begin{aligned}
\langle \mathcal{O}_1(x, t) \mathcal{O}_2(0) \rangle^R = & \langle \mathcal{O}_1 \rangle^R \langle \mathcal{O}_2 \rangle^R + \\
& + (\langle \mathcal{O}_1(x, t) \mathcal{O}_2(0) \rangle - \langle \mathcal{O}_1 \rangle \langle \mathcal{O}_2 \rangle) + (\langle \mathcal{O}_1(x, R-t) \mathcal{O}_2(0) \rangle - \langle \mathcal{O}_1 \rangle \langle \mathcal{O}_2 \rangle) \tag{5.35} \\
& + \int \frac{d\theta_1}{2\pi} \frac{d\theta_2}{2\pi} F_2^{\mathcal{O}_1}(\theta_1 + i\pi, \theta_2) F_2^{\mathcal{O}_2}(\theta_2 + i\pi, \theta_1) e^{i(\sinh(\theta_1) - \sinh(\theta_2))mx} e^{-m(R-t) \cosh(\theta_1) - mt \cosh(\theta_2)} \\
& + \mathcal{O}(e^{-2mR})
\end{aligned}$$

Equation (5.35) is a new result of this work and it can serve as a starting point to calculate higher order terms.¹

5.3.1 Comparison with the LeClair-Mussardo proposal

Based on the TBA approach LeClair and Mussardo proposed the following formula for the thermal two-point function (equation (3.3) in [30])

$$\begin{aligned}
\langle \mathcal{O}(x, t) \mathcal{O}(0, 0) \rangle^R = & \left(\langle \mathcal{O} \rangle^R \right)^2 + \sum_{N=1}^{\infty} \frac{1}{N!} \sum_{\sigma_i = \pm 1} \int \frac{d\theta_1}{2\pi} \cdots \frac{d\theta_N}{2\pi} \left[\prod_{j=1}^N f_{\sigma_j}(\theta_j) \exp \left(-\sigma_j (t\varepsilon_j + ixk_j) \right) \right] \\
& \times \left| \langle 0 | \mathcal{O} | \theta_1 \dots \theta_N \rangle_{\sigma_1 \dots \sigma_N} \right|^2 \tag{5.36}
\end{aligned}$$

¹We wish to note, that similar techniques are used in a recent work [116] which appeared after the completion of this thesis. In addition to the results above, the regularized finite contributions of I_{12} and I_{21} are also determined in [116].

where $f_{\sigma_j}(\theta_j) = 1/(1 + e^{-\sigma_j \varepsilon(\theta_j)})$, $\varepsilon_j = \varepsilon(\theta_j)/R$ and $k_j = k(\theta_j)$ with $\varepsilon(\theta)$ being the solution of the TBA equations (5.6) and $k(\theta)$ given by

$$\begin{aligned} k(\theta) &= m \sinh(\theta) + \int d\theta' \delta(\theta - \theta') \rho_1(\theta') \\ 2\pi \rho_1(\theta)(1 + e^{\varepsilon(\theta)}) &= m \cosh(\theta) + \int d\theta' \varphi(\theta - \theta') \rho_1(\theta') \end{aligned}$$

The form factors appearing in (5.36) are defined by

$$\langle 0 | \mathcal{O} | \theta_1 \dots \theta_N \rangle_{\sigma_1 \dots \sigma_N} = F_N^{\mathcal{O}}(\theta_1 - i\pi \tilde{\sigma}_1, \dots, \theta_N - i\pi \tilde{\sigma}_N) \quad \tilde{\sigma}_j = (1 - \sigma_j)/2 \in \{0, 1\}$$

We do not attempt here a thorough analysis of (5.36); nevertheless we wish to point out, that to order $\mathcal{O}(e^{-mR})$ it coincides with our result (5.35). The double integral (5.34) is given for example by the $N = 2$, $\sigma_{1,2} = (+1, -1)$ term in (5.36) after one substitutes the 0th-order approximations

$$\varepsilon(\theta) = mR \cosh(\theta) + \mathcal{O}(e^{-mR}) \quad k(\theta) = m \sinh(\theta) + \mathcal{O}(e^{-mR})$$

The validity of the LeClair-Mussardo proposal was doubted by two different authors [31, 35]. We did not find a discrepancy at order $\mathcal{O}(e^{-mR})$; it is a subject of future research to decide whether all terms in our low-temperature expansion are properly reproduced by (5.36).

Chapter 6

Conclusions

In this thesis we investigated finite size effects in 1+1 dimensional integrable quantum field theories; we considered massive integrable models with diagonal scattering. There were two main subjects of interest: finite volume form factors of local operators and finite size effects to correlation functions.

In the first main part of the work we gave a description of finite volume form factors in terms of the infinite volume form factors (solutions of the form factor bootstrap) and the S-matrix of the theory.

First we compared the spectral representation of correlation functions in an infinite system and in a finite volume L . We showed that the matrix elements in finite volume essentially coincide with the infinite volume form factors up to a nontrivial normalization factor, which is related to the particle densities of the finite volume spectrum. We showed, that our results capture all finite size corrections which scale as powers of $1/L$. We also showed that the residual finite size effects are of order $e^{-\mu L}$ with μ a universal characteristic mass scale of the theory, which does not depend on the particular form factor in question.

As a second step, we conjectured a formula for generic matrix elements without disconnected pieces. Together with the elementary case this is a new result of the author, although it can be considered as a generalization of partial results which appeared in [8] and independently in [52, 112]. Disconnected terms occur if there is a particle with a given rapidity, which present in both the "bra" and the "ket" vector. We showed that in finite volume this only happens in the case of diagonal form factors and matrix elements of "parity-symmetric" states including zero-momentum particles.

The diagonal matrix elements require special care because of the presence of various disconnected terms and the ambiguity of the infinite volume diagonal form factors. We used form factor perturbation theory to derive the first two cases (diagonal matrix elements of one-particle and two-particle states) in terms of the symmetric evaluation of the infinite volume diagonal form factors. Based on this result, we conjectured a general

formula, which we expressed with both the symmetric and connected evaluations. The latter expression was used to prove that our result coincides with a conjecture made independently by Saleur in [31]. The rigorous proofs concerning the two simplest cases (eqs. (2.32) and (2.33)) are new results of the author, together with the determination of the general relation between the symmetric and the connected form factors (Theorem 1).

To complete the description of finite volume matrix elements we also conjectured a formula for the case of states with zero-momentum particles. The most general result concerns situations with possibly more than one zero-momentum particles present in both states; this only occurs in theories with multiple particle species. In [117] we published the result for theories with only one particle type; the generalization (2.54) is an unpublished result of this work.

Following the analytic study, in section 3 we turned to numerical methods to confirm our results and conjectures. We investigated the massive Lee-Yang model and the critical Ising model in a magnetic field and considered form factors of the perturbing field, and the energy operator, respectively. We used TCSA as a numerical tool to obtain finite volume spectra and form factors. First we identified finite volume states at different values of the volume L : we matched the numerical data with predictions of the Bethe-Yang equations. We then calculated the finite volume form factors and compared them to our analytic formulas (the infinite volume form factors were already available in both models). In all cases (including form factors with disconnected pieces) we observed a satisfactory agreement in the scaling region, where both the residual finite size effects and the truncation errors are negligible.

We stress that our numerical investigation not only confirms our results about matrix elements in finite volume, but it is also the first direct test of the infinite volume form factors. These functions are obtained by solving the form factor axioms of the bootstrap program and then selecting the solutions with the desired symmetry and scaling properties. Although the identification of scattering theories as perturbed conformal field theories is well-established, there were only a few direct tests of the individual form factor functions prior to our work; the usual tests in the literature proceed through evaluation of correlation functions, sum-rules, etc. In this work, on the other hand, we directly compared the form factor functions at different values of the rapidity parameters to TCSA data, thus providing evidence for the applicability of the bootstrap approach to form factors.

In the case of the Ising model we observed that in some situations there is no scaling region, ie. the residual finite size corrections remain relevant even in large volumes, which are out of the reach of our TCSA routines. The large exponential corrections were explained by the presence of a μ -term with a small exponent. These findings served as

a motivation for section 4, where we investigated the μ -terms associated to finite size energies and finite volume form factors.

It is well-known that the μ -term is always connected with the inner structure of the particles, ie. their composition under the bootstrap procedure. We applied a simple quantum mechanical picture of bound state quantization in finite volume: the momenta of the constituents take complex values but they are still determined by the analytical continuation of the Bethe-Yang equations. We showed that if this principle is implemented properly, the μ -term can always be obtained by analytically continuing the usual formulas to the complex rapidities of the constituents. Moreover it was shown, that in some circumstances it is possible for the constituents of a bound state to unbind. This phenomenon was demonstrated numerically in case of the Ising model, where moving A_3 states with odd momentum quantum numbers dissociate in small volume into conventional A_1A_1 scattering states.

In the second part of the work (section 5) we investigated finite temperature corrections to vacuum expectation values and correlation functions. We introduced finite volume as a regulator of the otherwise ill-defined Boltzmann sum and established the spectral representation of n -point functions in terms of the finite volume form factors. We showed that it is possible to derive a systematic low temperature expansion with a well-defined $L \rightarrow \infty$ limit.

In the case of the one-point function we calculated the first three nontrivial terms and found complete agreement with the LeClair-Mussardo approach. It was pointed out, that the Delfino proposal differs from the LeClair-Mussardo formula exactly at this order; the discrepancy is easily explained in light of our results. Any evaluation scheme of thermal averages based on a spectral representation has to deal with infinities, which are introduced by disconnected terms of the form factors and by different contributions to the partition function itself. These infinities cancel as expected, however a well-defined regularization procedure is needed to obtain the left-over finite pieces. This point was missed in the proposals prior to our work. The LeClair-Mussardo formula is believed to be correct to all orders, however a general proof (possibly based on a re-summation scheme of our low-temperature expansion) is not available.

In our calculations the volume L served as a cutoff to regulate the divergent disconnected contributions. Those terms in the low-temperature expansion which scale with positive powers of L add up to zero, as it is necessary to obtain a meaningful result. We stress that in order to obtain the correct $\mathcal{O}(1)$ terms it was crucial to use the interacting densities $\rho^{(n)}$, which differ from the free-theory densities by sub-leading terms.

In this work we also considered the two-point function. We only calculated the first non-trivial term, which is a new (unpublished) result of this work. Our leading-order calculation showed agreement with the LeClair-Mussardo approach. A study of higher

order terms is left for future work, which will hopefully shed more light on the validity of the LeClair-Mussardo proposal.

There are several directions to generalize our results on finite volume form factors.

The extension to boundary field theories has already been established [118] together with the evaluation of finite temperature expectation values of boundary operators [119].

The generalization to non-diagonal scattering theories would be desirable, since these theories (for example the $O(3)$ σ -model) serve as effective field theories describing long-range interactions in real-world condensed matter systems (Heisenberg spin chains, etc.). We expect that the principles laid out in this work (finite volume matrix elements and infinite volume form factors connected by a density factor) carry over to the non-diagonal case. However, non-diagonal scattering poses technical difficulties. On one hand, the quantization of scattering states in finite volume is more complicated, since it involves a diagonalization of the transfer matrix. On the other hand, infinite volume form factors (decomposed into the different channels of the scattering) are also more difficult to obtain.

It is an interesting question whether some of our results can be extended to massless scattering theories. These models can be used to study renormalization group flows with a nontrivial conformal IR fixed point [75, 76, 120]. Although the form factor bootstrap for massless theories has already been established [120, 121], it is not clear what happens in a finite volume. In the absence of a mass-gap one does not have control over residual finite size effects, which decay exponentially in a massive theory. The situation is even worse in the case of thermal expectation values and correlation functions: there is no suitable variable (such as e^{-mR} in a massive theory) to perform a low-temperature expansion.

Finally we would like to remark that an exact description of finite volume form factors would be desirable, since they could be used to calculate correlations at finite temperature in a different way, than the one presented in this work. Instead of dealing with a theory defined in infinite volume and finite temporal extent $R = 1/T$ one can perform an Euclidean rotation $(\tau, x) \rightarrow (-x, \tau)$ to deal with a zero-temperature system defined in a finite volume R . Thermal corrections then become finite size corrections which can be readily calculated by a conventional zero-temperature form factor expansion. Obviously one needs the exact finite volume form factors in this approach: the summation over form factors not including the exponential corrections only reproduces the infinite volume correlation functions.

As far as we know, the only exact results available concern the form factors of the order and disorder operators in Ising model with zero magnetic field [43, 44, 45]. However, these calculations are rather model-specific and it is not clear at all how to approach more complicated (interacting) models. A TBA-like integral equation similar to the one describing excited state energies [25] would be desirable; however, it is not clear how to solve this problem.

Bibliography

- [1] M. E. Fisher and M. N. Barber, *Scaling Theory for Finite-Size Effects in the Critical Region*, Phys. Rev. Lett. **28** (1972) 1516-1519.
- [2] J. L. Cardy, *Operator Content of Two-Dimensional Conformally Invariant Theories*, Nucl. Phys. **B270** (1986) 186-204.
- [3] H. B. G. Casimir, *On the Attraction Between Two Perfectly Conducting Plates*, Indag. Math. **10** (1948) 261-263.
- [4] M. Lüscher, *Volume Dependence of the Energy Spectrum in Massive Quantum Field Theories. 1. Stable Particle States*, Commun. Math. Phys. **104** (1986) 177.
- [5] M. Lüscher, *Volume Dependence of the Energy Spectrum in Massive Quantum Field Theories. 2. Scattering States*, Commun. Math. Phys. **105** (1986) 153-188.
- [6] M. Lüscher and U. Wolff, *How to calculate the elastic scattering matrix in two dimensional quantum field theories by numerical simulation*, Nucl. Phys. **B339** (1990) 222-252.
- [7] M. Lüscher, *Signatures of unstable particles in finite volume*, Nucl. Phys. **B364** (1991) 237-254.
- [8] B. Pozsgay and G. Takacs, *Characterization of resonances using finite size effects*, Nucl. Phys. **B748** (2006) 485-523, [hep-th/0604022](#).
- [9] I. Affleck, *Conformal Field Theory Approach to the Kondo Effect*, Acta Phys. Polon. **B26** (1995) 1869-1932, [cond-mat/9512099](#).
- [10] P. Fendley, F. Lesage and H. Saleur, *A unified framework for the Kondo problem and for an impurity in a Luttinger liquid*, J. Statist. Phys. **85** (1996) 211, [cond-mat/9510055](#).
- [11] J. S. Caux, H. Saleur and F. Siano, *The two-boundary sine-Gordon model*, Nucl. Phys. **B672** (2003) 411-461, [cond-mat/0306328](#).

- [12] J. S. Caux, H. Saleur and F. Siano, *The Josephson current in Luttinger liquid-superconductor junctions*, Phys. Rev. Lett. **88** (2002) 106402, [cond-mat/0109103](#).
- [13] H. Saleur, *Lectures on Non Perturbative Field Theory and Quantum Impurity Problems: Part II*, [arXiv:cond-mat/0007309](#).
- [14] H. Saleur, *Lectures on Non Perturbative Field Theory and Quantum Impurity Problems: Part I*, [arXiv:cond-mat/9812110](#).
- [15] A. B. Zamolodchikov, *Integrable field theory from conformal field theory*, Adv. Stud. Pure Math. **19** (1989) 641-674.
- [16] A. B. Zamolodchikov, *Higher Order Integrals of Motion in Two-Dimensional Models of the Field Theory with a Broken Conformal Symmetry*, JETP Lett. **46** (1987) 160-164.
- [17] A. B. Zamolodchikov, *Renormalization Group and Perturbation Theory Near Fixed Points in Two-Dimensional Field Theory*, Sov. J. Nucl. Phys. **46** (1987) 1090.
- [18] F. A. Smirnov, *Form-factors in completely integrable models of quantum field theory*, Adv. Ser. Math. Phys. **14** (1992) 1-208.
- [19] A. B. Zamolodchikov, *Two point correlation function in scaling Lee-Yang model*, Nucl. Phys. **B348** (1991) 619-641.
- [20] V. E. Korepin and N. A. Slavnov, *The determinant representation for quantum correlation functions of the sinh-Gordon model*, J. Phys. **A31** (1998) 9283-9295, [hep-th/9801046](#).
- [21] V. E. Korepin and T. Oota, *The determinant representation for a correlation function in scaling Lee-Yang model*, J. Phys. **A31** (1998) L371-L380, [hep-th/9802003](#).
- [22] T. Oota, *Two-point correlation functions in perturbed minimal models*, J. Phys. **A31** (1998) 7611-7626, [hep-th/9804050](#).
- [23] A. B. Zamolodchikov, *Thermodynamic Bethe Ansatz in relativistic models. Scaling three state Potts and Lee-Yang models*, Nucl. Phys. **B342** (1990) 695-720.
- [24] A. LeClair, G. Mussardo, H. Saleur and S. Skorik, *Boundary energy and boundary states in integrable quantum field theories*, Nucl. Phys. **B453** (1995) 581-618, [hep-th/9503227](#).
- [25] P. Dorey and R. Tateo, *Excited states by analytic continuation of TBA equations*, Nucl. Phys. **B482** (1996) 639-659, [hep-th/9607167](#).

- [26] V. V. Bazhanov, S. L. Lukyanov and A. B. Zamolodchikov, *Quantum field theories in finite volume: Excited state energies*, Nucl. Phys. **B489** (1997) 487-531, [hep-th/9607099](#).
- [27] C. Destri and H. J. d Vega, *New thermodynamic Bethe ansatz equations without strings*, Phys. Rev. Lett. **69** (1992) 2313-2317.
- [28] C. Destri and H. J. De Vega, *Unified approach to thermodynamic Bethe Ansatz and finite size corrections for lattice models and field theories*, Nucl. Phys. **B438** (1995) 413-454, [hep-th/9407117](#).
- [29] A. LeClair, F. Lesage, S. Sachdev and H. Saleur, *Finite temperature correlations in the one-dimensional quantum Ising model*, Nuclear Physics B **482** (1996) 579.
- [30] A. Leclair and G. Mussardo, *Finite temperature correlation functions in integrable QFT*, Nucl. Phys. **B552** (1999) 624-642, [hep-th/9902075](#).
- [31] H. Saleur, *A comment on finite temperature correlations in integrable QFT*, Nucl. Phys. **B567** (2000) 602-610, [hep-th/9909019](#).
- [32] S. Lukyanov, *Finite temperature expectation values of local fields in the sinh-Gordon model*, Nuclear Physics B **612** (2001) 391.
- [33] G. Delfino, *One-point functions in integrable quantum field theory at finite temperature*, J. Phys. **A34** (2001) L161-L168, [hep-th/0101180](#).
- [34] G. Mussardo, *On the finite temperature formalism in integrable quantum field theories*, J. Phys. **A34** (2001) 7399-7410, [hep-th/0103214](#).
- [35] O. A. Castro-Alvaredo and A. Fring, *Finite temperature correlation functions from form factors*, Nucl. Phys. **B636** (2002) 611-631, [hep-th/0203130](#).
- [36] F. H. L. Essler and R. M. Konik. *Applications of Massive Integrable Quantum Field Theories to Problems in Condensed Matter Physics*, (2004).
- [37] B. L. Altshuler, R. M. Konik and A. M. Tsvelik, *Low temperature correlation functions in integrable models: Derivation of the large distance and time asymptotics from the form factor expansion*, Nuclear Physics B **739** (2006) 311.
- [38] F. H. L. Essler and R. M. Konik, *Finite-temperature lineshapes in gapped quantum spin chains*, Phys. Rev. **B78** (2008) 100403, [arxiv:0711.2524\[cond-mat.str-el\]](#).
- [39] R. M. K. A. J. A. James, F. H. L. E, *Finite Temperature Dynamical Structure Factor of Alternating Heisenberg Chains*, Phys. Rev. **B78** (2008) 094411.

- [40] A. J. A. James, W. D. Goetze and F. H. L. Essler. *Finite Temperature Dynamical Structure Factor of the Heisenberg-Ising Chain*, (2009).
- [41] F. A. Smirnov, *Quasi-classical study of form factors in finite volume*, (1998) , [hep-th/9802132](#).
- [42] G. Mussardo, V. Riva and G. Sotkov, *Finite-volume form factors in semiclassical approximation*, Nucl. Phys. **B670** (2003) 464-478, [hep-th/0307125](#).
- [43] A. I. Bugrij, *Form factor representation of the correlation function of the two dimensional Ising model on a cylinder*, (2001) , [hep-th/0107117](#).
- [44] A. I. Bugrij and O. Lisovyy, *Spin matrix elements in 2D Ising model on the finite lattice*, Physics Letters A **319** (2003) 390.
- [45] P. Fonseca and A. Zamolodchikov, *Ising field theory in a magnetic field: Analytic properties of the free energy*, (2001) , [hep-th/0112167](#).
- [46] A. Koubek and G. Mussardo, *On the operator content of the sinh-Gordon model*, Phys. Lett. **B311** (1993) 193-201, [hep-th/9306044](#).
- [47] A. Koubek, *Form-factor bootstrap and the operator content of perturbed minimal models*, Nucl. Phys. **B428** (1994) 655-680, [hep-th/9405014](#).
- [48] G. Delfino, *On the space of quantum fields in massive two-dimensional theories*, Nucl. Phys. **B807** (2009) 455-470, [arxiv:0806.1883\[hep-th\]](#).
- [49] A. A. Belavin, V. A. Belavin, A. V. Litvinov, Y. P. Pugai and A. B. Zamolodchikov, *On correlation functions in the perturbed minimal models $M(2,2n+1)$* , Nucl. Phys. **B676** (2004) 587-614, [hep-th/0309137](#).
- [50] A. B. Zamolodchikov, *Irreversibility of the Flux of the Renormalization Group in a 2D Field Theory*, JETP Lett. **43** (1986) 730-732.
- [51] G. Delfino, P. Simonetti and J. L. Cardy, *Asymptotic factorisation of form factors in two- dimensional quantum field theory*, Phys. Lett. **B387** (1996) 327-333, [hep-th/9607046](#).
- [52] L. Lellouch and M. Lüscher, *Weak transition matrix elements from finite-volume correlation functions*, Commun. Math. Phys. **219** (2001) 31-44, [hep-lat/0003023](#).
- [53] C. J. D. Lin, G. Martinelli, C. T. Sachrajda and M. Testa, *$K \rightarrow \pi \pi$ decays in a finite volume*, Nucl. Phys. **B619** (2001) 467-498, [hep-lat/0104006](#).

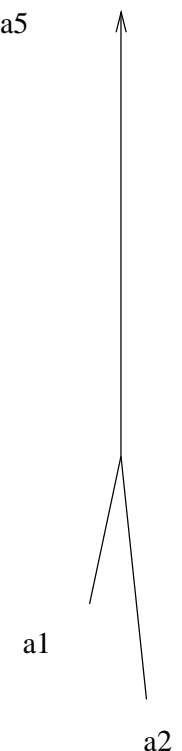
- [54] G. Mussardo, *Off critical statistical models: Factorized scattering theories and bootstrap program*, Phys. Rept. **218** (1992) 215-379.
- [55] C.-N. Yang, *Some exact results for the many body problems in one dimension with repulsive delta function interaction*, Phys. Rev. Lett. **19** (1967) 1312-1314.
- [56] R. J. Baxter, *Partition function of the eight-vertex lattice model*, Annals Phys. **70** (1972) 193-228.
- [57] A. B. Zamolodchikov and A. B. Zamolodchikov, *Factorized S-matrices in two dimensions as the exact solutions of certain relativistic quantum field models*, Annals Phys. **120** (1979) 253-291.
- [58] S. R. Coleman and H. J. Thun, *On the prosaic origin of the double poles in the Sine-Gordon S matrix*, Commun. Math. Phys. **61** (1978) 31.
- [59] C. J. Goebel, *On the sine-Gordon S matrix*, Prog. Theor. Phys. Suppl. **86** (1986) 261-273.
- [60] H. W. Braden, E. Corrigan, P. E. Dorey and R. Sasaki, *Multiple poles and other features of affine Toda field theory*, Nucl. Phys. **B356** (1991) 469-498.
- [61] S. R. Beane, W. Detmold and M. J. Savage, *n-Boson Energies at Finite Volume and Three-Boson Interactions*, Phys. Rev. **D76** (2007) 074507, [arxiv:0707.1670\[hep-lat\]](#).
- [62] W. Detmold and M. J. Savage, *The Energy of n Identical Bosons in a Finite Volume at $O(L^{-7})$* , Phys. Rev. **D77** (2008) 057502, [arxiv:0801.0763\[hep-lat\]](#).
- [63] T. Luu, *Three fermions in a box*, (2008) , [arxiv:0810.2331\[hep-lat\]](#).
- [64] T. R. Klassen and E. Melzer, *On the relation between scattering amplitudes and finite size mass corrections in QFT*, Nucl. Phys. **B362** (1991) 329-388.
- [65] H. Bethe, *Zur Theorie der Metalle. I. Eigenwerte und Eigenfunktionen der linearen Atomkette.*, Zeitschrift für Physik **A71** (1931) 205-226.
- [66] A. M. Polyakov, *Conformal symmetry of critical fluctuations*, JETP Lett. **12** (1970) 381-383.
- [67] A. A. Belavin, A. M. Polyakov and A. B. Zamolodchikov, *Infinite conformal symmetry in two-dimensional quantum field theory*, Nucl. Phys. **B241** (1984) 333-380.
- [68] P. H. Ginsparg, *Applied conformal field theory*, (1988) , [hep-th/9108028](#).

- [69] J. Cardy, *Conformal Field Theory and Statistical Mechanics*, (2008) , arxiv:0807.3472[cond-mat.stat-mech].
- [70] A. M. Polyakov, A. A. Belavin and A. B. Zamolodchikov, *Infinite Conformal Symmetry of Critical Fluctuations in Two-Dimensions*, J. Statist. Phys. **34** (1984) 763.
- [71] A. W. W. Ludwig and J. L. Cardy, *Perturbative Evaluation of the Conformal Anomaly at New Critical Points with Applications to Random Systems*, Nucl. Phys. **B285** (1987) 687-718.
- [72] G. Mussardo and P. Simon, *Bosonic-type S-matrix, vacuum instability and CDD ambiguities*, Nucl. Phys. **B578** (2000) 527-551, hep-th/9903072.
- [73] A. B. Zamolodchikov, *Integrals of Motion in Scaling Three State Potts Model Field Theory*, Int. J. Mod. Phys. **A3** (1988) 743-750.
- [74] A. B. Zamolodchikov, *Thermodynamic Bethe ansatz for RSOS scattering theories*, Nucl. Phys. **B358** (1991) 497-523.
- [75] A. B. Zamolodchikov, *From tricritical Ising to critical Ising by thermodynamic Bethe ansatz*, Nucl. Phys. **B358** (1991) 524-546.
- [76] P. Fendley, H. Saleur and A. B. Zamolodchikov, *Massless flows, 2. The Exact S matrix approach*, Int. J. Mod. Phys. **A8** (1993) 5751-5778, hep-th/9304051.
- [77] T. R. Klassen and E. Melzer, *Purely Elastic Scattering Theories and their Ultraviolet Limits*, Nucl. Phys. **B338** (1990) 485-528.
- [78] T. R. Klassen and E. Melzer, *The Thermodynamics of purely elastic scattering theories and conformal perturbation theory*, Nucl. Phys. **B350** (1991) 635-689.
- [79] C.-N. Yang and T. D. Lee, *Statistical theory of equations of state and phase transitions. I: Theory of condensation*, Phys. Rev. **87** (1952) 404-409.
- [80] T. D. Lee and C.-N. Yang, *Statistical theory of equations of state and phase transitions. II: Lattice gas and Ising model*, Phys. Rev. **87** (1952) 410-419.
- [81] J. L. Cardy, *Conformal invariance and the Yang-Lee edge singularity in two dimensions*, Phys. Rev. Lett. **54** (1985) 1354-1356.
- [82] G. Parisi and N. Surlas, *Critical behavior of branched polymers and the Lee-Yang edge singularity*, Phys. Rev. Lett. **46** (1981) 871.
- [83] J. L. Cardy and G. Mussardo, *S Matrix of the Yang-Lee Edge Singularity in Two-Dimensions*, Phys. Lett. **B225** (1989) 275.

- [84] A. B. Zamolodchikov, *Integrals of Motion and S Matrix of the (Scaled) $T=T(c)$ Ising Model with Magnetic Field*, Int. J. Mod. Phys. **A4** (1989) 4235.
- [85] V. A. Fateev, *The Exact relations between the coupling constants and the masses of particles for the integrable perturbed conformal field theories*, Phys. Lett. **B324** (1994) 45-51.
- [86] V. P. Yurov and A. B. Zamolodchikov, *Truncated Conformal Space Approach to Scaling Lee-Yang model*, Int. J. Mod. Phys. **A5** (1990) 3221-3246.
- [87] M. Karowski and P. Weisz, *Exact Form-Factors in (1+1)-Dimensional Field Theoretic Models with Soliton Behavior*, Nucl. Phys. **B139** (1978) 455.
- [88] B. Berg, M. Karowski and P. Weisz, *Construction of Green Functions from an Exact S Matrix*, Phys. Rev. **D19** (1979) 2477.
- [89] G. Delfino and G. Mussardo, *The Spin spin correlation function in the two-dimensional Ising model in a magnetic field at $T = T(c)$* , Nucl. Phys. **B455** (1995) 724-758, [hep-th/9507010](#).
- [90] G. Delfino, P. Grinza and G. Mussardo, *Decay of particles above threshold in the Ising field theory with magnetic field*, Nucl. Phys. **B737** (2006) 291-303, [hep-th/0507133](#).
- [91] G. Delfino, G. Mussardo and P. Simonetti, *Non-integrable Quantum Field Theories as Perturbations of Certain Integrable Models*, Nucl. Phys. **B473** (1996) 469-508, [hep-th/9603011](#).
- [92] G. Delfino, P. Grinza and G. Mussardo, *Decay of particles above threshold in the Ising field theory with magnetic field*, Nucl. Phys. **B737** (2006) 291-303, [hep-th/0507133](#).
- [93] J. Balog, *Field theoretical derivation of the TBA integral equation*, Nucl. Phys. **B419** (1994) 480-506.
- [94] N. B. V.E. Korepin and A. Izergin. *Quantum inverse scattering method and correlation functions*. Cambridge University Press, (1993).
- [95] H. Kausch, G. Takacs and G. Watts, *On the relation between $\Phi(1,2)$ and $\Phi(1,5)$ perturbed minimal models and unitarity*, Nucl. Phys. **B489** (1997) 557-579, [hep-th/9605104](#).
- [96] V. P. Yurov and A. B. Zamolodchikov, *Truncated fermionic space approach to the critical 2-D Ising model with magnetic field*, Int. J. Mod. Phys. **A6** (1991) 4557-4578.

- [97] G. Delfino and P. Simonetti, *Correlation Functions in the Two-dimensional Ising Model in a Magnetic Field at $T = T_c$* , Phys. Lett. **B383** (1996) 450-456, [hep-th/9605065](#).
- [98] V. Fateev, S. L. Lukyanov, A. B. Zamolodchikov and A. B. Zamolodchikov, *Expectation values of local fields in Bullough-Dodd model and integrable perturbed conformal field theories*, Nucl. Phys. **B516** (1998) 652-674, [hep-th/9709034](#).
- [99] G. Delfino, <http://www.sissa.it/~delfino/isingff.html>.
- [100] R. Guida and N. Magnoli, *Vacuum expectation values from a variational approach*, Phys. Lett. **B411** (1997) 127-133, [hep-th/9706017](#).
- [101] G. M. D. Fioravanti and P. Simon, *Universal Amplitude Ratios of The Renormalization Group: Two-Dimensional Tricritical Ising Model*, Phys.Rev. **E63** (2001) 016103, [cond-mat/0008216](#).
- [102] Z. Bajnok, L. Palla, G. Takacs and F. Wagner, *The k-folded sine-Gordon model in finite volume*, Nucl. Phys. **B587** (2000) 585-618, [hep-th/0004181](#).
- [103] K. Rummukainen and S. A. Gottlieb, *Resonance scattering phase shifts on a nonrest frame lattice*, Nucl. Phys. **B450** (1995) 397-436, [hep-lat/9503028](#).
- [104] B. Pozsgay and G. Takacs, *Form factors in finite volume I: form factor bootstrap and truncated conformal space*, Nucl. Phys. **B788** (2008) 167-208, [arxiv:0706.1445\[hep-th\]](#).
- [105] R. A. Janik and T. Lukowski, *Wrapping interactions at strong coupling – the giant magnon*, Phys. Rev. **D76** (2007) 126008, [arxiv:0708.2208\[hep-th\]](#).
- [106] M. P. Heller, R. A. Janik and T. Lukowski, *A new derivation of Lüscher F-term and fluctuations around the giant magnon*, JHEP **06** (2008) 036, [arxiv:0801.4463\[hep-th\]](#).
- [107] Z. Bajnok and R. A. Janik, *Four-loop perturbative Konishi from strings and finite size effects for multiparticle states*, Nucl. Phys. **B807** (2009) 625-650, [arxiv:0807.0399\[hep-th\]](#).
- [108] Y. Hatsuda and R. Suzuki, *Finite-Size Effects for Multi-Magnon States*, JHEP **09** (2008) 025, [arxiv:0807.0643\[hep-th\]](#).
- [109] Z. Bajnok, L. Palla and G. Takacs, *Boundary states and finite size effects in sine-Gordon model with Neumann boundary condition*, Nucl. Phys. **B614** (2001) 405-448, [hep-th/0106069](#).

- [110] Z. Bajnok, L. Palla and G. Takacs, *(Semi)classical analysis of sine-Gordon theory on a strip*, Nucl. Phys. **B702** (2004) 448-480, [hep-th/0406149](#).
- [111] L. Maiani and M. Testa, *Final state interactions from Euclidean correlation functions*, Phys. Lett. **B245** (1990) 585-590.
- [112] C. J. D. Lin, G. Martinelli, C. T. Sachrajda and M. Testa, *$K \rightarrow \pi \pi$ decays in a finite volume*, Nucl. Phys. **B619** (2001) 467-498, [hep-lat/0104006](#).
- [113] V. P. Yurov and A. B. Zamolodchikov, *Correlation functions of integrable 2-D models of relativistic field theory. Ising model*, Int. J. Mod. Phys. **A6** (1991) 3419-3440.
- [114] J. L. Cardy and G. Mussardo, *Form-factors of descendant operators in perturbed conformal field theories*, Nucl. Phys. **B340** (1990) 387-402.
- [115] R. M. Konik, *Haldane Gapped Spin Chains: Exact Low Temperature Expansions of Correlation Functions*, (2001).
- [116] F. H. L. Essler and R. M. Konik, *Finite Temperature Dynamical Correlations in Massive Integrable Quantum Field Theories*, (2009) , [arxiv:0907.0779\[cond-mat\]](#).
- [117] B. Pozsgay and G. Takacs, *Form factors in finite volume II: disconnected terms and finite temperature correlators*, Nucl. Phys. **B788** (2008) 209-251, [arxiv:0706.3605\[hep-th\]](#).
- [118] M. Kormos and G. Takacs, *Boundary form factors in finite volume*, Nucl. Phys. **B803** (2008) 277-298, [arxiv:0712.1886\[hep-th\]](#).
- [119] G. Takacs, *Finite temperature expectation values of boundary operators*, Nucl. Phys. **B805** (2008) 391-417, [arxiv:0804.4096\[hep-th\]](#).
- [120] G. Delfino, G. Mussardo and P. Simonetti, *Correlation functions along a massless flow*, Phys. Rev. **D51** (1995) 6620-6624, [hep-th/9410117](#).
- [121] P. Mejean and F. A. Smirnov, *Form factors for principal chiral field model with Wess- Zumino-Novikov-Witten term*, Int. J. Mod. Phys. **A12** (1997) 3383-3396, [hep-th/9609068](#).



sim

